NUCLEAR MAGNETIC RESONANCE SPECTROSCOPY

Part Three: Spin–Spin Coupling

C hapters 3 and 4 covered only the most essential elements of nuclear magnetic resonance (NMR) theory. Now we will consider applications of the basic concepts to more complicated situations. In this chapter, the emphasis is on the origin of coupling constants and what information can be deduced from them. Enantiotopic and diastereotopic systems will be covered as well as more advanced instances of spin–spin coupling, such as second-order spectra.

5.1 COUPLING CONSTANTS: SYMBOLS

Chapter 3, Sections 3.17 and 3.18, introduced coupling constants. For simple multiplets, the coupling constant J is easily determined by measuring the spacing (in Hertz) between the individual peaks of the multiplet. This coupling constant has the same value regardless of the field strength or operating frequency of the NMR spectrometer. J is a *constant*.[1]

Coupling between two nuclei of the same type is called **homonuclear coupling.** Chapter 3 examined the homonuclear three-bond couplings between hydrogens on adjacent carbon atoms (vicinal coupling, Section 5.2C), which gave multiplets governed by the $n + 1$ Rule. Coupling between two different types of nuclei is called **heteronuclear coupling**. The couplings between ^{13}C and attached hydrogens are one-bond heteronuclear couplings (Section 5.2A).

The magnitude of the coupling constant depends to a large extent on the number of bonds intervening between the two atoms or groups of atoms that interact. Other factors also influence the strength of interaction between two nuclei, but in general, one-bond couplings are larger than two-bond couplings, which in turn are larger than three-bond couplings, and so forth. Consequently, the symbols used to represent coupling are often extended to include additional information about the type of atoms involved and the number of bonds through which the coupling constant operates.

We frequently add a superscript to the symbol J to indicate the number of bonds through which the interaction occurs. If the identity of the two nuclei involved is not obvious, we add this information in parentheses. Thus, the symbol

$$^1J\,(^{13}C-^1H) = 156 \text{ Hz}$$

indicates a one-bond coupling between a carbon-13 atom and a hydrogen atom (C—H) with a value of 156 Hz. The symbol

$$^3J\,(^1H-^1H) = 8 \text{ Hz}$$

---

[1] We will see, however, the magnitude of J is dependent on the bond angles between the interacting nuclei and can therefore vary with temperature or solvent, to the extent these influence the conformation of the compound.
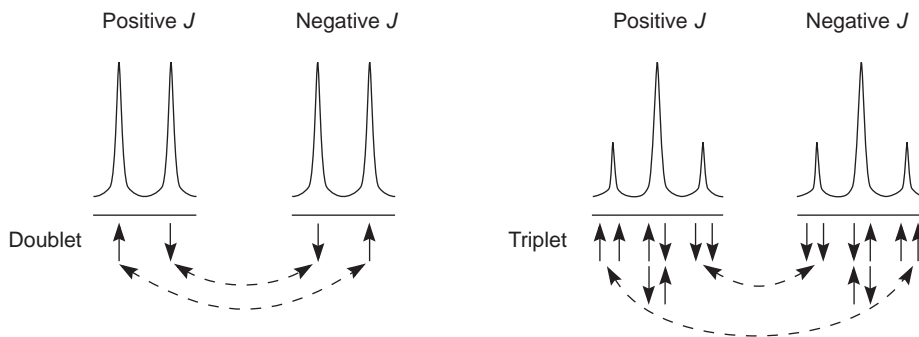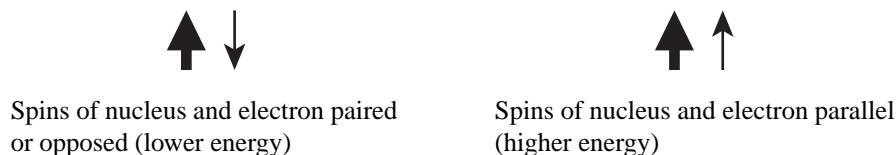
F I G U R E   5 . 1   The dependence of multiplet assignments on the sign of J, the coupling constant.

indicates a three-bond coupling between two hydrogen atoms, as in $H-C-C-H$. Subscripts may also be used to give additional information. $J_{1,3}$, for instance, indicates a coupling between atoms 1 and 3 in a structure or between protons attached to carbons 1 and 3 in a structure. J_{CH} or J_{HH} clearly indicates the types of atoms involved in the coupling interaction. The different coupling constants in a molecule might be designated simply as J_1, J_2, J_3, and so forth. Expect to see many variants in the usage of J symbols.

Although it makes no difference to the gross appearance of a spectrum, some coupling constants are positive, and others are negative. With a negative J, the meanings of the individual lines in a multiplet are reversed—the upfield and downfield peaks exchange places—as shown in Figure 5.1. In the simple measurement of a coupling constant from a spectrum, it is impossible to tell whether the constant is positive or negative. Therefore, a measured value should always be regarded as the *absolute value* of J ($|J|$).

## 5.2 COUPLING CONSTANTS: THE MECHANISM OF COUPLING

A physical picture of spin–spin coupling, the way in which the spin of one nucleus influences the spin of another, is not easy to develop. Several theoretical models are available. The best theories we have are based on the Dirac vector model. This model has limitations, but it is fairly easy for the novice to understand, and its predictions are substantially correct. According to the Dirac model, the electrons in the intervening bonds between the two nuclei transfer spin information from one nucleus to another by means of interaction between the nuclear and electronic spins. An electron near the nucleus is assumed to have the lowest energy of interaction with the nucleus when the spin of the electron (small arrow) has its spin direction opposed to (or "paired" with) that of the nucleus (heavy arrow).

Spins of nucleus and electron paired   Spins of nucleus and electron parallel
or opposed (lower energy)   (higher energy)

This picture makes it easy to understand why the size of the coupling constant diminishes as the number of intervening bonds increases. As we will see, it also explains why some coupling constants are negative while others are positive. Theory shows that couplings involving an odd number of intervening bonds (^1J, ^3J, . . .) are expected to be positive, while those involving an even number of intervening bonds (^2J, ^4J, . . .) are expected to be negative.

A. One-Bond Couplings (^1J)

A one-bond coupling occurs when a single bond links two spin-active nuclei. The bonding electrons in a single bond are assumed to avoid each other such that when one electron is near nucleus A, the other is near nucleus B. According to the Pauli Principle, pairs of electrons in the same orbital have opposed spins; therefore, the Dirac model predicts that the most stable condition in a bond is when both nuclei have opposed spins. Following is an illustration of a $^{13}C-^1H$ bond; the nucleus of the ^{13}C atom (heavy solid arrow) has a spin opposite to that of the hydrogen nucleus (heavy open arrow). The alignments shown would be typical for a $^{13}C-^1H$ bond or for any other type of bond in which both nuclei have spin (for instance, $^1H-^1H$ or $^{31}P-H$).

$$^{13}C-H$$
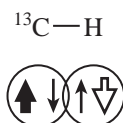
Notice that in this arrangement the two nuclei prefer to have opposite spins. When two spin-active nuclei prefer an opposed alignment (have opposite spins), the coupling constant J is usually positive. If the nuclei are parallel or aligned (have the same spin), J is usually negative. Thus, most one-bond couplings have positive J values. Keep in mind, however, that there are some prominent exceptions, such as $^{13}C-^{19}F$, for which the coupling constants are negative (see Table 5.1).

It is not unusual for coupling constants to depend on the hybridization of the atoms involved. ^1J values for $^{13}C-^1H$ coupling constants vary with the amount of s character in the carbon hybrid, according to the following relationship:

$$^1J_{CH} = (500 \text{ Hz}) \left(\frac{1}{n+1}\right) \text{ for hybridization type } sp^n \qquad \textbf{Equation 5.1}$$

Notice the specific values given for the $^{13}C-^1H$ couplings of ethane, ethene, and ethyne in Table 5.1.

Using the Dirac nuclear–electronic spin model, we can also develop an explanation for the origin of the spin–spin splitting multiplets that are the results of coupling. As a simple example, consider a $^{13}C-^1H$ bond. Recall that a ^{13}C atom that has one hydrogen attached appears as a doublet (two peaks) in a proton-coupled ^{13}C NMR spectrum (Section 4.3 and Fig. 4.3, p. 182). There are two lines (peaks) in the ^{13}C NMR spectrum because the hydrogen nucleus can have two spins (+1/2 or –1/2), leading to two different energy transitions for the ^{13}C nucleus. Figure 5.2 illustrates these two situations.

TABLE 5.1
SOME ONE-BOND COUPLING CONSTANTS (^1J)

$^{13}C-^1H$	110 –270 Hz
	sp^3 115–125 Hz (ethane = 125 Hz)
	sp^2 150–170 Hz (ethene = 156 Hz)
	sp 240–270 Hz (ethyne = 249 Hz)
$^{13}C-^{19}F$	−165 to −370 Hz
$^{13}C-^{31}P$	48–56 Hz
$^{13}C-D$	20 –30 Hz
$^{31}P-^1H$	190 –700 Hz
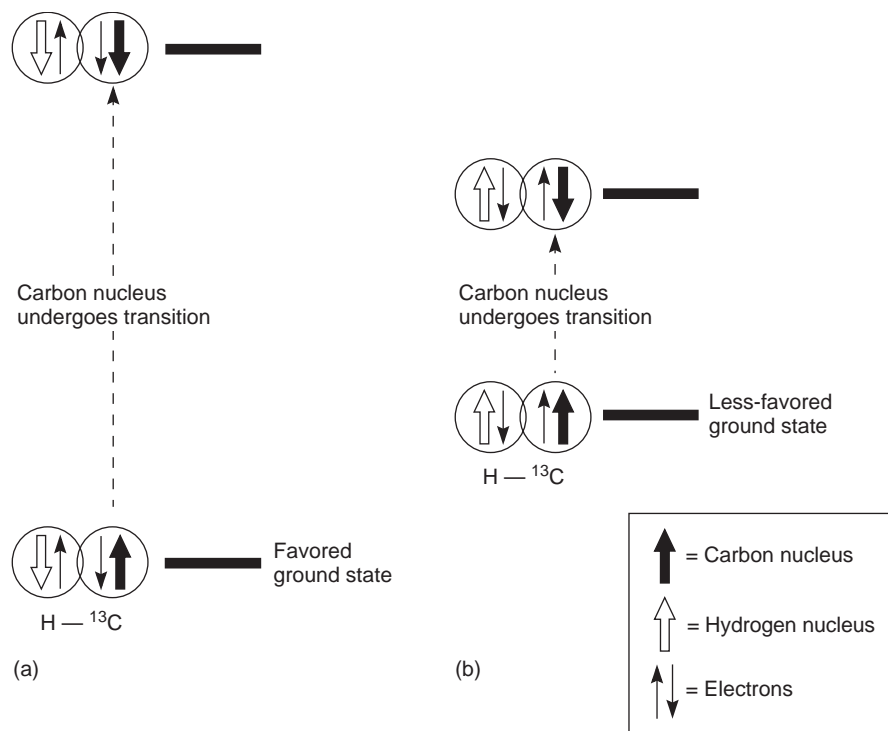
F I G U R E 5 . 2   The two different energy transitions for a ^{13}C nucleus in a C—H bond. (a) The favored ground state (all spins paired); (b) the less-favored ground state (impossible to pair all spins).

At the bottom of Figure 5.2a is the favored ground state for the $^{13}C-^{1}H$ bond. In this arrangement, the carbon nucleus is in its lowest energy state [spin (^{1}H) = +1/2], and all of the spins, both nuclear and electronic, are paired, resulting in the lowest energy for the system. The spin of the nucleus of the hydrogen atom is opposed to the spin of the ^{13}C nucleus. A higher energy results for the system if the spin of the hydrogen is reversed [spin (^{1}H) = –1/2]. This less-favored ground state is shown at the bottom of Figure 5.2b.

Now, assume that the carbon nucleus undergoes transition and inverts its spin. The excited state that results from the less-favored ground state (seen at the top of Fig. 5.2b) turns out to have a lower energy than the one resulting from the favored ground state (top of Fig. 5.2a) because all of its nuclear and electronic spins are paired. Thus, we see two different transitions for the ^{13}C nucleus [spin(^{13}C) = +1/2], depending on the spin of the attached hydrogen. As a result, in a proton-coupled NMR spectrum a doublet is observed for a methine carbon ($^{13}C-^{1}H$).

B. Two-Bond Couplings (^{2}J)

Two-bond couplings are quite common in NMR spectra. They are usually called **geminal couplings** because the two nuclei that interact are attached to the same central atom (Latin *gemini* = "twins"). Two-bond coupling constants are abbreviated ^{2}J. They occur in carbon compounds whenever two or more spin-active atoms are attached to the same carbon atom. Table 5.2 lists some two-bond coupling constants that involve carbon as the central atom. Two-bond coupling constants are typically, although not always, smaller in magnitude than one-bond couplings (Table 5.2). Notice that the most common type of two-bond coupling, HCH, is frequently (but not always) negative.

TABLE 5.2
SOME TWO-BOND COUPLING CONSTANTS (^2J)

C$\overset{H}{\underset{H}{<}}$	-9 to -15 Hz		C$\overset{H}{\underset{^{19}F}{<}}$	~ 50 Hz[a]
=C$\overset{H}{\underset{H}{<}}$	0 to 2 Hz		C$\overset{H}{\underset{^{13}C}{<}}$	~ 5 Hz[a]
C$\overset{H}{\underset{D}{<}}$	~ 2 Hz[a]		C$\overset{H}{\underset{^{31}P}{<}}$	$7 - 14$ Hz[a]
C$\overset{^{19}F}{\underset{^{19}F}{<}}$	~ 160 Hz[a]			

[a]*Absolute values.*

The mechanistic picture for geminal coupling (^2J) invokes nuclear–electronic spin coupling as a means of transmitting spin information from one nucleus to the other. It is consistent with the Dirac model that we discussed at the beginning of Section 5.2 and in Section 5.2A. Figure 5.3 shows this mechanism. In this case, another atom (without spin) intervenes between two interacting orbitals. When this happens, theory predicts that the interacting electrons, and hence the nuclei, prefer to have parallel spins, resulting in a negative coupling constant. The preferred alignment is shown on the left side of Figure 5.3.

The amount of geminal coupling depends on the HCH angle α. The graph in Figure 5.4 shows this dependence, where the amount of *electronic* interaction between the two C−H orbitals determines the magnitude of the coupling constant ^2J. In general, ^2J geminal coupling constants increase as the angle α decreases. As the angle α decreases, the two orbitals shown in Figure 5.3 move closer, and the electron spin correlations become greater. Note, however, that the graph in Figure 5.4 is very approximate, showing only the general trend; actual values vary quite widely.
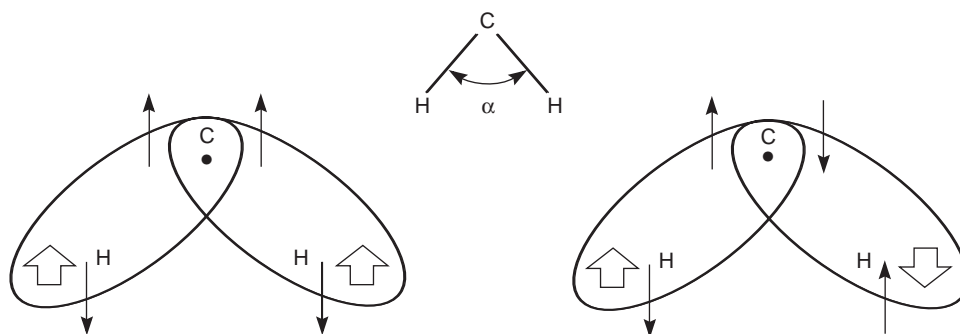
FIGURE 5.3   The mechanism of geminal coupling.
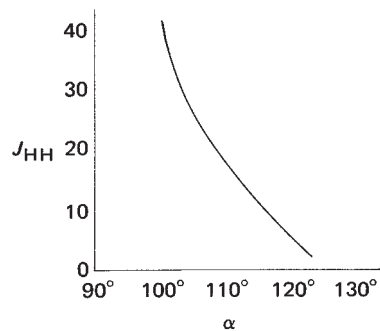
FIGURE 5.4 The dependence of the magnitude of $^2J_{HCH}$, the geminal coupling constant, on the HCH bond angle α.

Following are some systems that show geminal coupling, along with their approximate HCH bond angles. Notice that the coupling constants become smaller, as predicted, when the HCH angle becomes larger. Note also that even small changes in bond angles resulting from stereochemical changes influence the geminal coupling constant.
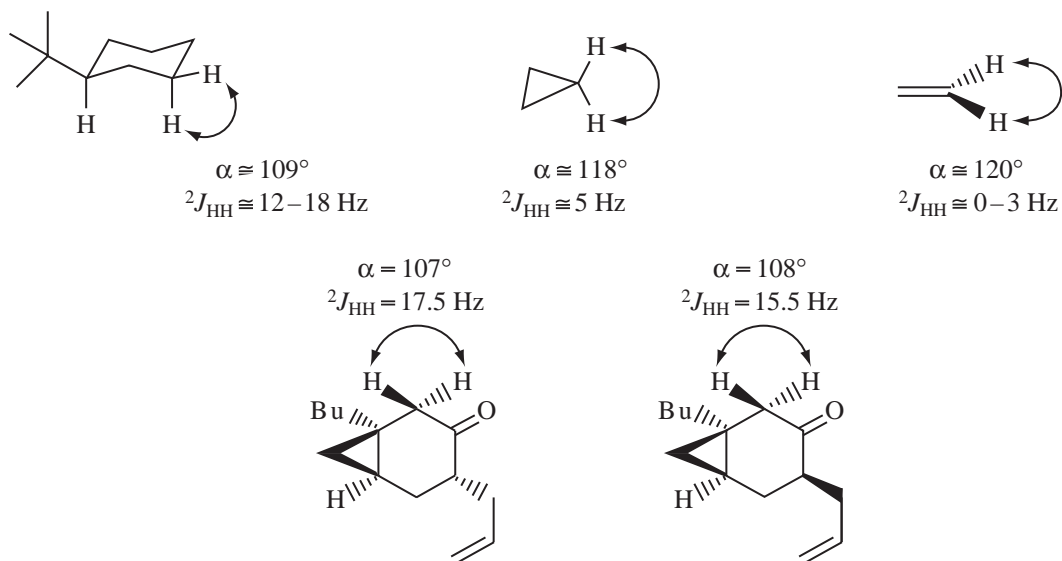

$\alpha \cong 109°$
$^2J_{HH} \cong 12-18$ Hz

$\alpha \cong 118°$
$^2J_{HH} \cong 5$ Hz

$\alpha \cong 120°$
$^2J_{HH} \cong 0-3$ Hz

$\alpha = 107°$
$^2J_{HH} = 17.5$ Hz

$\alpha = 108°$
$^2J_{HH} = 15.5$ Hz

Table 5.3 shows a larger range of variation, with approximate values for a selected series of cyclic compounds and alkenes. Notice that as ring size decreases, the absolute value of the coupling constant

TABLE 5.3
VARIATIONS IN $^2J_{HH}$ WITH HYBRIDIZATION AND RING SIZE

| +2 | −2 | −4 | −9 | −11 | −13 | −9 to −15 Hz |

^2J also decreases. Compare, for instance, cyclohexane, where ^2J is –13, and cyclopropane, where ^2J is –4. As the angle CCC in the ring becomes smaller (as p character increases), the complementary HCH angle grows larger (s character increases), and consequently the geminal coupling constant decreases. Note that hybridization is important, and that the sign of the coupling constant for alkenes changes to positive, except where they have an electronegative element attached.


Plane of symmetry— no splitting

Free rotation— no splitting
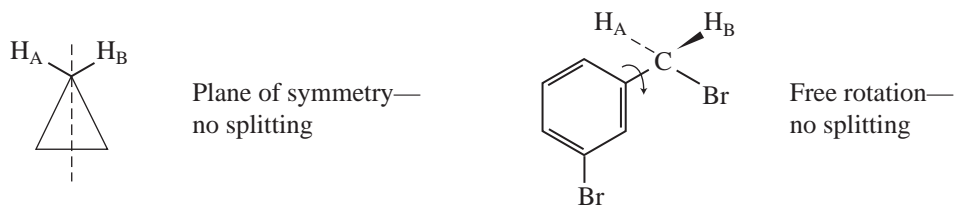
Geminal coupling between nonequivalent protons is readily observed in the ^1H NMR spectrum, and the magnitude of the coupling constant ^2J is easily measured from the line spacings when the resonances are first order (see Sections 5.6 and 5.7). In second-order spectra, the value of ^2J cannot be directly measured from the spectrum but may be determined by computational methods (spectral simulation). In many cases, however, no geminal HCH coupling (no spin–spin splitting) is observed because the geminal protons are magnetically equivalent (see Section 5.3). You have already seen in our discussions of the $n + 1$ Rule that in a hydrocarbon chain the protons attached to the same carbon may be treated as a group and do not split one another. How, then, can it be said that coupling exists in such cases if no spin–spin splitting is observed in the spectrum? The answer comes from deuterium substitution experiments. If one of the hydrogens in a compound that shows no spin–spin splitting is replaced by a deuterium, geminal splitting with deuterium ($I = 1$) is observed. Since deuterium and hydrogen are electronically the same atom (they differ only by a neutron, of course), it can be assumed that if there is interaction for HCD there is also interaction for HCH. The HCH and HCD coupling constants are related by the gyromagnetic ratios of hydrogen and deuterium:

$$^2J_{HH} = \gamma H/\gamma D \, (^2J_{HD}) = 6.51(^2J_{HD})$$ **Equation 5.2**

In the following sections of this chapter, whenever coupling constant values are given for seemingly equivalent protons (excluding cases of magnetic inequivalence, see Section 5.3), the coupling values were derived from spectra of deuterium-labeled isomers.

C. Three-Bond Couplings (^3J)

In a typical hydrocarbon, the spin of a hydrogen nucleus in one C—H bond is coupled to the spins of those hydrogens in adjacent C—H bonds. These H—C—C—H couplings are usually called **vicinal couplings** because the hydrogens are on neighboring carbon atoms (Latin *vicinus* = "neighbor"). Vicinal couplings are three-bond couplings and have a coupling constant designated as ^3J. In Sections 3.13 through 3.17, you saw that these couplings produce spin–spin splitting patterns that follow the $n + 1$ Rule in simple aliphatic hydrocarbon chains.

Three-bond vicinal coupling
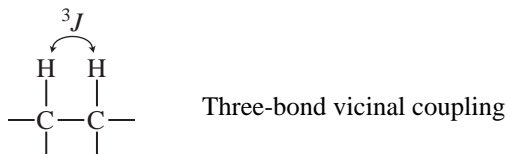
Once again, nuclear and electronic spin interactions carry the spin information from one hydrogen to its neighbor. Since the σ C—C bond is nearly orthogonal (perpendicular) to the σ C—H bonds, there is no overlap between the orbitals, and the electrons cannot interact strongly through the sigma bond system. According to theory, they transfer the nuclear spin information via the small amount of parallel orbital *overlap* that exists between adjacent C—H bond orbitals. The spin interaction between the electrons in the two adjacent C—H bonds is the major factor determining the size of the coupling constant.
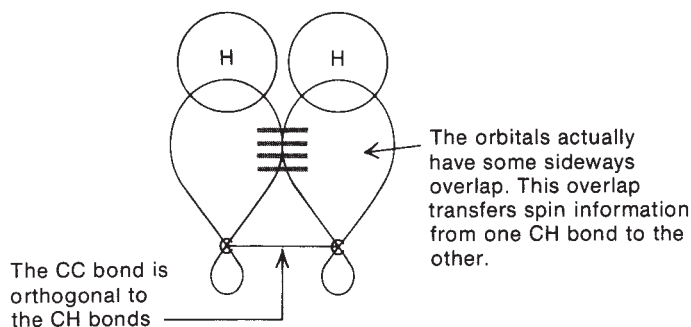
Figure 5.5 illustrates the two possible arrangements of nuclear and electronic spins for two coupled protons that are on adjacent carbon atoms. Recall that the carbon nuclei (^{12}C) have zero spin. The drawing on the left side of the figure, where the spins of the hydrogen nuclei are paired and where the spins of the electrons that are interacting through orbital overlap are also paired, is expected to represent the lowest energy and have the favored interactions. Because the interacting nuclei are spin paired in the favored arrangement, three-bond H—C—C—H couplings are expected to be positive. In fact, most three-bond couplings, regardless of atom types, are found to be positive.

That our current picture of three-bond vicinal coupling is substantially correct can be seen best in the effect of the dihedral angle between adjacent C—H bonds on the magnitude of the spin inter-action. Recall that two nonequivalent adjacent protons give rise to a pair of doublets, each proton splitting the other.

The parameter $^3J_{HH}$, the vicinal coupling constant, measures the magnitude of the splitting and is equal to the separation in Hertz between the multiplet peaks. The actual magnitude of the coupling
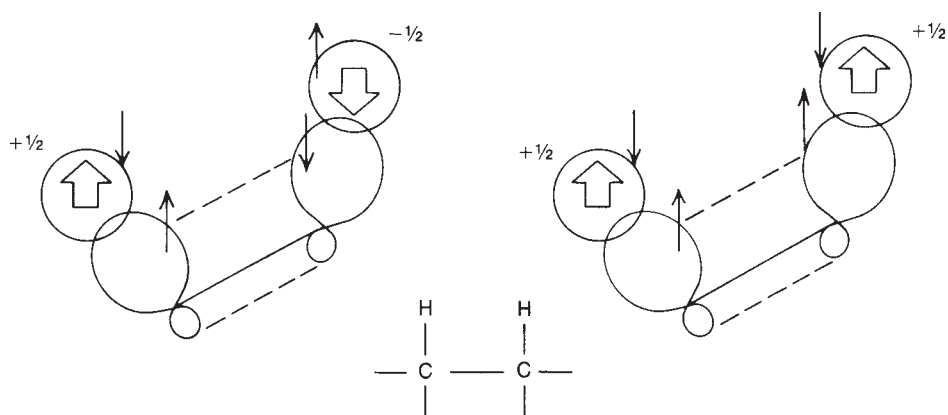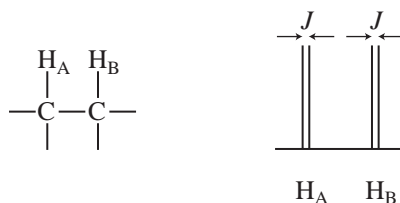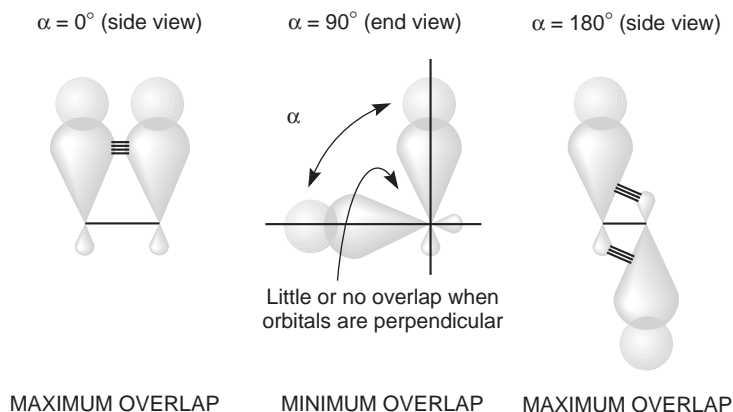

F I G U R E 5 . 5   The method of transferring spin information between two adjacent C—H bonds.

constant between two adjacent C—H bonds can be shown to depend directly on the dihedral angle α between these two bonds. Figure 5.6 defines the dihedral angle α as a perspective drawing and a Newman diagram.

The magnitude of the splitting between H_A and H_B is greatest when $\alpha = 0°$ or $180°$ and is smallest when $\alpha = 90°$. The side-to-side overlap of the two C—H bond orbitals is at a maximum at $0°$, where the C—H bond orbitals are parallel, and at a minimum at $90°$, where they are perpendicular. At $\alpha = 180°$, overlap with the back lobes of the sp^3 orbitals occurs.

$\alpha = 0°$ (side view) $\alpha = 90°$ (end view) $\alpha = 180°$ (side view)

Little or no overlap when orbitals are perpendicular

MAXIMUM OVERLAP   MINIMUM OVERLAP   MAXIMUM OVERLAP

Martin Karplus was the first to study the variation of the coupling constant $^3J_{HH}$ with the dihedral angle α and developed an equation (Eq. 5.3) that gave a good fit to the experimental data shown in the graph in Figure 5.7. The **Karplus relationship** takes the form

$$^3J_{HH} = A + B \cos \alpha + C \cos 2\alpha$$

$$A = 7 \qquad B = -1 \qquad C = 5 \qquad\qquad \textbf{Equation 5.3}$$

Many subsequent workers have modified this equation—particularly its set of constants, A, B, and C—and several different forms of it are found in the literature. The constants shown are accepted as
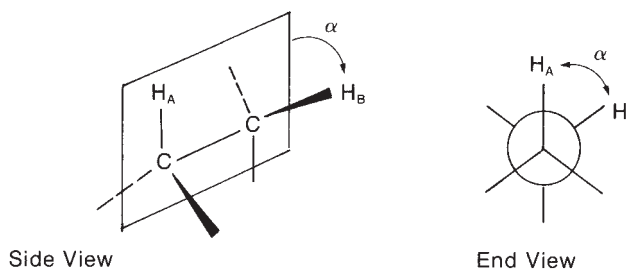
**FIGURE 5.6** The definition of a dihedral angle α.

Side View

End View
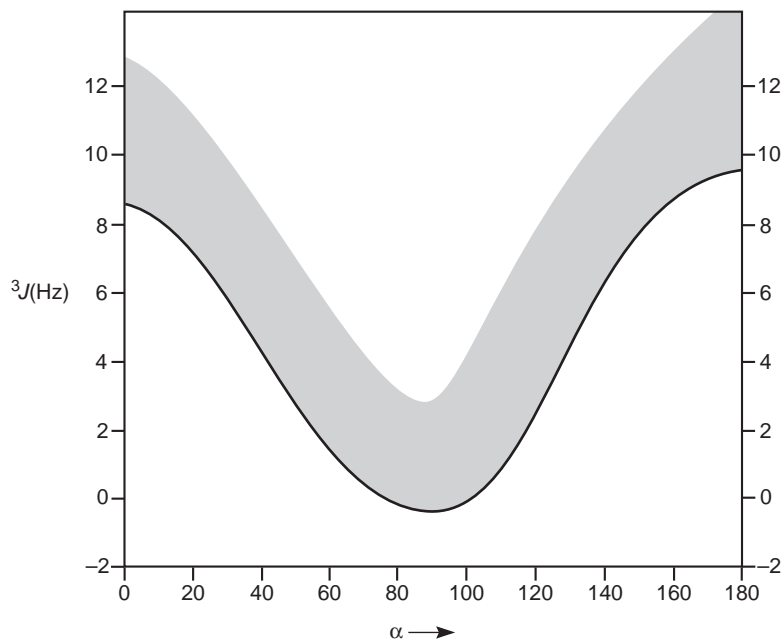
FIGURE 5.7 The Karplus relationship—the approximate variation of the coupling constant ^3J with the dihedral angle α.

those that give the best general predictions. Note, however, that actual experimental data exhibit a wide range of variation, as shown by the shaded area of the curve (sometimes called the **Karplus curve**) in Figure 5.7.

The Karplus relationship makes perfect sense according to the Dirac model. When the two adjacent C—H σ bonds are orthogonal ($\alpha = 90°$, perpendicular), there should be minimal orbital overlap, with little or no spin interaction between the electrons in these orbitals. As a result, nuclear spin information is not transmitted, and $^3J_{HH} \cong 0$. Conversely, when these two bonds are parallel ($\alpha = 0°$) or antiparallel ($\alpha = 180°$), the coupling constant should have its greatest magnitude ($^3J_{HH} = $ max).

The variation of $^3J_{HH}$ indicated by the shaded area in Figure 5.7 is a result of factors other than the dihedral angle α. These factors (Fig. 5.8) include the bond length R_{CC}, the valence angles θ_1 and θ_2, and the electronegativity of any substituents X attached to the carbon atoms.
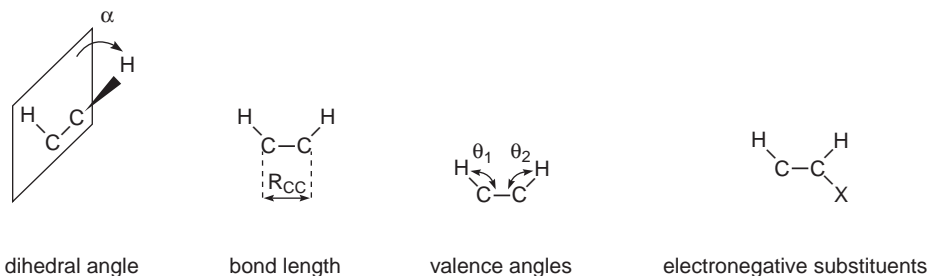
FIGURE 5.8 Factors influencing the magnitude of $^3J_{HH}$.

In any hydrocarbon, the magnitude of interaction between any two adjacent C–H bonds is always close to the values given in Figure 5.7. Cyclohexane derivatives that are conformationally biased are the best illustrative examples of this principle. In the following molecule, the ring is substantially biased to favor the conformation with the bulky *tert*-butyl group in an equatorial position. The coupling constant between two axial hydrogens J_{aa} is normally 10 to 14 Hz ($\alpha = 180°$), whereas the magnitude of interaction between an axial hydrogen and an equatorial hydrogen J_{ae} is generally 2 to 6 Hz ($\alpha = 60°$). A diequatorial interaction also has $J_{ee} = 2$ to 5 Hz ($\alpha = 60°$), but the equatorial-equatorial vicinal coupling constant (J_{ae}) is usually about 1 Hz smaller than the axial-equatorial vicinal coupling constant (J_{ae}) in the same ring system. For cyclohexane derivatives that have more than one solution conformation at room temperature, the observed coupling constants will be the weighted average of the coupling constants for each individual conformation (Fig. 5.9). Cyclopropane derivatives and epoxides are examples of conformationally rigid systems. Notice that J_{cis} ($\alpha = 0°$) is larger than J_{trans} ($\alpha = 120°$) in three-membered rings (Fig. 5.10).

Table 5.4 lists some representative three-bond coupling constants. Notice that in the alkenes the *trans* coupling constant is always larger than the *cis* coupling constant. Spin–spin coupling in alkenes will be discussed in further detail in Sections 5.8 and 5.9. In Table 5.5, an interesting variation is seen with ring size in cyclic alkenes. Larger HCH valence angles in the smaller ring sizes result in smaller coupling constants ($^3J_{HH}$).
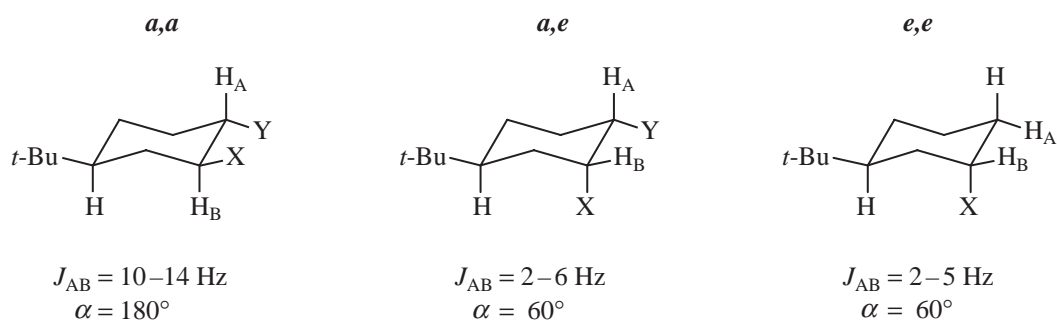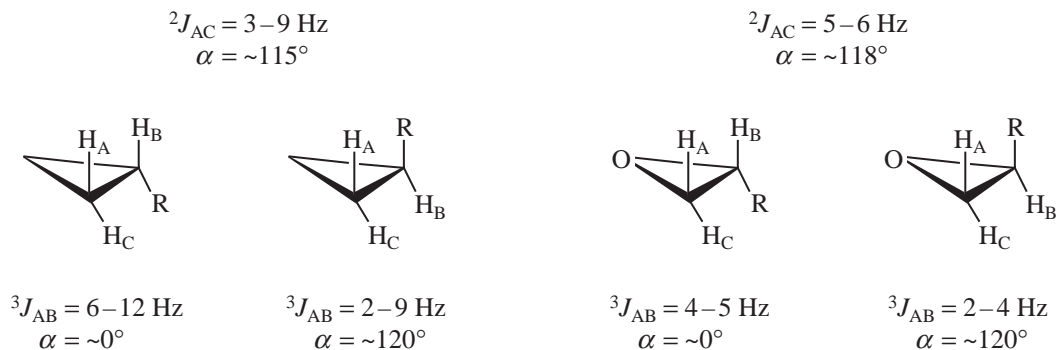

FIGURE 5.9 Vicinal couplings in cyclohexane derivatives.

For three-membered rings, $J_{cis} > J_{trans}$

FIGURE 5.10 Vicinal couplings in three-membered ring derivatives.

TABLE 5.4
SOME THREE-BOND COUPLING CONSTANTS ($^3J_{XY}$)

H–C–C–H	6–8 Hz	H–C=C–H	*cis*	6–15 Hz
			trans	11–18 Hz
^{13}C–C–C–H	5 Hz	H–C=C–^{19}F	*cis*	18 Hz
			trans	40 Hz
^{19}F–C–C–H	5–20 Hz	^{19}F–C=C–^{19}F	*cis*	30–40 Hz
			trans	–120 Hz
^{19}F–C–C–^{19}F	–3 to –20			
^{31}P–C–C–H	13 Hz			
^{31}P–O–C–H	5–15 Hz			

TABLE 5.5
VARIATION OF $^3J_{HH}$ WITH VALENCE ANGLES IN CYCLIC ALKENES (Hz)

| 0–2 | 2–4 | 5–7 | 8–11 | 6–15 |

D. Long-Range Couplings (^4J–^nJ)

As discussed above, proton–proton coupling is normally observed between protons on *adjacent* atoms (vicinal coupling) and is sometimes observed between protons on the *same* atom (geminal coupling), provided the protons in question are nonequivalent. Only under special circumstances does coupling occur between protons that are separated by four or more covalent bonds, and these are collectively referred to as **long-range couplings.** Long-range couplings are common in allylic systems, aromatic rings, and rigid bicyclic systems. Long-range coupling in aromatic systems will be covered in Section 5.10.

Long-range couplings are communicated through specific overlap of a series of orbitals and as a result have a stereochemical requirement. In alkenes, small couplings between the alkenyl hydrogens and protons on the carbon(s) α to the opposite end of the double bond are observed:

$|^4J_{ad}| = 0$ - 3 Hz
$|^4J_{bd}| = 0$ - 3 Hz
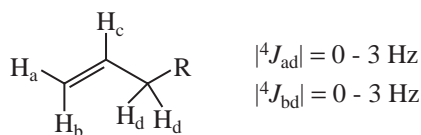
This four-bond coupling (^4J) is called **allylic coupling.** The π electrons of the double bond help to transmit the spin information from one nucleus to the other, as shown in Figure 5.11. When the allylic C–H bond is aligned with the plane of the C–C π bond, there is maximum overlap between
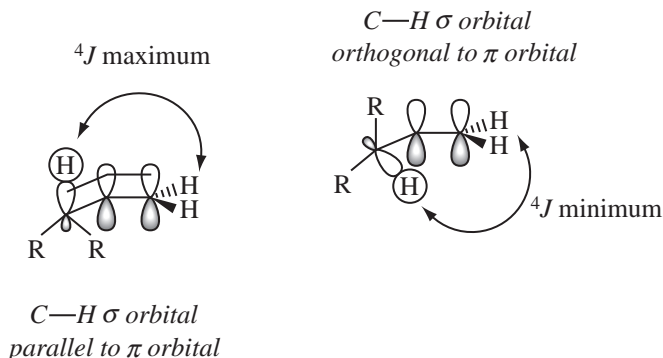
FIGURE 5.11 Geometric arrangements that maximize and minimize allylic coupling.

the allylic C—H σ orbital and the π orbital, and the allylic coupling interaction assumes the maximum value ($^4J = 3$–4 Hz). When the allylic C—H bond is perpendicular to the C—C π bond, there is *minimum* overlap between the allylic C—H σ orbital and the π orbital, and the allylic coupling is very small ($^4J = {\sim}0$ Hz). At intermediate conformations, there is partial overlap of the allylic C—H bond with the π orbital, and intermediate values for ^4J are observed.

In alkenes, the magnitude of allylic coupling (^4J) depends on the extent of overlap of the carbon–hydrogen σ bond with the π bond. A similar type of interaction occurs in alkynes, but with an important difference. In the case of **propargylic coupling** (Fig. 5.12), a C—H σ orbital on the carbon α to the triple bond *always* has partial overlap with the alkyne π system because the triple bond consists of two perpendicular π bonds, effectively creating a cylinder of electron density surrounding the C—C internuclear axis.

In some alkenes, coupling can occur between the C—H σ bonds on either side of the double bond. This **homoallylic coupling** occurs over five bonds (^5J) but is naturally weaker than allylic coupling (^4J) because it occurs over a greater distance. Homoallylic coupling is generally not observed except when *both* C—H σ bonds on either side of the double bond are parallel to the π orbital of the double bond *simultaneously* (Fig. 5.13). This is common when two allylic methyl groups are interacting because of the inherent threefold symmetry of the CH_3 group—one of the C—H σ bonds will be partially overlapped with the alkene π bond at all times. For larger or branched alkene substituents, however, the conformations that allow such overlap suffer from significant steric strain ($A^{1,3}$ strain) and are unlikely to be a significant contribution to the solution structure of such compounds, unless other, more significant, constraints are present, such as rings or steric congestion elsewhere in the molecule. For example, 1,4-cyclohexadiene and 6-methyl-3,4-dihydro-2H-pyran both have fairly large homoallylic couplings (^5J, Fig. 5.13). Allenes are also effective at communicating spin–spin splitting over long distances in a type of homoallylic coupling. An example is 1,1-dimethylallene, where $^5J = 3$ Hz (Fig. 5.13).

Unlike the situation for homoallylic coupling in most acyclic alkenes, **homopropargylic coupling** is almost always observed in the ^1H NMR spectra of internal alkynes. As we saw above, essentially all conformations of the C—H σ bond on the carbon α to the triple bond allow for partial overlap with the π system of the alkyne, resulting in coupling constants significantly larger than those observed for
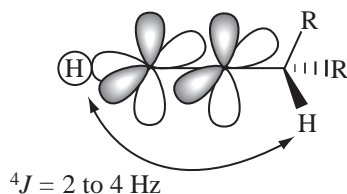

$^4J = 2$ to 4 Hz

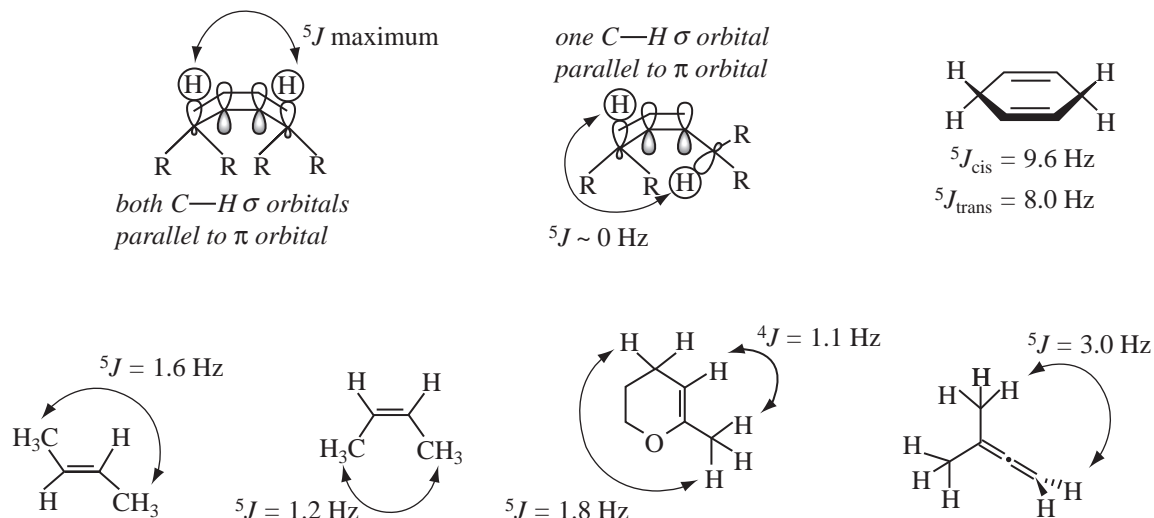**FIGURE 5.12** Propargylic coupling.

F I G U R E 5 . 1 3 Homoallylic coupling in alkenes and allenes.

homoallylic coupling (Fig. 5.14). In conjugated enyne compounds, ^6J is often observed, a result of combination homoallylic/propargylic coupling.

Long-range couplings in compounds without π systems are less common but do occur in special cases. One case of long-range coupling in saturated systems occurs through a rigid arrangement of bonds in the form of a W (^4J), with hydrogens occupying the end positions. Two possible types of orbital overlap have been suggested to explain this type of coupling (Fig. 5.15). The magnitude of ^4J for **W coupling** is usually small except in highly strained ring systems in which the rigid structures reinforce the favorable geometry for the overlaps involved (Fig. 5.16).
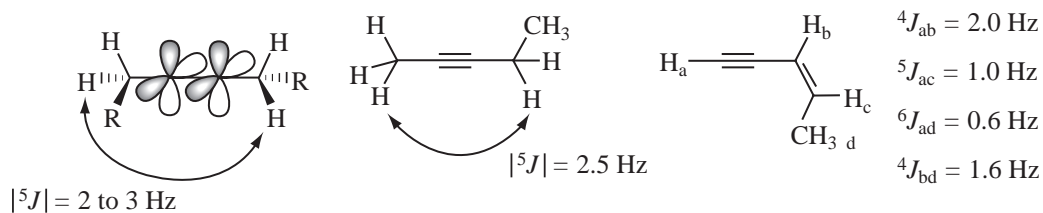
F I G U R E 5 . 1 4 Homopropargylic coupling in alkynes.
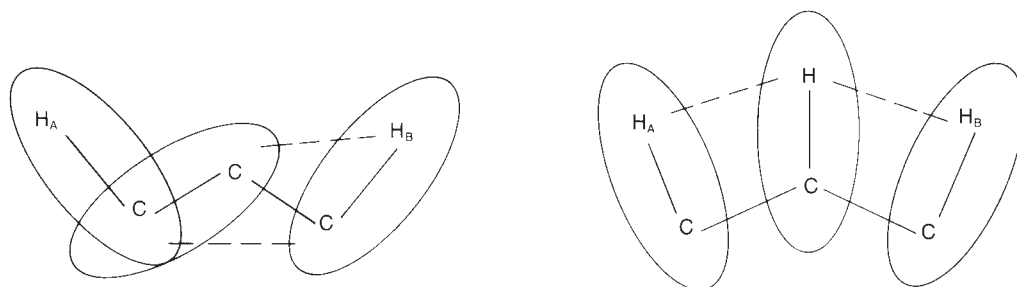
F I G U R E 5 . 1 5 Possible orbital overlap mechanisms to explain ^4J W coupling.
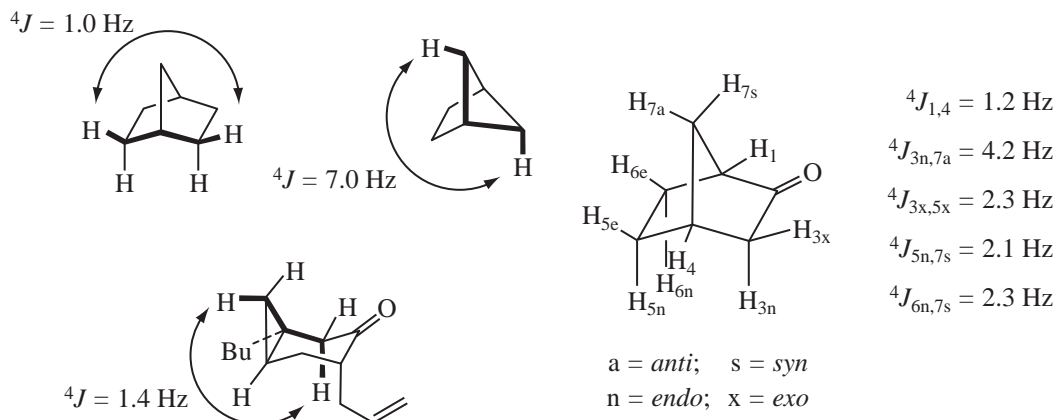
FIGURE 5.16 Examples of ^4J W coupling in rigid bicyclic compounds.
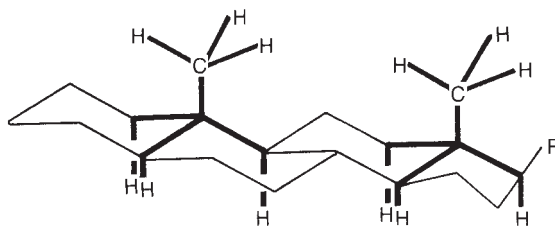
**FIGURE 5.17** A steroid ring skeleton showing several possible W couplings (^4J).

In other systems, the magnitude of ^4J is often less than 1 Hz and is not resolved even on high-field spectrometers. Peaks that have spacings less than the resolving capabilities of the spectrometer are usually broadened; that is, two lines very close to each other appear as a single "fat," or broad, peak. Many W couplings are of this type, and small allylic couplings ($^4J < 1$ Hz) can also give rise to peak broadening rather than discrete splitting. Angular methyl groups in steroids and those at the ring junctions in *trans*-decalin systems often exhibit peak broadening due to W coupling with several hydrogens of the ring (Fig. 5.17). Because these systems are relatively unstrained, ^4J_w is usually quite small.

☐ 5.3 MAGNETIC EQUIVALENCE

In Chapter 3, Section 3.8, we discussed the idea of chemical equivalence. If a plane of symmetry or an axis of symmetry renders two or more nuclei equivalent by symmetry, they are said to be **chemically equivalent.**

In acetone, a plane of symmetry (and a C_2 axis) renders the two methyl groups chemically equivalent. The two methyl carbon atoms yield a single peak in the ^{13}C NMR spectrum. In addition, free rotation of the methyl group around the C—C bond ensures that all six hydrogen atoms are equivalent and resonate at the same frequency, producing a singlet in the ^1H NMR spectrum. In l,2-dichloroethane, there is also a plane of symmetry, rendering the two methylene (CH$_2$) groups equivalent. Even though the hydrogens on these two carbon atoms are close enough for vicinal (three-bond) coupling ^3J, all four hydrogens appear as a single peak in the ^1H NMR spectrum, and no spin–spin splitting is seen. In fumaric acid, there is a twofold axis of symmetry that renders

the carbons and hydrogens chemically equivalent. Because of symmetry, the adjacent *trans* vinyl hydrogens in fumaric acid do not show spin–spin splitting, and they appear as a singlet (both hydrogens having the same resonance frequency). The two ring hydrogens and methyl groups in *trans*-2,3-dimethylcyclopropanone (axis of symmetry) are also chemically equivalent, as are the two ring hydrogens and methyl groups in *cis*-2,3-dimethylcyclopropanone (plane of symmetry).

plane of symmetry

plane of symmetry

axis of symmetry

fumaric acid

axis of symmetry

plane of symmetry
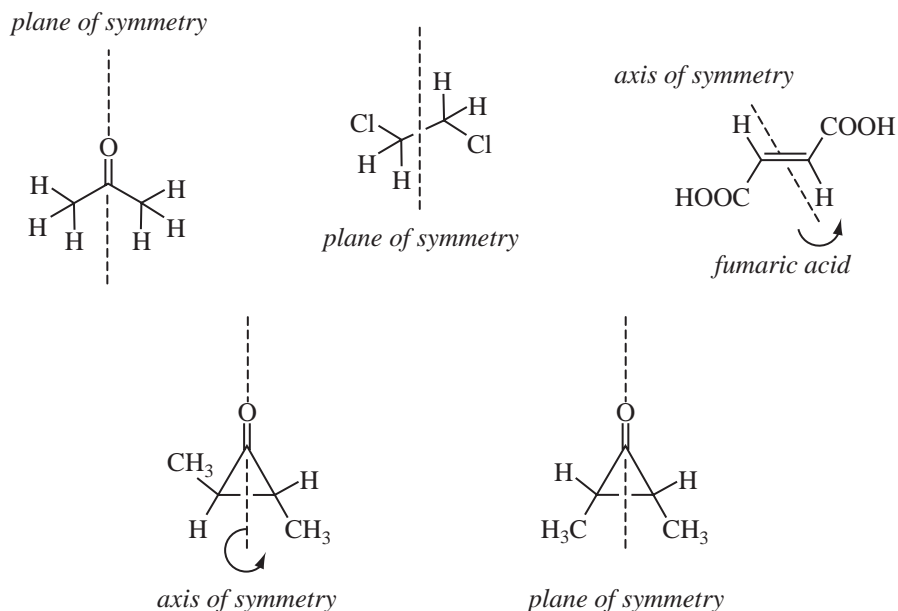
In most cases, chemically equivalent nuclei have the same resonance frequency (chemical shift), do not split each other, and give a single NMR signal. When this happens, the nuclei are said to be **magnetically equivalent** as well as chemically equivalent. However, it is possible for nuclei to be chemically equivalent but magnetically *inequivalent.* As we will show, magnetic equivalence has requirements that are more stringent than those for chemical equivalence. For a group of nuclei to be magnetically equivalent, their magnetic environments, including *all coupling interactions*, must be of identical types. Magnetic equivalence has two strict requirements:

1. Magnetically equivalent nuclei must be **isochronous;** that is, they must have identical chemical shifts.

   and

2. Magnetically equivalent nuclei must have equal coupling (same *J* values) to all other nuclei in the molecule.

A corollary that follows from magnetic equivalence is that magnetically equivalent nuclei, even if they are close enough to be coupled, do not split one another, and they give only one signal (for both nuclei) in the NMR spectrum. This corollary does not imply that no coupling occurs between magnetically equivalent nuclei; it means only that no observable spin–spin splitting results from the coupling.

Some simple examples will help you understand these requirements. In chloromethane, all of the hydrogens of the methyl group are chemically and magnetically equivalent because of the threefold axis of symmetry (coincident with the C—Cl bond axis) and three planes of symmetry (each containing one hydrogen and the C—Cl bond) in this molecule. In addition, the methyl group rotates

freely about the C−Cl axis. Taken alone, this rotation would ensure that all three hydrogens experience the same *average* magnetic environment. The three hydrogens in chloromethane give a single resonance in the NMR (they are isochronous). Because there are no adjacent hydrogens in this one-carbon compound, by default all three hydrogens are equally coupled to all adjacent nuclei (a null set) and equally coupled to each other.
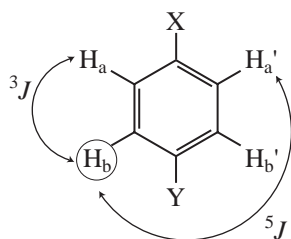
When a molecule has a plane of symmetry that divides it into equivalent halves, the observed spectrum is that for "half" of the molecule. The ^{1}H NMR spectrum of 3-pentanone shows only one quartet (CH_2 with three neighbors) and one triplet (CH_3 with two neighbors). A plane of symmetry renders the two ethyl groups equivalent; that is, the two methyl groups are chemically equivalent, and the two methylene groups are chemically equivalent. The coupling of any of the hydrogens in the methyl group to any of the hydrogens in the methylene group (^3J) is also equivalent (due to free rotation), and the coupling is the same on one "half" of the molecule as on the other. Each type of hydrogen is chemically equivalent.

$$3\text{-Pentanone} \quad CH_3CH_2 \overset{\overset{\displaystyle O}{\displaystyle \|}}{-C} -CH_2CH_3$$

Now, consider a *para*-disubstituted benzene ring, in which the *para* substituents X and Y are not the same. This molecule has a plane of symmetry that renders the hydrogens on opposite sides of the ring chemically equivalent. You might expect the ^{1}H spectrum to be that of one-half of the molecule—two doublets. It is not, however, since the corresponding hydrogens in this molecule are not *magnetically equivalent.* Let us label the chemically equivalent hydrogens H_a and H_a' (and H_b and H_b'). We would expect both H_a and H_a' or H_b and H_b' to have the same chemical shift (be isochronous), but *their coupling constants to the other nuclei are not the same.* H_a, for instance, does not have the same coupling constant to H_b (three bonds, ^3J) as H_a' has to H_b (five bonds, ^5J). Because H_a and H_a' do not have the same coupling constant to H_b, they cannot be magnetically equivalent, even though they are chemically equivalent. This analysis also applies to H_a', H_b, and H_b', none of which has equivalent couplings to the other hydrogens in the molecule.

Why is this subtle difference between the two kinds of equivalence important? Often, protons that are chemically equivalent are also magnetically equivalent; however, when chemically equivalent protons are *not* magnetically equivalent, there are usually consequences in the appearance of the NMR spectrum. Nuclei that are magnetically equivalent will give "first-order spectra" that can be analyzed using the $n + 1$ Rule or a simple "tree diagram" (Section 5.5). Nuclei that are not magnetically equivalent sometimes give second-order spectra, in which unexpected peaks may appear in multiplets (Section 5.7).

A simpler case than benzene, which has chemical equivalence (due to symmetry) but not magnetic equivalence, is 1,1-difluoroethene. Both hydrogens couple to the fluorines (^{19}F, $I = \frac{1}{2}$); how-


para-Disubstituted benzene   1, 1-Difluoroethene
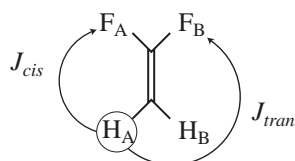
ever, the two hydrogens are not magnetically equivalent because H_a and H_b do not couple to F_a with the same coupling constant ($^3J_{HF}$). One of these couplings is *cis* ($^3J_{cis}$), and the other is *trans* ($^3J_{trans}$). In Table 5.4, it was shown that *cis* and *trans* coupling constants in alkenes were different in magnitude, with $^3J_{trans}$ having the larger value. Because these hydrogens have *different coupling constants to the same atom,* they cannot be magnetically equivalent. A similar argument applies to the two fluorine atoms, which also are magnetically inequivalent.

Now consider 1-chloropropane. The hydrogens within a group (those on C1, C2, and C3) are isochronous, but each group is on a different carbon, and as a result, each *group* of hydrogens has a different chemical shift. The hydrogens in each group experience identical *average* magnetic environments, mainly because of free rotation, and are magnetically equivalent. Furthermore, also because of rotation, the hydrogens in each group are equally coupled to the hydrogens in the other groups. If we consider the two hydrogens on C2, H_b and H_b' and pick any other hydrogen on either C1 or C3, both H_b and H_b' will have the same coupling constant to the designated hydrogen. Without free rotation (see the preceding illustration) there would be no magnetic equivalence. Because of the fixed unequal dihedral angles ($H_a-C-C-C_b$ versus $H_a-C-C-H_b'$), J_{ab} and J_{ab}' would not be the same. Free rotation can be slowed or stopped by lowering the temperature, in which case H_b and H_b' would become magnetically inequivalent. This type of magnetic inequivalence is often seen in 1,2-disubstituted ethane groups in which the substituents have sufficient steric bulk to hinder free rotation around the C–C axis enough that it becomes slow on the NMR time-scale.

1-Chloropropane $CH_3-CH_2-CH_2-Cl$
            c   **b**   **a**

If conformation is locked (no rotation)
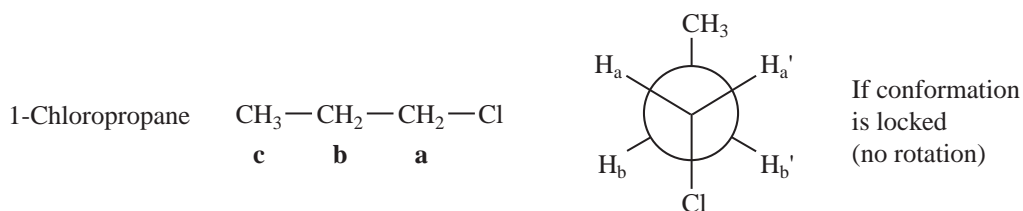
As one can see, it is a frequent occurrence that one needs to determine whether two groups attached to the same carbon (geminal groups) are equivalent or nonequivalent. Methylene groups (geminal protons) and isopropyl groups (geminal methyl groups) are frequently the subjects of interest. It turns out that there are three possible relationships for such geminal groups: They can be homotopic, enantiotopic, or diastereotopic.

Methylene group: Geminal dimethyl group:
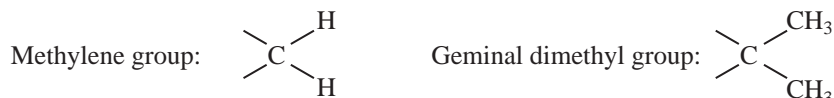
Homotopic groups are always equivalent, and in the absence of couplings from another group of nuclei, they are isochronous and give a single NMR absorption. Homotopic groups are interchangeable by rotational symmetry. The simplest way to recognize homotopic groups is by means of a substitution test. In this test, first one member of the group is substituted for a different group, then the other is substituted in the same fashion. The results of the substitution are examined to see the relationship of the resulting new structures. If the new structures are *identical*, the two original groups are homotopic. Figure 5.18a shows the substitution procedure for a molecule with two

Replace H_A   *Replace H_B*
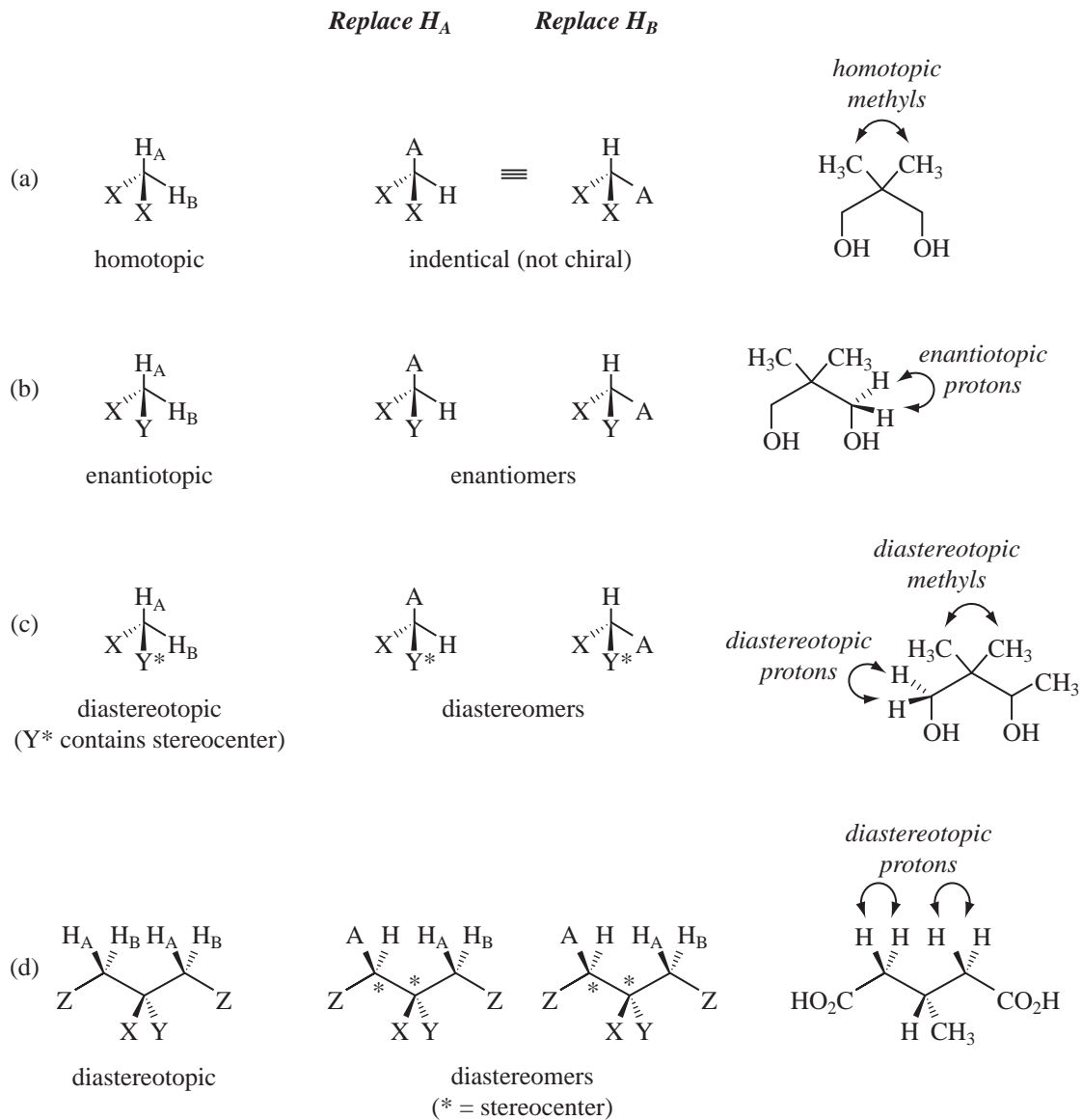
FIGURE 5.18 Replacement tests for homotopic, enantiotopic, and diastereotopic groups.

homotopic methylene hydrogens. In this molecule, the structures resulting from the replacement of first H_A and then H_B are identical. Notice that for this homotopic molecule, the substituents X are the same. The starting compound is completely symmetric because it has both a plane and a twofold axis of symmetry.

Enantiotopic groups appear to be equivalent, and they are typically isochronous and give a single NMR absorption—except when they are placed in a chiral environment or acted on by a chiral reagent. Enantiotopic groups can also be recognized by the substitution test. Figure 5.18b shows the substitution procedure for a molecule with two enantiotopic methylene hydrogens. In this molecule, the resultant structures from the replacement of first H_A and then H_B are *enantiomers*. Although

these two hydrogens appear to be equivalent and are isochronous in a typical NMR spectrum, they are not equivalent on replacement, each hydrogen giving a different enantiomer. Notice that the structure of this enantiotopic molecule is not chiral, but that substituents X and Y are different groups. There is a *plane* of symmetry, but no rotational axis of symmetry. Enantiotopic groups are sometimes called **prochiral** groups. When one or the other of these groups is replaced by a different one, a *chiral* molecule results. The reaction of prochiral molecules with a chiral reagent, such as an enzyme in a biological system, produces a chiral result. If these molecules are placed in a chiral environment, the two groups are no longer equivalent. We will examine a chiral environment induced by chiral shift reagents in Chapter 6 (Section 6.9).

   Diastereotopic groups are not equivalent and are not isochronous; they have different chemical shifts in the NMR spectrum. When the diastereotopic groups are hydrogens, they frequently split each other with a geminal coupling constant ^2J. Figure 5.18c shows the substitution procedure for a molecule with two diastereotopic hydrogens. In this molecule, the replacement of first H_A and then H_B yields a pair of *diastereomers*. Diastereomers are produced when substituent Y* already contains an adjacent stereocenter. Diastereotopic groups are also found in prochiral compounds in which the substitution test simultaneously creates two stereogenic centers (Figure 5.18d). Section 5.4 covers both types of diastereotopic situations in detail.

5.4 SPECTRA OF DIASTEREOTOPIC SYSTEMS

In this section, we examine some molecules that have diastereotopic groups (discussed in Section 5.3). Diastereotopic groups are not equivalent, and two different NMR signals are observed. The most common instance of diastereotopic groups is when two similar groups, G and G', are substituents on a carbon *adjacent to a stereocenter*. If first group G and then group G' are replaced by another group, a pair of diastereomers forms (see Fig. 5.18c).[2]
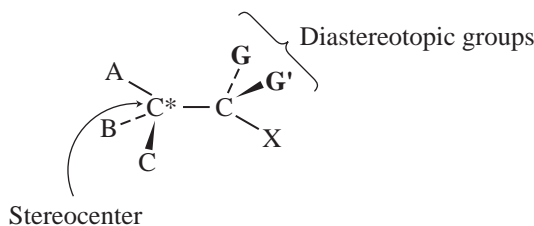
A. Diastereotopic Methyl Groups: 4-Methyl-2-pentanol

As a first example, examine the ^{13}C and ^1H NMR spectra of 4-methyl-2-pentanol in Figures 5.19 and 5.20, respectively. This molecule has diastereotopic methyl groups (labeled 5 and 5') on carbon 4. First, examine the ^{13}C spectrum in Figure 5.19. If this compound did not have diastereotopic groups, we would expect only two different peaks for methyl carbons as there are only two chemically distinct types of methyl groups. However, the spectrum shows three methyl peaks. A very closely spaced pair of resonances is observed at 23.18 and 22.37 ppm, representing the diastereotopic methyl groups, and a third resonance at 23.99 ppm from the C-1 methyl group. There are two peaks for the geminal dimethyl groups! Carbon 4, to which the methyl groups are attached, is seen at 24.8 ppm,

---

[2] Note that groups farther down the chain are also diastereotopic, but the effect becomes smaller as the distance from the stereocenter increases and eventually becomes unobservable. Note also that it is not essential that the stereocenter be a carbon atom.
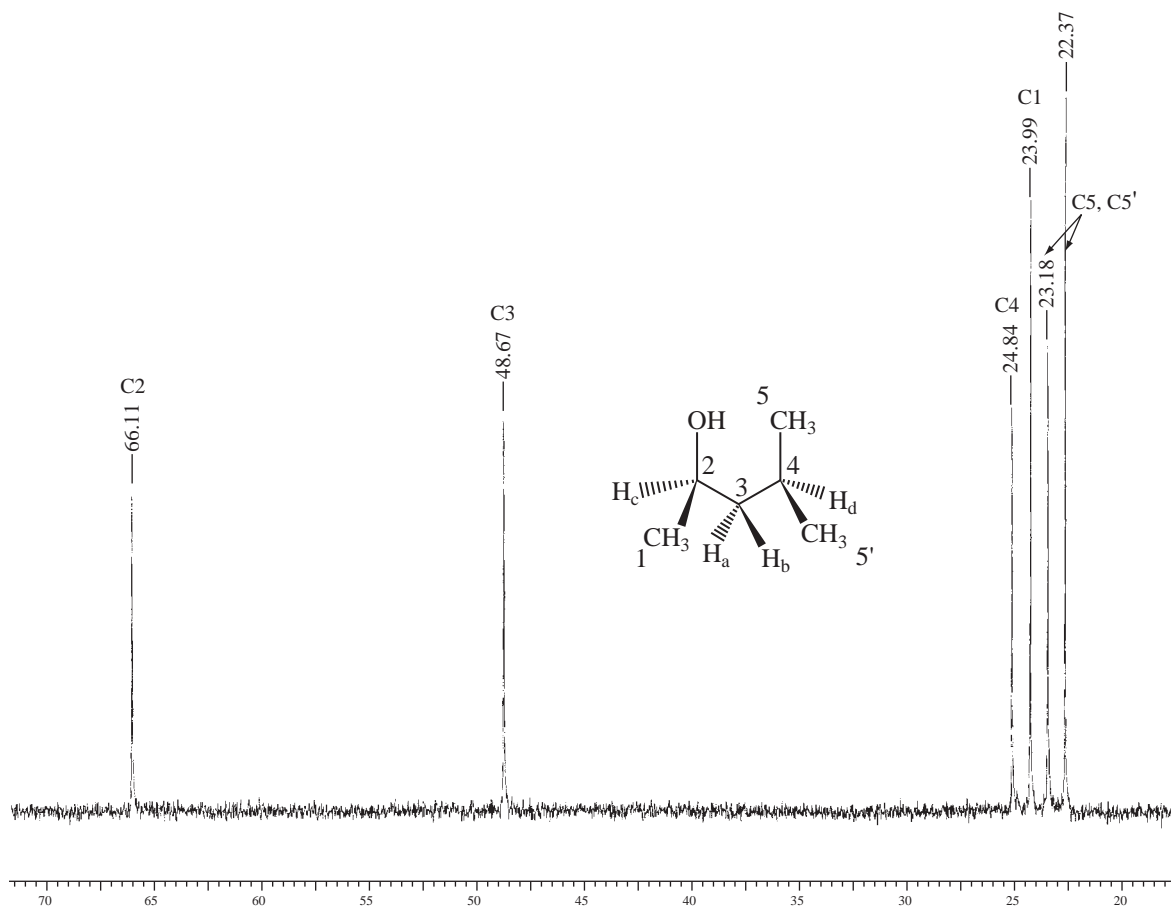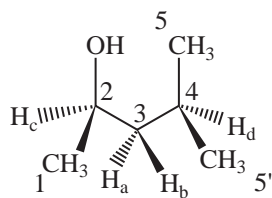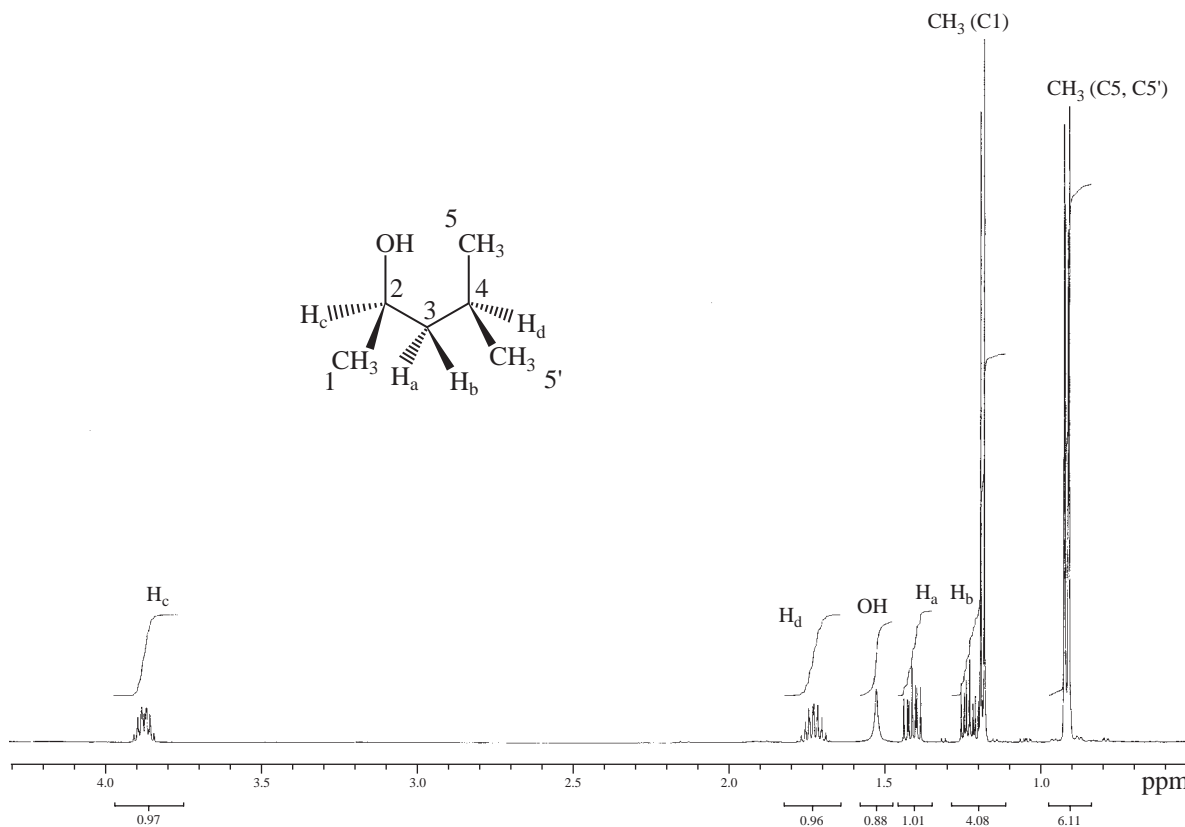
FIGURE 5.19 ^{13}C spectrum of 4-methyl-2-pentanol showing diastereotopic methyl groups.

carbon 3 is at 48.7 ppm, and carbon 2, which has the deshielding hydroxyl attached, is observed downfield at 66.1 ppm.


4-methyl-2-pentanol

The two methyl groups have slightly different chemical shifts because of the nearby stereocenter at C-2. The two methyl groups are always nonequivalent in this molecule, even in the presence of free rotation. You can confirm this fact by examining the various fixed, staggered rotational

FIGURE 5.20 ^{1}H spectrum of 4-methyl-2-pentanol showing diastereotopic methyl and methylene groups (500 MHz, CDCL$_3$).

conformations using Newman projections. There are no planes of symmetry in any of these conformations; neither of the methyl groups is ever enantiomeric.
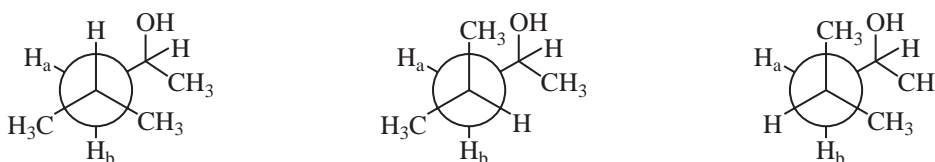
The ^{1}H proton NMR spectrum (Figs. 5.20 and 5.21) is a bit more complicated, but just as the two diastereotopic methyl carbons have different chemical shifts, so do the diastereotopic methyl hydrogens. The hydrogen atom attached to C-4 splits each methyl group into a doublet. The chemical shift difference between the methyl protons is very small, however, and the two doublets are partially overlapped. One of the methyl doublets is observed at 0.92 ppm (J = 6.8 Hz), and the other diastereotopic methyl doublet is seen at 0.91 ppm (J = 6.8 Hz). The C-1 methyl group is also a doublet at 1.18 ppm, split by the hydrogen on C-2 (J = 5.9 Hz).

B.   Diastereotopic Hydrogens: 4-Methyl-2-pentanol

As with diastereotopic methyl groups, a pair of hydrogens located on a carbon atom adjacent to a stereocenter is expected to be diastereotopic. In some compounds expected to have diastereotopic hydrogens, the difference between the chemical shifts of the diastereotopic geminal hydrogens H_A and H_B is so small that neither this difference nor any coupling between H_A and H_B is easily

CH₃ (C1)

594.92
589.06

CH₃ (C5, C5')

461.68
460.22
454.85
453.39

1.15   1.10   1.05   1.00   0.95   0.90   ppm
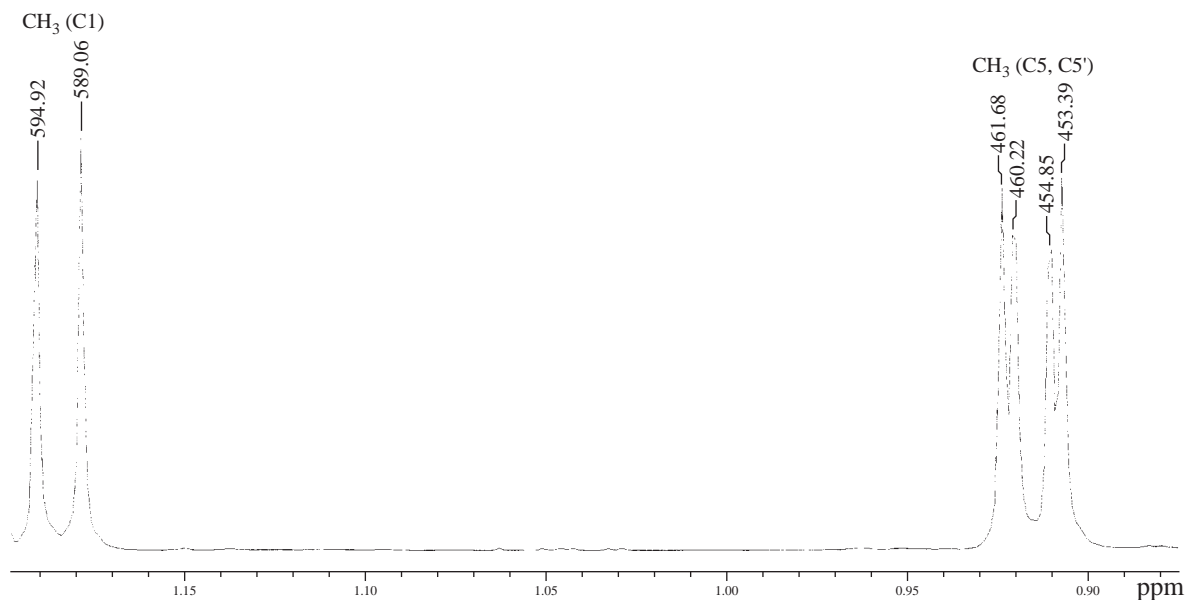
FIGURE 5.21   Upfield region of the ¹H spectrum of 4-methyl-2-pentanol showing diastereotopic methyl groups.

detectable. In this case, the two protons act as a single group. In many other compounds, however, the chemical shifts of H_A and H_B are quite different, and they split each other ($^2J_{AB}$) into doublets. If there are other adjacent protons, large differences in the magnitude of the vicinal coupling constants are seen as well due to unequal populations of conformers arising from differential steric and torsional strain.

Figure 5.22 is an expansion from the ¹H NMR spectrum of 4-methyl-2-pentanol, showing the diastereotopic hydrogens on C-3 in order to make the splitting patterns clear. Figure 5.23 is an

886.28
879.44
877.98
873.10
871.63
866.75
864.80
860.41
858.46
853.58
852.11
845.28

H_d

OH

763.29

H_a

718.39
712.53
710.09
704.73
698.87
696.43
690.57

H_b

625.66
620.78
617.37
612.00
607.12
603.70
598.82

1.80   1.75   1.70   1.65   1.60   1.55   1.50   1.45   1.40   1.35   1.30   1.25   ppm
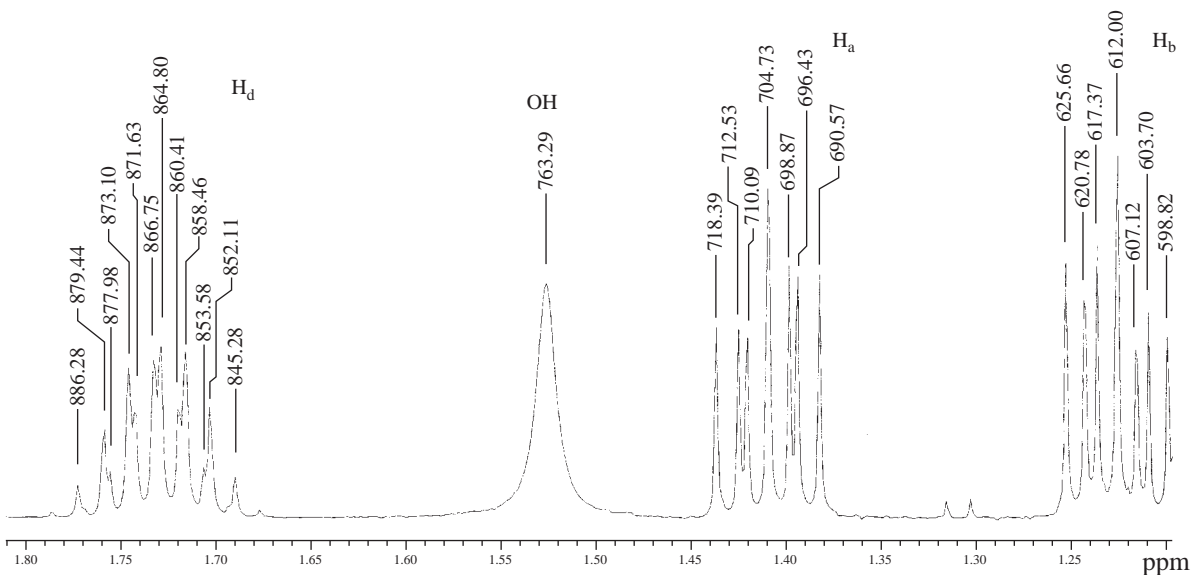
FIGURE 5.22   Expansion of the ¹H spectrum of 4-methyl-2-pentanol showing diastereotopic methylene protons.
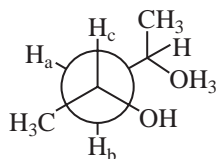
lowest energy conformation
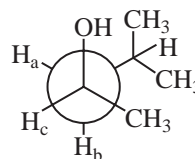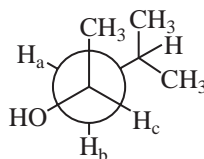
highest energy conformation

4-methyl-2-pentanol

δ 1.41 ppm

δ 1.22 ppm
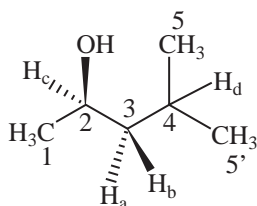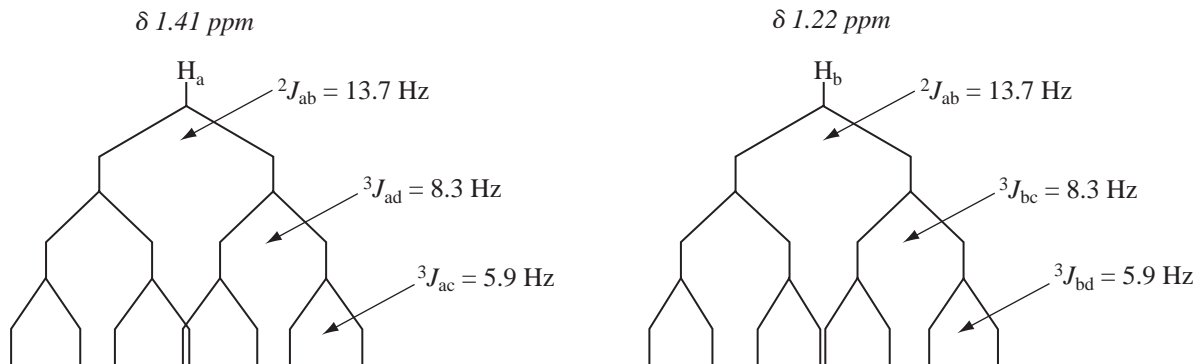
FIGURE 5.23 Splitting diagrams for the diastereotopic methylene protons in 4-methyl-2-pentanol.

analysis of the diastereotopic protons H_a and H_b. The geminal coupling constant $^2J_{ab}$ = 13.7 Hz, which is a typical value for diastereotopic geminal coupling in acyclic aliphatic systems (Section 5.2B). The coupling constant $^3J_{bc}$ (8.3 Hz) is somewhat larger than $^3J_{ac}$ (5.9 Hz), which is in agreement with the average dihedral angles predicted from the relevant conformations and the Karplus relationship (Section 5.2C). The hydrogen on C-2, H_c, is coupled not only to H_a and H_b but also to the C-1 methyl group, with ^3J (H_cC-CH_3) = 5.9 Hz. Because of the more complex splitting of H_c, a splitting analysis tree is not shown for this proton. Similarly, the hydrogen on C-4 (seen at 1.74 ppm in Fig. 5.22) has a complex splitting pattern due to coupling to both H_a and H_b as well as the two sets of diastereotopic methyl protons on C-5 and C-5'. Measurement of coupling constants from complex first-order resonances like these is discussed in detail in Sections 5.5 and 5.6.

An interesting case of diastereotopic hydrogens is found in citric acid, shown in Figure 5.24. Citric acid is an achiral molecule, yet the methylene protons H_a and H_b are diastereotopic, and they not only have different chemical shifts, but they also split each other. This is an example illustrating the type of diastereotopic groups first shown in Figure 5.18d.

921.78   905.97   865.89   850.08

3.10   3.05   3.00   2.95   2.90   2.85   2.80

$^2J_{ab} = 15.8$ Hz
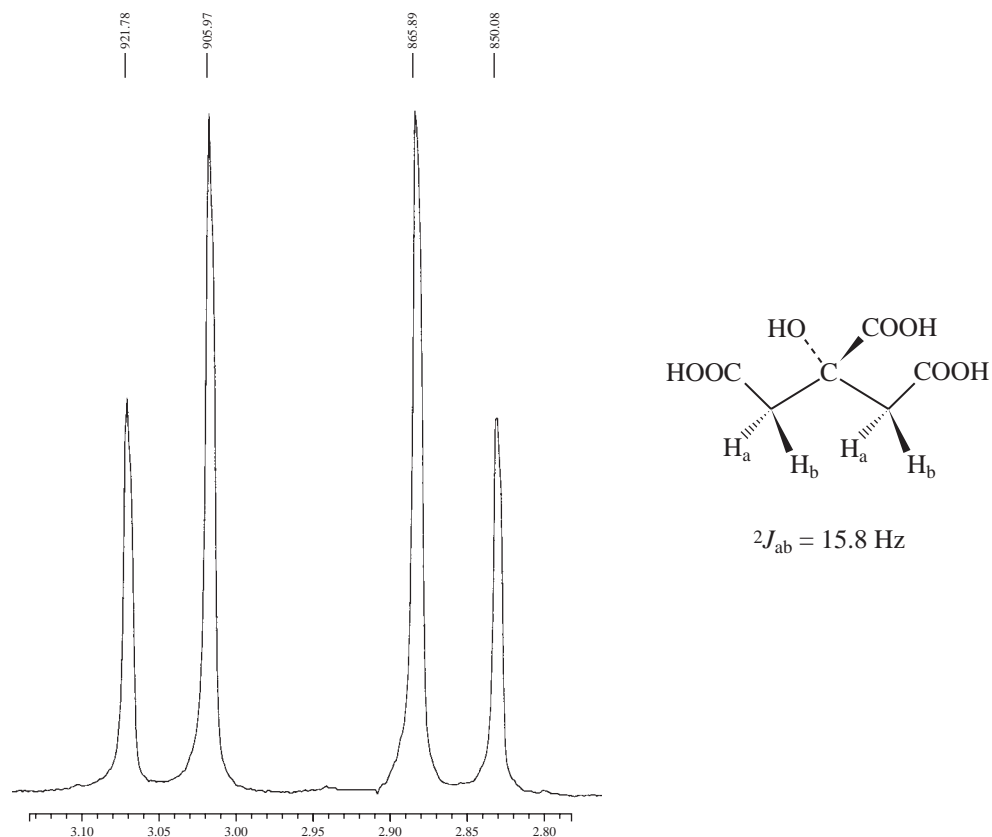
F I G U R E   5 . 2 4   The 300-MHz ^{1}H spectrum of the diastereotopic methylene protons in citric acid.

5.5 NONEQUIVALENCE WITHIN A GROUP—THE USE OF TREE DIAGRAMS WHEN THE *n* + 1 RULE FAILS

When the protons attached to a single carbon are chemically equivalent (have the same chemical shift), the *n* + 1 Rule successfully predicts the splitting patterns. In contrast, when the protons attached to a single carbon are chemically nonequivalent (have different chemical shifts), the *n* + 1 Rule no longer applies. We shall examine two cases, one in which the *n* +1 Rule applies (1,1,2-trichloroethane) and one in which it fails (styrene oxide).

Chapter 3, Section 3.13, and Figure 3.25 (p.131), addressed the spectrum of 1,1,2-trichloroethane. This symmetric molecule has a three-proton system, $-CH_2-CH-$ in which the methylene protons are equivalent. Due to free rotation around the C—C bond, the methylene protons each experience the same averaged environment, are isochronous (have the same chemical shift), and do not split each other. In addition, the rotation ensures that they both have the same averaged coupling constant *J* to the methine (CH) hydrogen. As a result, they behave as a group, and geminal coupling between them does not lead to any splitting. The *n* + 1 Rule correctly predicts a doublet for the CH_2 protons (one neighbor) and a triplet for the CH proton (two neighbors). Figure 5.25a illustrates the parameters for this molecule.

Figure 5.26, the ^{1}H spectrum of styrene oxide, shows how chemical nonequivalence complicates the spectrum. The three-membered ring prevents rotation, causing protons H_A and H_B to have different chemical shift values; they are chemically and magnetically inequivalent. Hydrogen H_A is on the same side of the ring as the phenyl group; hydrogen H_B is on the opposite side of the ring. These

(a) Free rotation
The *n* + 1 rule applies

$$\delta_A = \delta_B$$
$$J_{AC} = J_{BC'}$$
$$J_{AB} = 0$$

(b) Biased conformation
A tree diagram is required

$$\delta_A \neq \delta_B$$
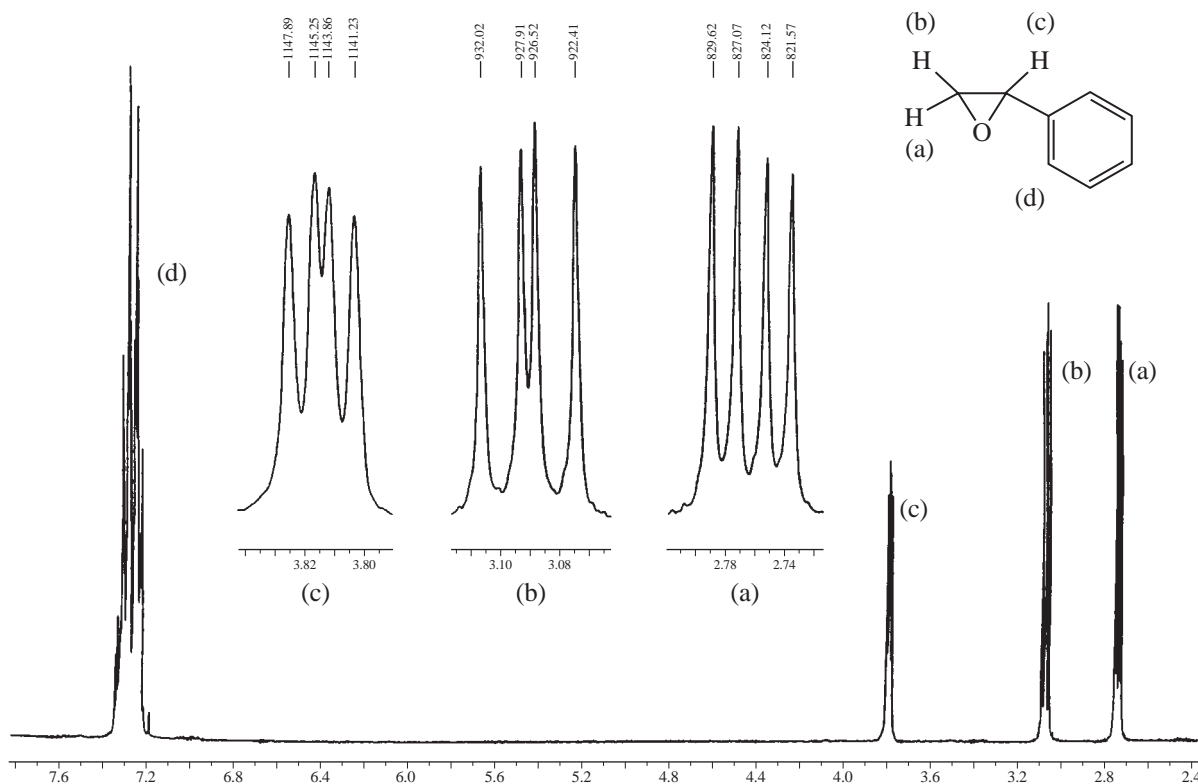$$J_{AC'} \neq J_{BC'}$$
$$J_{AB} \neq 0$$
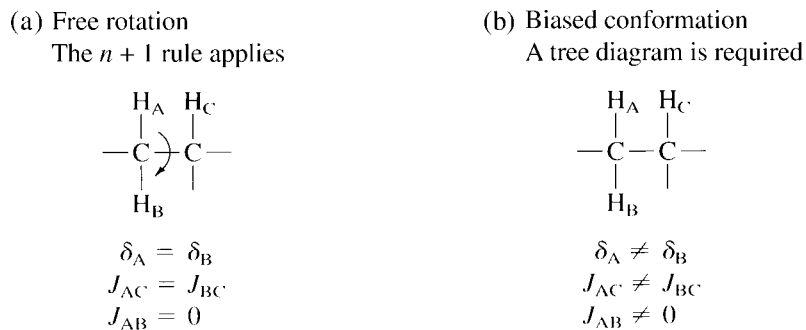
FIGURE 5.25   Two cases of splitting.

FIGURE 5.26   The ^{1}H NMR spectrum of styrene oxide.

hydrogens have different chemical shift values, H_A = 2.75 ppm and H_B = 3.09 ppm, and they show geminal splitting with respect to each other. The third proton, H_c, appears at 3.81 ppm and is coupled *differently* to H_A (which is *trans*) than to H_B (which is *cis*). Because H_A and H_B are nonequivalent and because H_c is coupled differently to H_A than to H_B ($^3J_{AC} \neq {}^3J_{BC}$), the *n* + 1 Rule fails, and the spectrum of styrene oxide becomes more complicated. To explain the spectrum, one must examine each hydrogen individually and take into account its coupling with every other hydrogen independent of the others. Figure 5.25b shows the parameters for this situation.
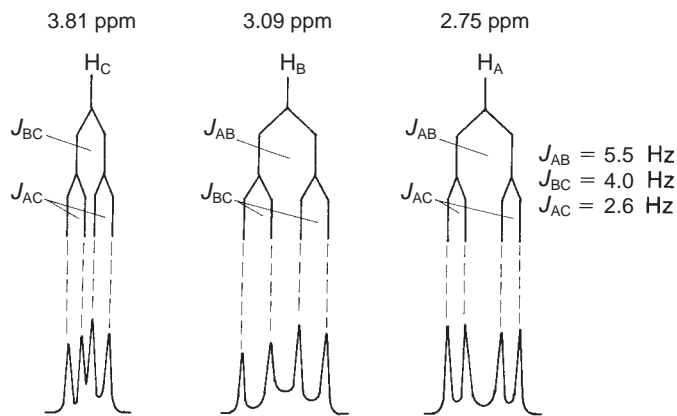
FIGURE 5.27 An analysis of the splitting pattern in styrene oxide.

An analysis of the splitting pattern in styrene oxide is carried out splitting-by-splitting with **graphical analyses, or tree diagrams** (Fig. 5.27). Begin with an examination of hydrogen H_C. First, the two possible spins of H_B split H_C ($^3J_{BC}$) into a doublet; second, H_A splits each of the doublet peaks ($^3J_{AC}$) into another doublet. The resulting pattern of two doublets is called a **doublet of doublets.** You may also look at the same splitting from H_A first and from H_B second. It is customary to *show the largest splitting first*, but it is not necessary to follow this convention to obtain the correct result. If the actual coupling constants are known, it is very convenient to perform this analysis (*to scale*) on graph paper with 1-mm squares.

Note that $^3J_{BC}$ (*cis*) is larger than $^3J_{AC}$ (*trans*). This is typical for small ring compounds in which there is more interaction between protons that are *cis* to each other than between protons that are *trans* to each other (see Section 5.2C and Fig. 5.10). Thus, we see that H_C gives rise to a set of *four* peaks (another doublet of doublets) centered at 3.81 ppm. Similarly, the resonances for H_A and H_B are each a doublet of doublets at 2.75 ppm and 3.09 ppm, respectively. Figure 5.27 also shows these splittings. Notice that the magnetically nonequivalent protons H_A and H_B give rise to geminal splitting ($^2J_{AB}$) that is quite significant.

As you see, the splitting situation becomes quite complicated for molecules that contain nonequivalent groups of hydrogens. In fact, you may ask, how can one be sure that the graphic analysis just given is the correct one? First, this analysis explains the entire pattern; second, it is internally consistent. Notice that the coupling constants have the same magnitude wherever they are used. Thus, in the analysis, $^3J_{BC}$ (*cis*) is given the same magnitude when it is used in splitting H_C as when it is used in splitting H_B. Similarly, $^3J_{AC}$ (*trans*) has the same magnitude in splitting H_C as in splitting H_A. The coupling constant $^2J_{AB}$ (geminal) has the same magnitude for H_A as for H_B. If this kind of self-consistency were not apparent in the analysis, the splitting analysis would have been incorrect. To complete the analysis, note that the NMR peak at 7.28 ppm is due to the protons of the phenyl ring. It integrates for five protons, while the other three multiplets integrate for one proton each.

We must sound one note of caution at this point. In some molecules, the splitting situation becomes so complicated that it is virtually impossible for the beginning student to derive it. Section 5.6 describes the process by which to determine coupling constants in greater detail to assist you. There are also situations involving apparently simple molecules for which a graphical analysis of the type we have just completed does not suffice (second-order spectra). Section 5.7 will describe a few of these cases.

We have now discussed three situations in which the $n + 1$ Rule fails: (1) when the coupling involves nuclei other than hydrogen that do not have spin = 1/2 (e.g., deuterium, Section 4.13), (2) when there is nonequivalence in a set of protons attached to the same carbon; and (3) when the chemical shift difference between two sets of protons is small compared to the coupling constant linking them (see Sections 5.7 and 5.8).

☐ 5.6 MEASURING COUPLING CONSTANTS FROM FIRST-ORDER SPECTRA

When one endeavors to measure the coupling constants from an actual spectrum, there is always some question of how to go about the task correctly. In this section, we will provide guidelines that will help you to approach this problem. The methods given here apply to first-order spectra; analysis of second-order spectra is discussed in Section 5.7. What does 'first-order' mean, as applied to NMR spectra? For a spectrum to be first-order, the frequency difference (Δv, in Hz) between any two coupled resonances must be significantly larger than the coupling constant that relates them. A first-order spectrum has $\Delta v/J > {\sim}6$.[3]

First-order resonances have a number of helpful characteristics, some of which are related to the number of individual couplings, n:

1. symmetry about the midpoint (chemical shift) of the multiplet. Note that a number of second-order patterns are also centrosymmetric, however (Section 5.7);

2. the maximum number of lines in the multiplet = 2^n; the actual number of lines is often less than the maximum number, though, due to overlap of lines arising from coincidental mathematical relationships among the individual J values;

3. the sum of the line intensities in the multiplet = 2^n;

4. the line intensities of the multiplet correspond to Pascal's triangle (Section 3.16);

5. the J values can be determined directly by measuring the appropriate line spacings in the multiplet;

6. the distance between the outermost lines in the multiplet is the sum of all the individual couplings, ΣJ.

A.   Simple Multiplets—One Value of *J* (One Coupling)

For simple multiplets, where only one value of J is involved (one coupling), there is little difficulty in measuring the coupling constant. In this case it is a simple matter of determining the spacing (in Hertz) between the successive peaks in the multiplet. This was discussed in Chapter 3, Section 3.17. Also discussed in that section was the method of converting differences in parts per million (ppm) to Hertz (Hz). The relationship

$$1 \text{ ppm (in Hertz)} = \text{Spectrometer Frequency in Hertz} \div 1{,}000{,}000$$

---

[3] The choice of $\Delta v/J > 6$ for a first-order spectrum is not a hard-and-fast rule. Some texts suggest a $\Delta v/J$ value of >10 for first-order spectra. In some cases, multiplets appear essentially first-order with $\Delta v/J$ values slightly less than 6.

TABLE 5.6
THE HERTZ EQUIVALENT OF A ppm UNIT AT
VARIOUS SPECTROMETER OPERATING FREQUENCIES

Spectrometer Frequency	Hertz Equivalent of 1 ppm
60 MHz	60 Hz
100 MHz	100 Hz
300 MHz	300 Hz
500 MHz	500 Hz

gives the simple correspondence values given in Table 5.6, which shows that if the spectrometer frequency is ***n* MHz,** one ppm of the resulting spectrum will be ***n* Hz.** This relationship allows an easy determination of the coupling constant linking two peaks when their chemical shifts are known only in ppm; just find the chemical shift difference in ppm and multiply by the Hertz equivalent.

The current processing software for most modern FT-NMR instruments allows the operator to display peak locations in both Hertz and ppm. Figure 5.28 is an example of the printed output from a modern 300-MHz FT-NMR. In this septet, the chemical shift values of the peaks (ppm) are obtained from the scale printed at the bottom of the spectrum, and the values of the peaks in Hertz are printed vertically above each peak. To obtain the coupling constant it is necessary only to subtract the Hertz values for the successive peaks. In doing this, however, you will note that not all of the differences are
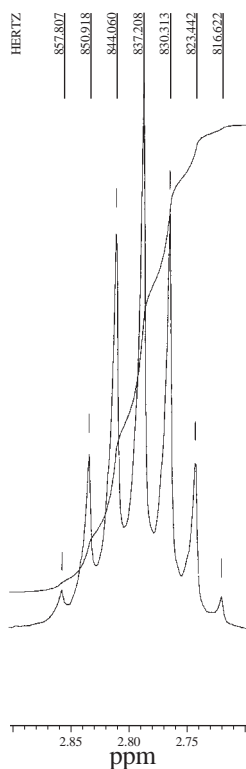
FIGURE 5.28 A septet determined at 300 MHz showing peak positions in ppm and Hz values.

TABLE 5.7
ANALYSIS OF FIRST-ORDER MULTIPLETS AS SERIES OF DOUBLETS

Number of Identical Couplings	Multiplet Appearance	Equivalent Series of Doublets	Sum of Line Intensities
1	d	d	2
2	t	dd	4
3	q	ddd	8
4	quintet (pentet)	dddd	16
5	sextet	ddddd	32
6	septet	dddddd	64
7	octet	ddddddd	128
8	nonet	dddddddd	256

identical. In this case (starting from the downfield side of the resonance) they are 6.889, 6.858, 6.852, 6.895, 6.871, and 6.820 Hz. There are two reasons for the inconsistencies. First, these values are given to more places than the appropriate number of significant figures would warrant. The inherent linewidth of the spectrum makes differences less than 0.1 Hz insignificant. When the above values are rounded off to the nearest 0.1 Hz, the line spacings are 6.9, 6.9, 6.9, 6.9, 6.9, and 6.8 Hz—excellent agreement. Second, the values given for the peaks are not always precise depending on the number of data points in the spectrum. If an insufficient number of points are recorded during the acquisition of the FID (large value of Hz/pt), the apex of a peak may not correspond exactly with a recorded data point and this situation results in a small chemical shift error.

When conflicting J values are determined for a multiplet it is usually appropriate to round them off to two significant figures, or to take an average of the similar values and round that average to two significant figures. For most purposes, it is sufficient if all the measured J values agree to <0.3 Hz difference. In the septet shown in Figure 5.28, the average of all the differences is 6.864 Hz, and an appropriate value for the coupling constant would be 6.9 Hz.

Before we consider multiplets with more than one distinct coupling relationship, it is helpful to review simple multiplets, those adequately described by the $n + 1$ Rule, and begin to consider them as series of doublets by considering each individual coupling relationship separately. For example, a triplet (t) can be considered a doublet of doublets (dd) where two identical couplings ($n = 2$) are present ($J_1 = J_2$). The sum of the triplet's line intensities (1:2:1) is equal to 2^n where $n = 2$ ($1 + 2 + 1$) $= 2^2 = 4$). Similarly, a quartet can be considered a doublet of doublet of doublets where three identical couplings ($n = 3$) are present ($J_1 = J_2 = J_3$) and the sum of the quartet's line intensities (1:3:3:1) equals 2^n where $n = 3$ ($1 + 3 + 3 + 1 = 2^3 = 8$). This analysis is continued in Table 5.7.

B.   Is the *n* + 1 Rule Ever *Really* Obeyed?

In a linear chain, the $n + 1$ Rule is strictly obeyed only if the vicinal inter-proton coupling constants (^3J) are *exactly the same* for every successive pair of carbons.

<div align="center">

(A)   (B)   (C)   (D)

—CH_2—CH_2—CH_2—CH_2—

$J_{AB} = J_{BC} = J_{CD}$, and so on
Condition under which the $n + 1$ Rule is strictly obeyed

</div>
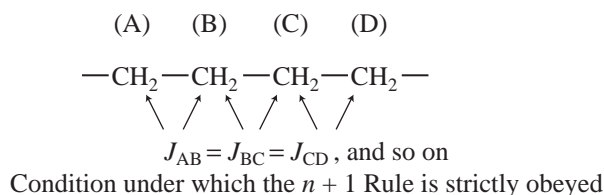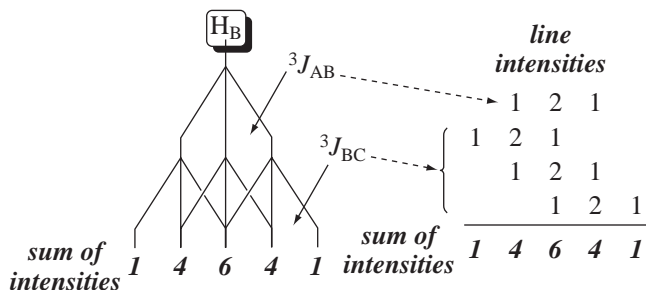
FIGURE 5.29 Construction of a quintet for a methylene group with four neighbors all with identical coupling values.

Consider a three-carbon chain as an example. The protons on carbons A and C split those on carbon B. If there is a total of four protons on carbons A and C, the $n + 1$ Rule predicts a pentet. This occurs only if $^3J_{AB} = {}^3J_{BC}$. Figure 5.29 represents the situation graphically.

One way to describe the situation is as a triplet of triplets, since the methylene protons labeled 'B' above should be split into a triplet by the neighboring methylene protons labeled 'A' and into a triplet by the neighboring methylene protons labeled 'C'. First, the protons on carbon A split those on carbon B ($^3J_{AB}$), yielding a triplet (intensities 1:2:1). The protons on carbon C then split *each component* of the triplet ($^3J_{BC}$) into another triplet (1:2:1). At this stage, many of the lines from the second splitting interaction *overlap* those from the first splitting interaction because they have the same spacings (J value). Because of this coincidence, only five lines are observed. But we can easily confirm that they arise in the fashion indicated by adding the intensities of the splittings to predict the intensities of the final five-line pattern (see Fig. 5.29). These intensities agree with those predicted by the use of Pascal's triangle (Section 3.16). Thus, the $n + 1$ Rule depends on a special condition—that all of the vicinal coupling constants are identical.
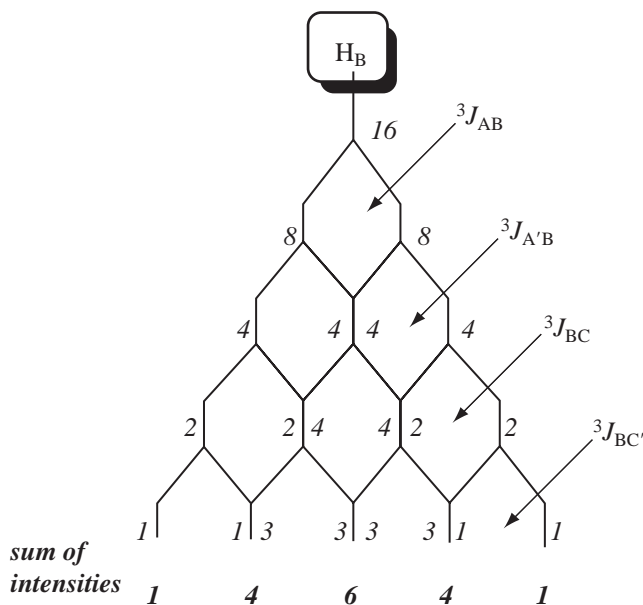
FIGURE 5.30 Construction of a quintet for a methylene group with four neighbors by considering as a dddd.
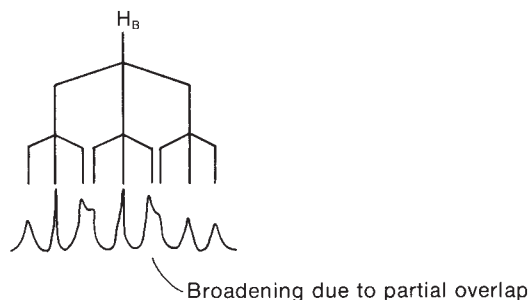
F I G U R E   5 . 3 1   Loss of a simple quintet when $^3J_{AB} \neq {}^3J_{BC}$.

Another way to describe the situation above is to consider the H_B methylene protons as a doublet of doublet of doublet of doublets (dddd) where $^3J_{AB} = {}^3J_{A'B} = {}^3J_{BC} = {}^3J_{AC'}$. With four distinct couplings, the sum of the line intensities for the H_B multiplet will be $2^4 = 16$. By constructing a splitting tree for H_B and distributing the intensities for each doublet, one arrives at the same conclusion: H_B is an apparent quintet with line intensities 1:4:6:4:1 = 16 (Figure 5.30).

In many molecules, however, J_{AB} is slightly different from J_{BC}. This leads to peak broadening in the multiplet, since the lines do not perfectly overlap. (Broadening occurs because the peak separation in Hertz is too small in magnitude for the NMR instrument to be able to distinguish the separate peak components.).

Sometimes the perturbation of the quintet is only slight, and then either a shoulder is seen on the side of a peak or a dip is obvious in the middle of a peak. At other times, when there is a large difference between $^3J_{AB}$ and $^3J_{BC}$, distinct peaks, more than five in number, can be seen. Deviations of this type are most common in a chain of the type $X{-}CH_2CH_2CH_2{-}Y$, where X and Y are widely different in character. Figure 5.31 illustrates the origin of some of these deviations.

Chains of any length can exhibit this phenomenon, whether or not they consist solely of methylene groups. For instance, the spectrum of the protons in the second methylene group of propylbenzene is simulated as follows. The splitting pattern gives a crude sextet, but the second line has a shoulder on the left, and the fourth line shows an unresolved splitting. The other peaks are somewhat broadened.
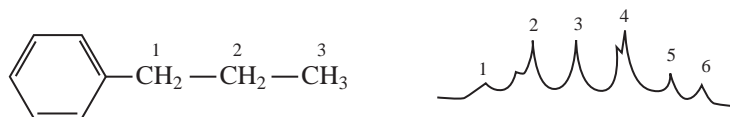
C.   More Complex Multiplets—More Than One Value of *J*

When analyzing more complicated resonances with more than one distinct coupling, measuring all of the coupling constants presents a challenge. Many chemists take the lazy way out and simply call a complex resonance a "multiplet." This presents problems on multiple levels. First, coupling constants give valuable information about both the two-dimensional (2-D) structure (connectivity) and three-dimensional (3-D) structure (stereochemistry) of compounds. With the availability of high-field instruments with pulsed field gradients (PFGs), chemists often turn immediately to 2-D NMR techniques such as COSY and NOESY (Chapter 10) to determine connectivity within spin systems and three-dimensional structure, respectively. Often the same information (provided the resonances are not too severely overlapping or second-order) may be extracted from the simple 1-D ^1H NMR spectrum if one knows how. Thus, *it is always worth the effort to determine all coupling constants from a first-order resonance.*

When measuring coupling constants in a system with more than one coupling you will often notice that none of the multiplet peaks is located at the appropriate chemical shift values to directly

determine a value for an intermediate J value. This is illustrated in Figure 5.32a where a doublet of doublets is illustrated. In this case, none of the peaks is located at the chemical shift values that would result from the first coupling J_1. To a beginning student, it may be tempting to average the
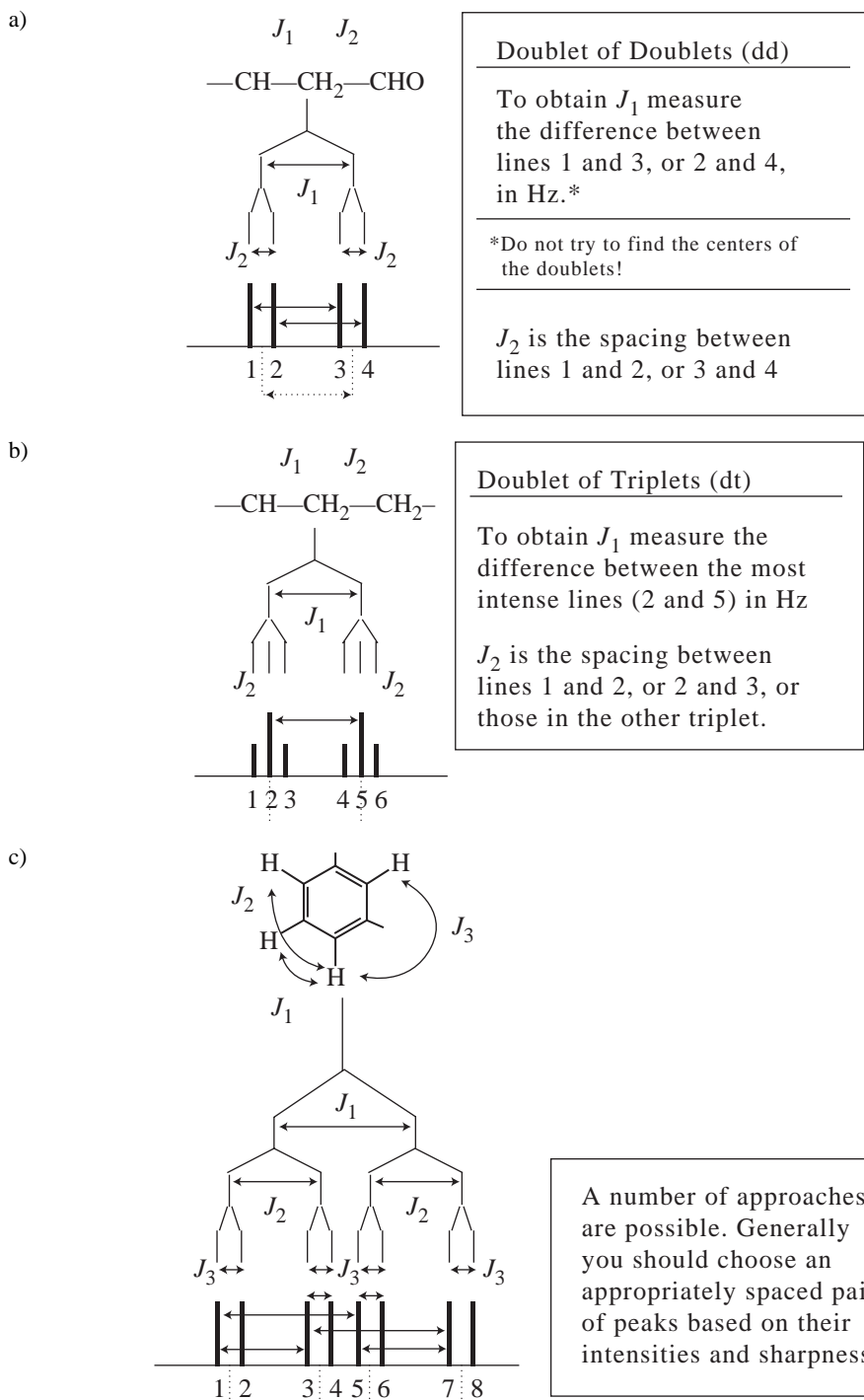
FIGURE 5.32 Determining coupling constants for a) doublet of doublets (dd), b) doublet of triplets (dt), and c) doublet of doublet of doublets (ddd) patterns.

chemical shift values for peaks 1 and 2, and for peaks 3 and 4, and then take the difference (dotted lines). This is not necessary. With a little thought you will see that the distance between peaks 1 and 3, and also the distance between peaks 2 and 4 (solid arrows), can yield the desired value with much less work. This type of situation will occur whenever there is an even number of sub-peaks (doublets, quartets, etc.) in the separated multiplets. In these systems you should look for an appropriately spaced pair of offset subpeaks that will yield the value you need. It will usually be necessary to construct a splitting diagram (tree) in order to decide which of the peaks are the appropriate ones.

When the separated multiplets have an odd number of subpeaks, one of the subpeaks will inevitably fall directly on the desired chemical shift value without a need to look for appropriate offset peaks. Figure 5.32b shows a doublet of triplets. Note that peaks 2 and 5 are ideally located for a determination of J_1.

Figure 5.32c shows a pattern that may be called a doublet of doublets of doublets. After constructing a tree diagram, it is relatively easy to select appropriate peaks to use for the determination of the three coupling constants (solid arrows).

A number of approaches to measuring coupling constants are possible. Generally you should choose an appropriately spaced pair of peaks based on their intensities and sharpness. With experience, most practicing synthetic chemists have the skills to measure coupling constants for all manner of resonances containing two or three unequal J values, i.e. doublet of doublet of doublet (ddd) resonances, including the doublet of triplets (dt) and triplet of doublet (td) permutations using the methods described above and in Fig. 5.32.

Even experienced chemists, however, often struggle to extract all of the coupling constants from resonances that have four couplings in them (doublet of doublet of doublet of doublets, or dddd) and even more complex multiplets. A straightforward systematic method exists, however, that allows for complete analysis of any (even the most complex) first-order multiplet. Practicing this method on the more easily analyzed ddd multiplets discussed above will allow the student to gain confidence in its usefulness. This systematic multiplet analysis was most succinctly presented by Hoye and Zhao, and is presented below.

Analysis of a first-order multiplet begins with numbering each line in the resonance from left-to-right.[4] The outermost line will be relative intensity = 1. Lines of relative intensity > 1 get more than one component number. A line of relative intensity 2 gets two component numbers, one with relative intensity 3 gets three component numbers, and so on. The line component numbers and the relative line intensities must sum to a 2^n number. This is illustrated in Figure 5.33. In Figure 5.33a, there are eight lines of equal intensity ($2^3 = 8$), and each line has one component number. In Figure 5.33b, there is some coincidence of lines; the middle line has double intensity and therefore gets two component numbers. Figure 5.33c and 5.33d show line numbering for multiplets with lines having relative intensity 3 and 6, respectively. The assignment of line components sometimes requires a bit of trial and error as partial overlap of lines and 'leaning' of the multiplet may make determining the relative intensities more difficult. Remember, though, that a first-order multiplet is always symmetric about its midpoint.

Once the relative intensities of the lines of the multiplet are determined and the component numbers assigned to arrive at 2^n components, the measurement of coupling constants is actually fairly easy. We will go through the analysis of a dddd pattern step-by-step (Figure 5.34). The distance between the first component and the second component (referred to as {1 to 2} by Hoye) is the

---

[4] Since first-order resonances are symmetric, one could number the lines of a resonance from right-to-left just as easily. This is useful when part of the multiplet is obscured due to overlap of another resonance. One should also check for internal consistency within a resonance, as on occasion one 'half' of the multiplet may be sharper than the other due to the digitization of the spectrum, as discussed previously in Section 5.6A.
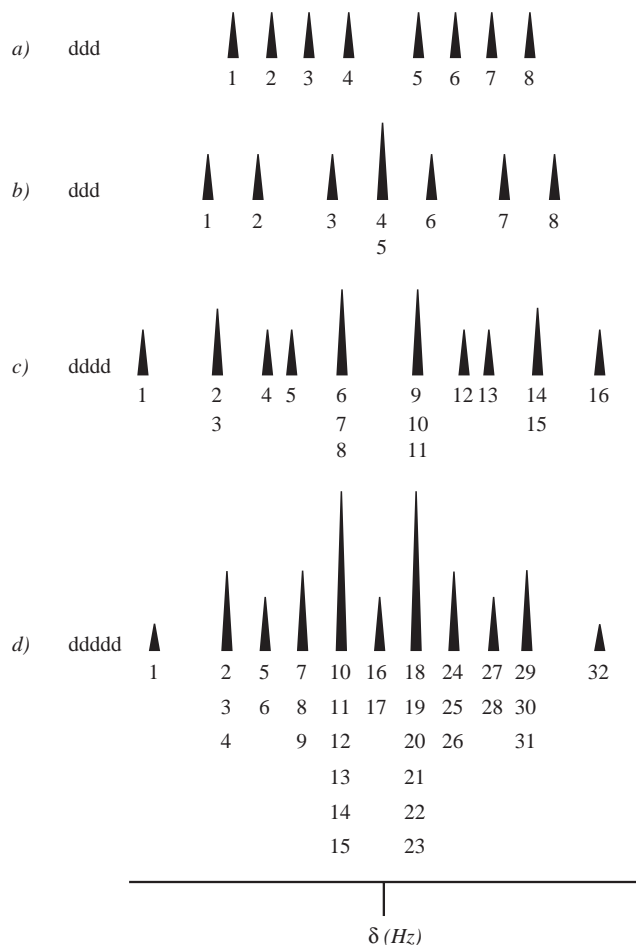
FIGURE 5.33 Numbering lines of a first-order multiplet to account for all 2^n components of the resonance. (From Hoye, T. R. and H. Zhao, *Journal of Organic Chemistry* 2002, 67, 4014–4016.) Reprinted by permission.

smallest coupling constant J_1 (Figure 5.34, step i). The distance between component 1 and component 3 of the multiplet ({1 to 3}) is the next largest coupling constant J_2 (Figure 5.34, step ii). Note that if the second line of the resonance has more than one component number, there will be more than one identical J value. If the second line of a resonance has three components, for example, there will be three identical J values, etc. After measuring J_1 and J_2, the next step in the analysis is to "remove" the component of the multiplet corresponding to ($J_1 + J_2$) (Figure 5.34 step iii, component 5 is crossed out). The reason for removing one of the components is to eliminate from consideration lines that are not due to a unique coupling interaction, but rather from coincidence of lines due to the sum of two smaller couplings. In other words, it shows whether or not the two 'halves' of the resonance have 'crossed' due to J_3 being smaller than the sum of $J_1 + J_2$. Now, J_3 is the distance between component 1 and the *next highest remaining* component (component 4 or 5, depending on which component was removed in step iii, in this example $J_3 = \{1$ to $4\}$) (Figure 5.34, step iv). This process now becomes iterative. The next step is to remove the component(s) that correspond to the remaining combinations of the first three J values: ($J_1 + J_3$), ($J_2 + J_3$), and ($J_1 + J_2 + J_3$) (Figure 5.34, step v, components 6, 7, and 9 are crossed out). The next coupling constant, J_4, will be the distance between the first component and the next highest remaining component. In the example case shown in Figure 5.34, J_4 corresponds to {1 to 8}. This iterative process repeats until all the coupling constants are found. Remember that the total number of coupling interactions and the total number of line
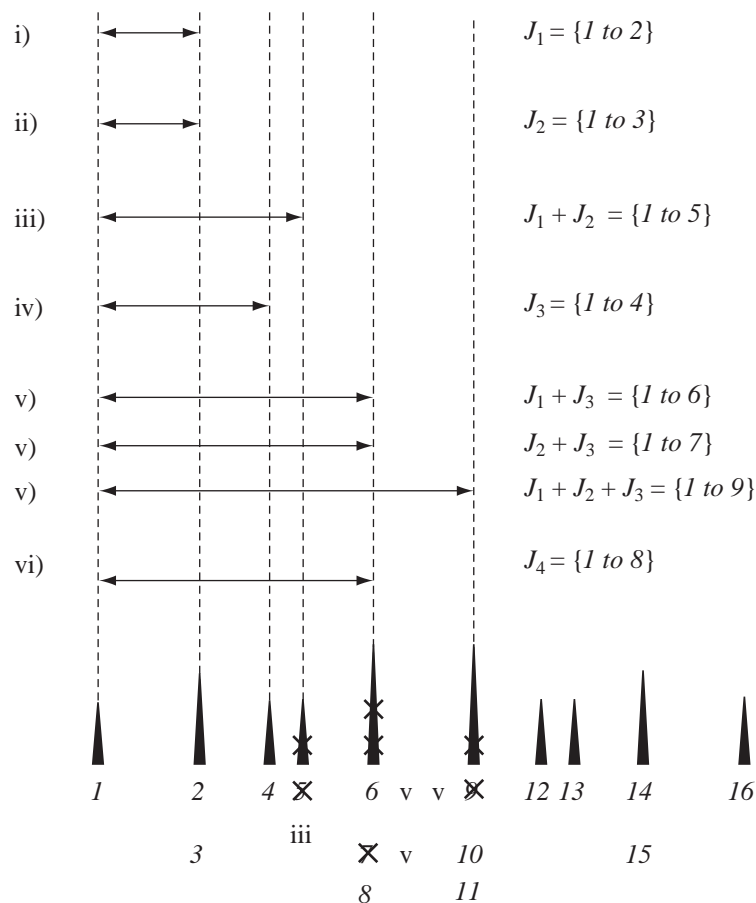
F I G U R E   5 . 3 4   Assignment of $J_1 – J_4$ of a dddd by systematic analysis. (From Hoye, T. R. and H. Zhao, *Journal of Organic Chemistry* 2002, *67,* 4014–4016.) Reprinted by permission.

components must equal 2^n, and the overall width of the multiplet *must* equal the sum of all the individual coupling constants! This is a convenient check of your work.

☐ 5.7 SECOND-ORDER SPECTRA—STRONG COUPLING

A. First-Order and Second-Order Spectra

In earlier sections, we have discussed **first-order spectra,** spectra that can be interpreted by using the $n + 1$ Rule or a simple graphical analysis (splitting trees). In certain cases, however, neither the $n + 1$ Rule nor graphical analysis suffices to explain the splitting patterns, intensities, and numbers of peaks observed. In these last cases, a mathematical analysis must be carried out, usually by computer, to explain the spectrum. Spectra that require such advanced analysis are said to be **second-order spectra.**

Second-order spectra are most commonly observed when the difference in chemical shift between two groups of protons is similar in magnitude (in Hertz) to the coupling constant J (also in Hertz), which links them. That is, second-order spectra are observed for couplings between nuclei that have *nearly equivalent chemical shifts* but are not exactly identical. In contrast, if two sets of nuclei are separated by a large chemical shift difference, they show first-order coupling.

Strong coupling, second-order spectra   Weak coupling, first-order spectra
($\Delta v/J$ small)   ($\Delta v/J$ large)
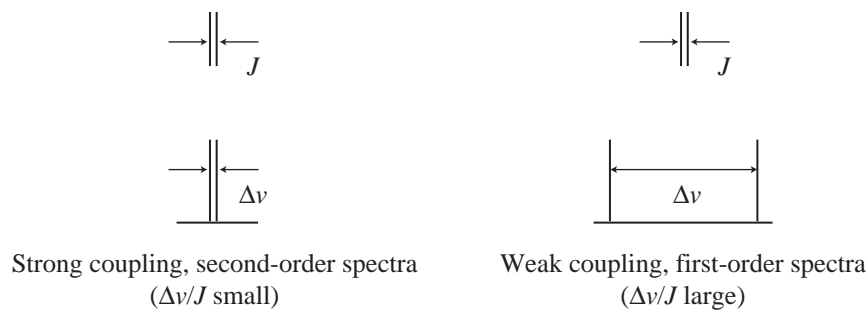
Another way of expressing this generalization is by means of the ratio $\Delta v/J$, where Δv is the chemical shift difference, and J is the coupling constant that links the two groups. Both values are expressed in Hertz, and their absolute values are used for the calculation. When $\Delta v/J$ is large (> ~6), the splitting pattern typically approximates first-order splitting. However, when the chemical shifts of the two groups of nuclei move closer together and $\Delta v/J$ approaches unity, we see second-order changes in the splitting pattern. When $\Delta v/J$ is large and we see first-order splitting, the system is said to be **weakly coupled;** if $\Delta v/J$ is small and we see second-order coupling, the system is said to be **strongly coupled.**

We have established that even complex looking first-order spectra may be analyzed in a straightforward fashion to determine all of the relevant coupling constants, which provide valuable information about connectivity and stereochemistry. Second-order spectra can be deceptive in their appearance and often tempt the novice into trying to extract coupling constant values, which ultimately proves an exercise in futility. How, then, does one determine if a resonance is first order or second order? How can one determine $\Delta v/J$ if one does not know the relevant coupling values in the first place? Herein lays the importance of being familiar with typical coupling constant values for commonly encountered structural features. One should first *estimate* $\Delta v/J$ by finding the chemical shift difference between resonances that are likely to be coupled (based on one's knowledge of the structure or in some cases the 2-D COSY spectra (Chapter 10, Section 10.6) and divide that value by a typical or *average* coupling constant for the relevant structural type. The estimated $\Delta v/J$ value allows one to make a judgment about whether detailed analysis of the resonance is likely to be useful ($\Delta v/J > \sim 6$) or not ($\Delta v/J < \sim 6$).

B.   Spin System Notation

Nuclear Magnetic Resonance (NMR) spectroscopists have developed a convenient shorthand notation, sometimes called **Pople notation,** to designate the type of spin system. Each chemically different type of proton is given a capital letter: A, B, C, and so forth. If a group has two or more protons of one type, they are distinguished by subscripts, as in A_2 or B_3. Protons of similar chemical shift values are assigned letters that are close to one another in the alphabet, such as A, B, and C. Protons of widely different chemical shift are assigned letters far apart in the alphabet: X, Y, Z versus A, B, C. A two-proton system where H_A and H_X are widely separated, and that exhibits first-order splitting, is called an AX system. A system in which the two protons have similar chemical shifts, and that exhibits second-order splitting, is called an AB system. When the two protons have identical chemical shifts, are magnetically equivalent, and give rise to a singlet, the system is designated A_2. Two protons that have the same chemical shift but are not magnetically equivalent are designated as AA'. If three protons are involved and they all have very different chemical shifts, a letter from the middle of the alphabet is used, usually M, as in AMX. The ^{1}H NMR spectrum of styrene oxide in Figure 5.26 is an example of an AMX pattern. In contrast, ABC would be used for the strongly coupled situation in which all three protons have similar chemical shifts. We will use designations similar to these throughout this section.
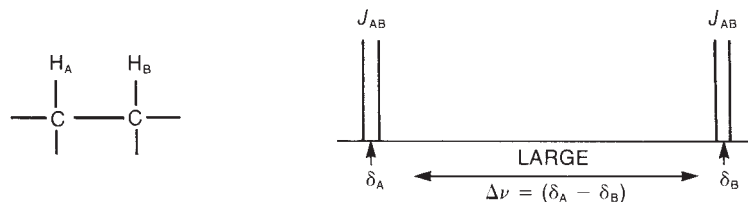
FIGURE 5.35 A first-order AX system: $\Delta\nu$ large, and $n + 1$ Rule applies.

C. The A$_2$, AB, and AX Spin Systems

Start by examining the system with two protons, H_A and H_B, on adjacent carbon atoms. Using the $n + 1$ Rule, we expect to see each proton resonance as a doublet with components of equal intensity in the ^1H NMR spectrum. In actuality, we see two doublets of equal intensity in this situation only if the difference in chemical shift ($\Delta\nu$) between H_A and H_B is large compared to the magnitude of the coupling constant ($^3J_{AB}$) that links them. Figure 5.35 illustrates this case.

Figure 5.36 shows how the splitting pattern for the two-proton system H_AH_B changes as the chemical shifts of H_A and H_B come closer together and the ratio $\Delta\nu/J$ becomes smaller. The figure is drawn to scale, with $^3J_{AB} = 7$ Hz. When $\delta H_A = \delta H_B$ (that is, when the protons H_A and H_B have the same chemical shift), then $\Delta\nu = 0$, and no splitting is observed; both protons give rise to a single absorption peak. Between one extreme, where there is no splitting due to chemical shift equivalence ($\Delta\nu/J = 0$), and the other extreme, the simple first-order spectrum ($\Delta\nu/J = 15$) that follows the $n + 1$ Rule, subtle and continuous changes in the splitting pattern take place. Most obvious is the decrease in intensity of the outer peaks of the doublets, with a corresponding increase in the intensity of the inner peaks. Other changes that are not as obvious also occur.

Mathematical analysis by theoreticians has shown that although the chemical shifts of H_A and H_B in the simple first-order AX spectrum correspond to the center point of each doublet, a more complex situation holds in the second-order cases: The chemical shifts of H_A and H_B are closer to the inner peaks than to the outer peaks. The actual positions of δ_A and δ_B must be calculated. The difference in chemical shift must be determined from the line positions (in Hertz) of the individual peak components of the group, using the equation

$$(\delta_A - \delta_B) = \sqrt{(\delta_1 - \delta_4)(\delta_2 - \delta_3)}$$

where δ_1 is the position (in Hertz downfield from TMS) of the first line of the group, and δ_2, δ_3, and δ_4 are the second, third, and fourth lines, respectively (Fig. 5.37). The chemical shifts of H_A and H_B are then displaced $\frac{1}{2}(\delta_A - \delta_B)$ to each side of the center of the group, as shown in Figure 5.37.

D. The AB$_2$ . . . AX$_2$ and A$_2$B$_2$ . . . A$_2$X$_2$ Spin Systems

To provide some idea of the magnitude of second-order variations from simple behavior, Figures 5.38 and 5.39 illustrate the calculated ^1H NMR spectra of two additional systems ($-CH-CH_2-$ and $-CH_2-CH_2-$). The first-order spectra appear at the top ($\Delta\nu/J > 10$), while increasing amounts of second-order complexity are encountered as we move toward the bottom ($\Delta\nu/J$ approaches zero).

The two systems shown in Figures 5.38 and 5.39 are, then, AB$_2$ ($\Delta\nu/J < 10$) and AX$_2$ ($\Delta\nu/J > 10$) in one case and A$_2$B$_2$ ($\Delta\nu/J < 10$) and A$_2$X$_2$ ($\Delta\nu/J > 10$) in the other. We will leave discussion of these types of spin systems to more advanced texts, such as those in the reference list at the end of this chapter.

Figures 5.40 through 5.43 (pp. 274–276) show actual 60-MHz ^1H NMR spectra of some molecules of the A$_2$B$_2$ type. It is convenient to examine these spectra and compare them with the expected patterns in Figure 5.39; which were calculated from theory using a computer.
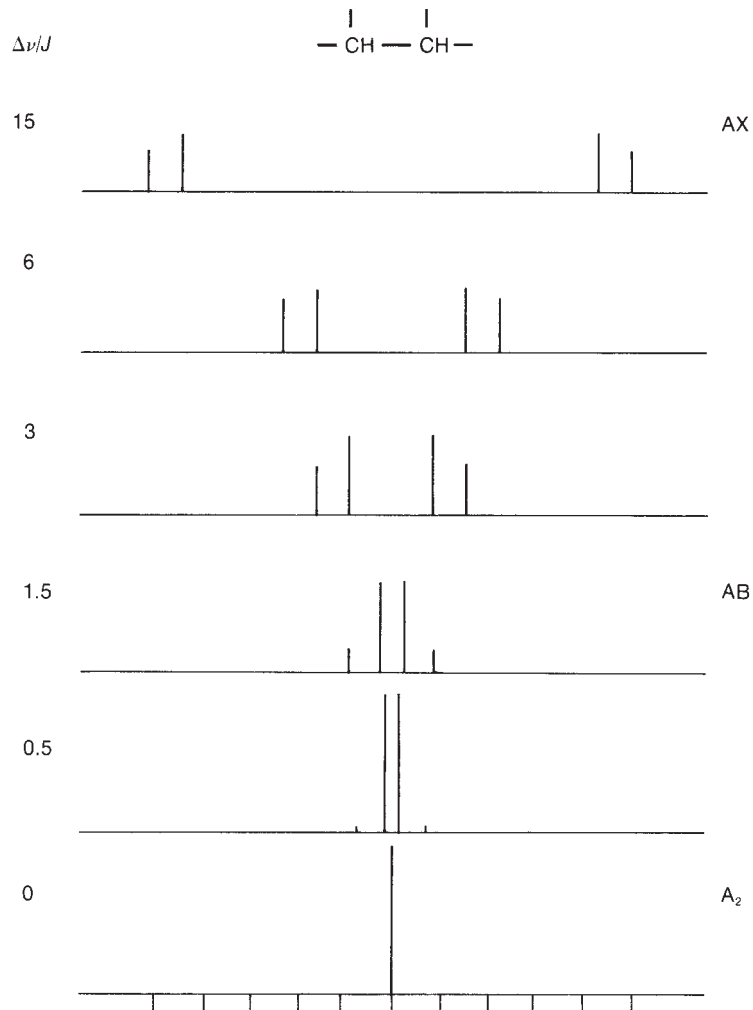
FIGURE 5.36 Splitting patterns of a two-proton system for various values of $\Delta\nu/J$. Transition from an AB to an AX pattern.
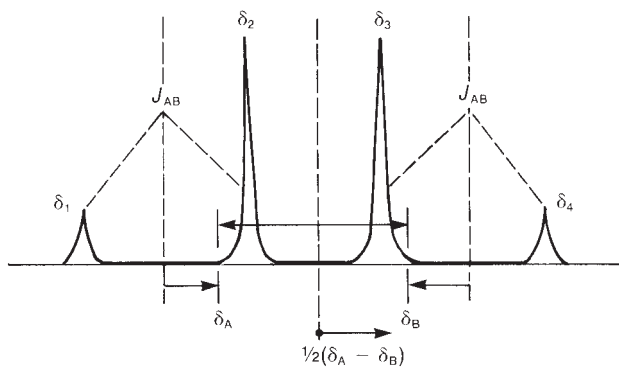
FIGURE 5.37 The relationships among the chemical shifts, line positions, and coupling constant in a two-proton AB system that exhibits second-order effects.
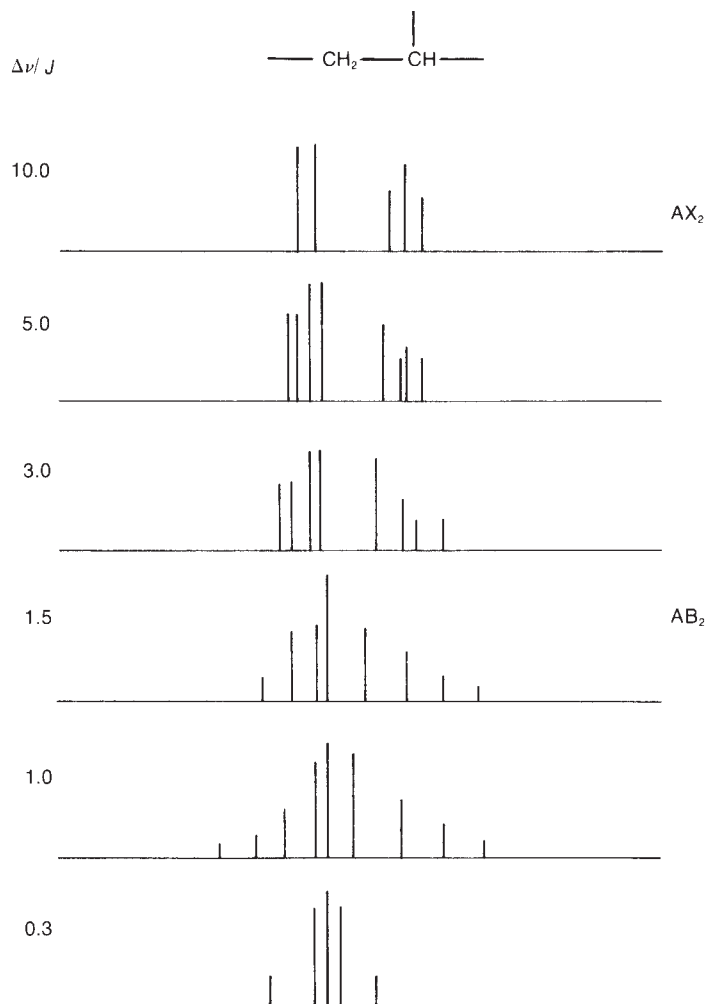
F I G U R E   5 . 3 8   The splitting patterns of a three-proton system $-CH-CH_2-$ for various $\Delta\nu/J$ values.

E.   Simulation of Spectra

We will not consider all the possible second-order spin systems in this text. Splitting patterns can often be more complicated than expected, especially when the chemical shifts of the interacting groups of protons are very similar. In many cases, only an experienced NMR spectroscopist using a computer can interpret spectra of this type. Today, there are many computer programs, for both PC and UNIX workstations, that can simulate the appearances of NMR spectra (at any operating frequency) if the user provides a chemical shift and a coupling constant for each of the peaks in the interacting spin system. In addition, there are programs that will attempt to match a calculated spectrum to an actual NMR spectrum. In these programs, the user initially provides a best guess at the parameters (chemical shifts and coupling constants), and the program varies these parameters until it finds the best fit. Some of these programs are included in the reference list at the end of this chapter.

F.   The Absence of Second-Order Effects at Higher Field

With routine access to NMR spectrometers with ^{1}H operating frequencies >300 MHz, chemists today encounter fewer second-order spectra than in years past. In Sections 3.17 and 3.18, you saw that the chemical shift increases when a spectrum is determined at higher field, but that the coupling
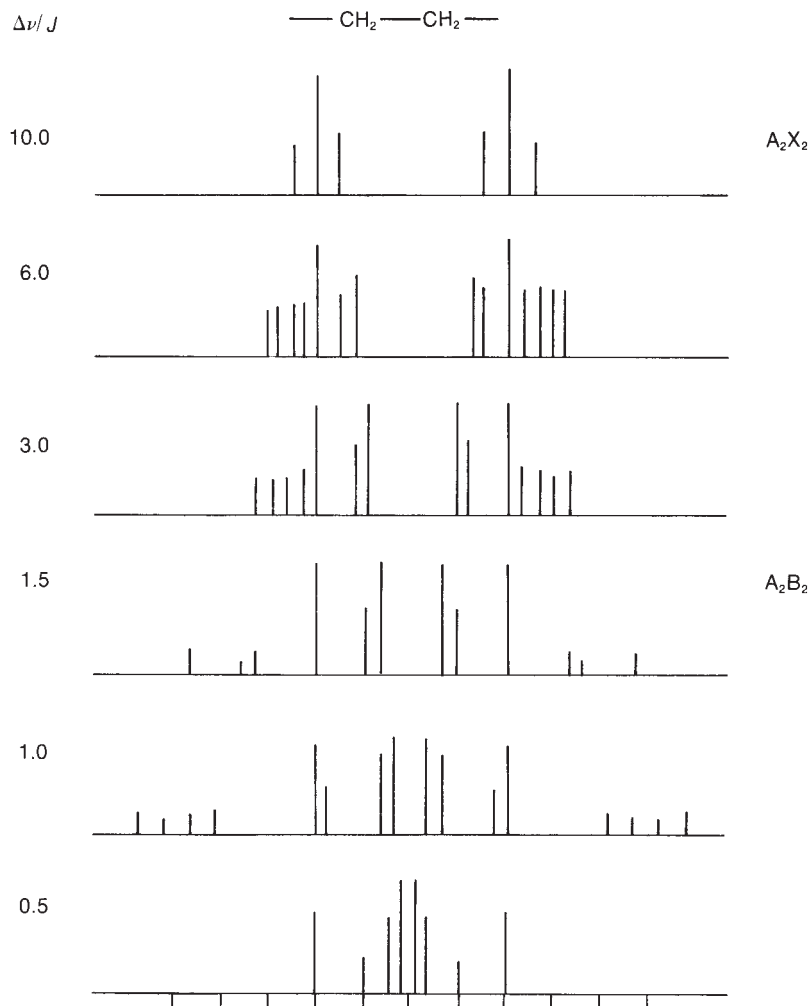
FIGURE 5.39 The splitting patterns of a four-proton system $-CH_2-CH_2-$ for various $\Delta v/J$ values.

constants do not change in magnitude (see Fig. 3.38). In other words, Δv (the chemical shift difference in Hertz) increases, but J (the coupling constant) does not. This causes the $\Delta v/J$ ratio to increase, and second-order effects begin to disappear. At high field, many spectra are first order and are therefore easier to interpret than spectra determined at lower field strengths.

As an example. Figure 5.43a is the 60-MHz ^1H NMR spectrum of 2-chloroethanol. This is an A_2B_2 spectrum showing substantial second-order effects ($\Delta v/J$ is between 1 and 3). In Figure 5.43b, which shows the ^1H spectrum taken at 300 MHz, the formerly complicated and second-order patterns have *almost* reverted to two triplets just as the $n + 1$ Rule would predict ($\Delta v/J$ is between 6 and 8). At 500 MHz (Figure 5.43c), the predicted A_2X_2 pattern ($\Delta v/J \sim 12$) is observed.

G. Deceptively Simple Spectra

It is not always obvious when a spectrum has become completely first order. Consider the A_2B_2 to A_2X_2 progression shown in Figure 5.39. At which value of $\Delta v/J$ does this spectrum become truly first order? Somewhere between $\Delta v/J = 6$ and $\Delta v/J = 10$ the spectrum seems to become A_2X_2. The
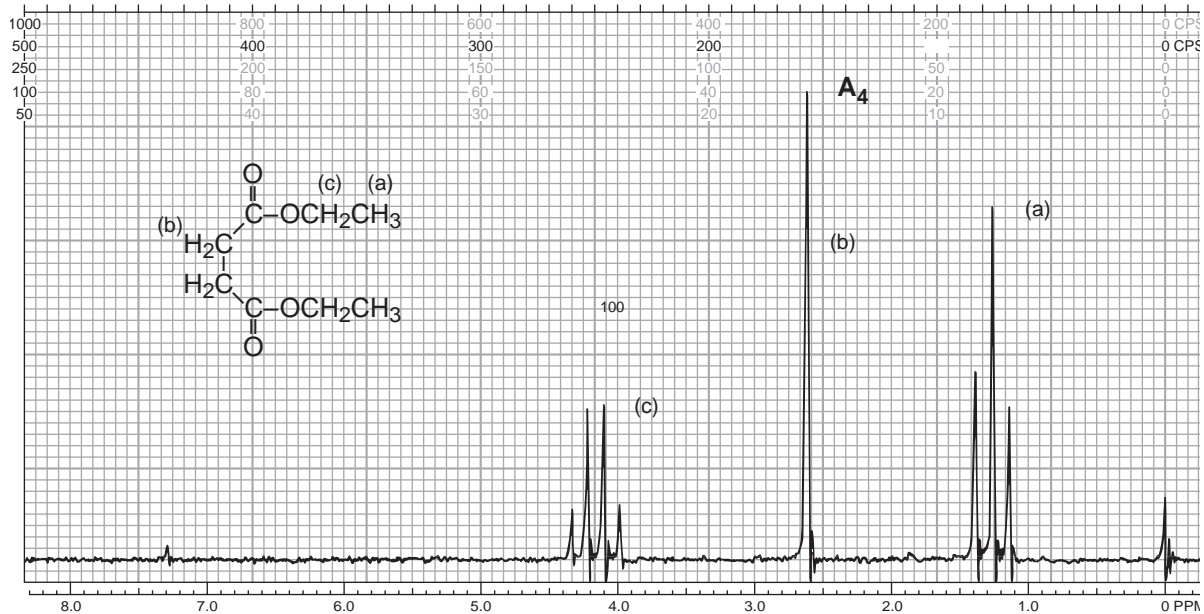
FIGURE 5.40 The 60-MHz ^{1}H NMR spectrum of diethyl succinate.
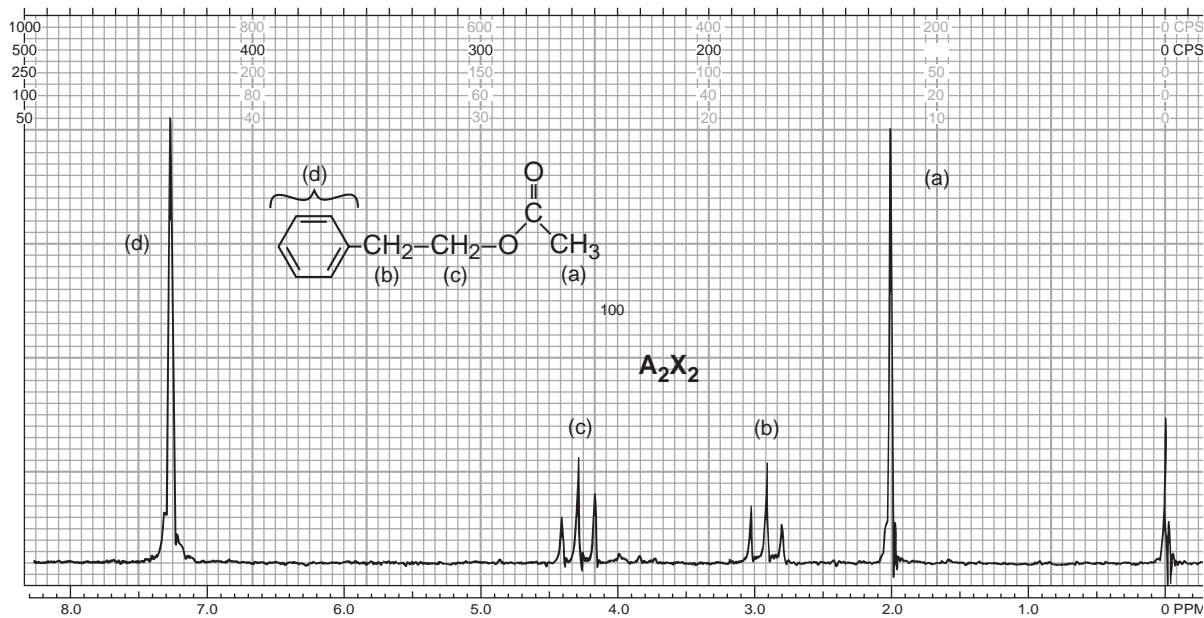
FIGURE 5.41 The 60-MHz ^{1}H NMR spectrum of phenylethyl acetate.

number of observed lines decreases from 14 lines to only 6 lines. However, if spectra are simulated, incrementally changing $\Delta\nu/J$ slowly from 6 to 10, we find that the change is not abrupt but gradual. Some of the lines disappear by decreasing in intensity, and some merge together, increasing their intensities. It is possible for weak lines to be lost in the noise of the baseline or for merging lines to

(a)

A_2B_2

(b)

Phenyl
2nd order

A_2X_2

(c)

Phenyl
1st order

A_2X_2
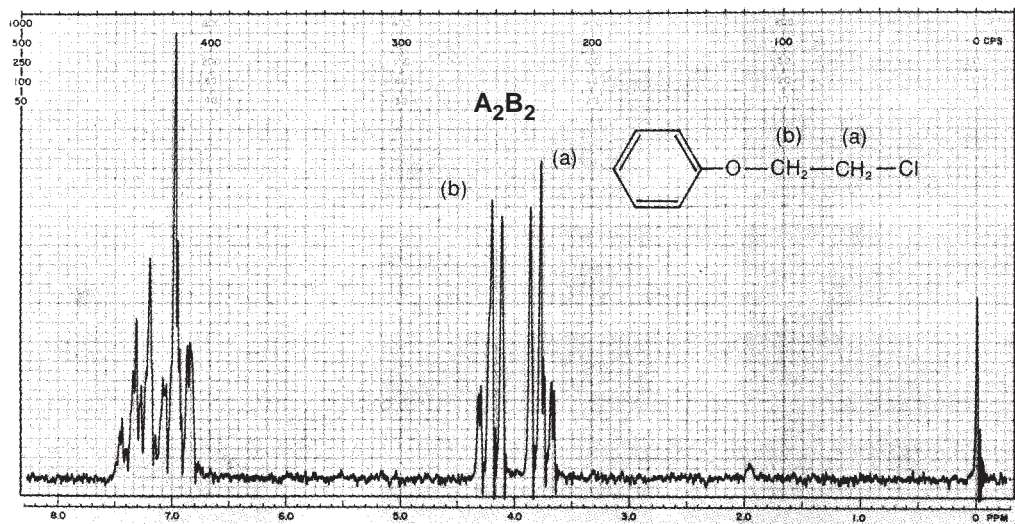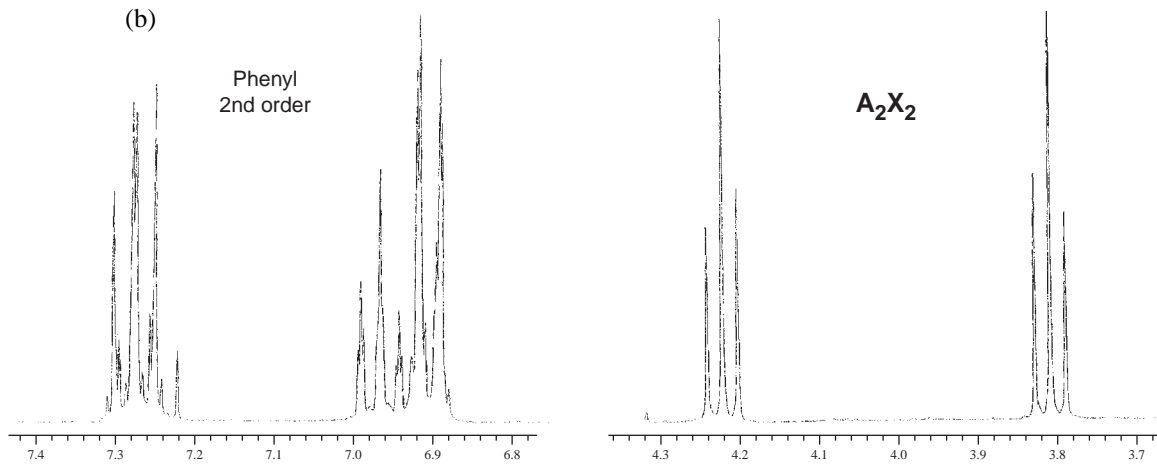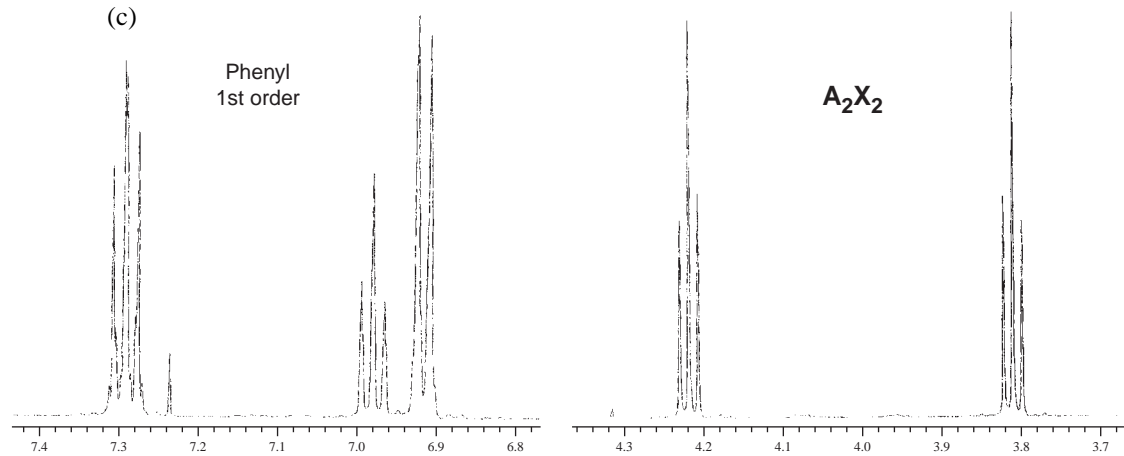
FIGURE 5.42 ¹H NMR spectrum of β-chlorophenetole: (a) 60 MHz, (b) 300 MHz (7.22 peak CHCl₃), (c) 500 MHz (7.24 peak CHCl₃).

(a)

Cl–CH$_2$–CH$_2$–OH   A$_2$B$_2$

(b)

A$_2$B$_2$

(c)

A$_2$X$_2$
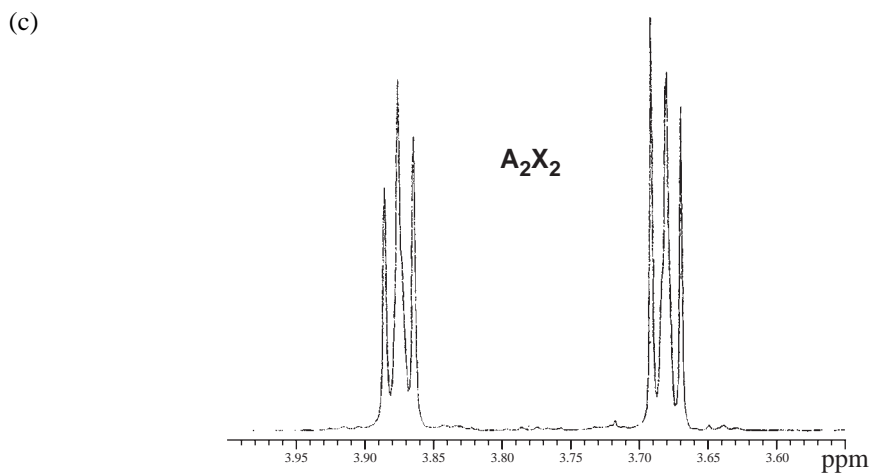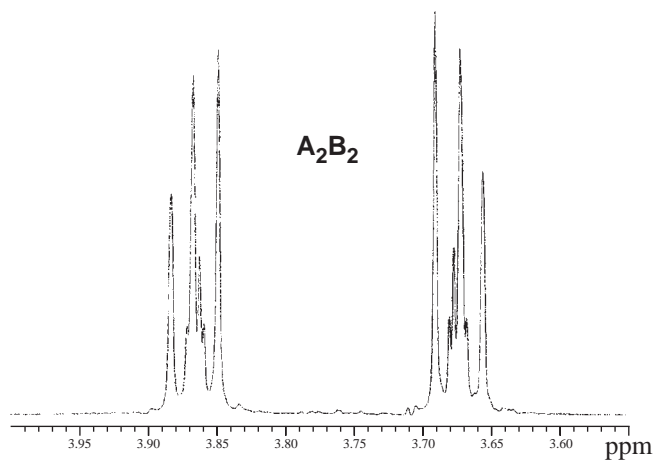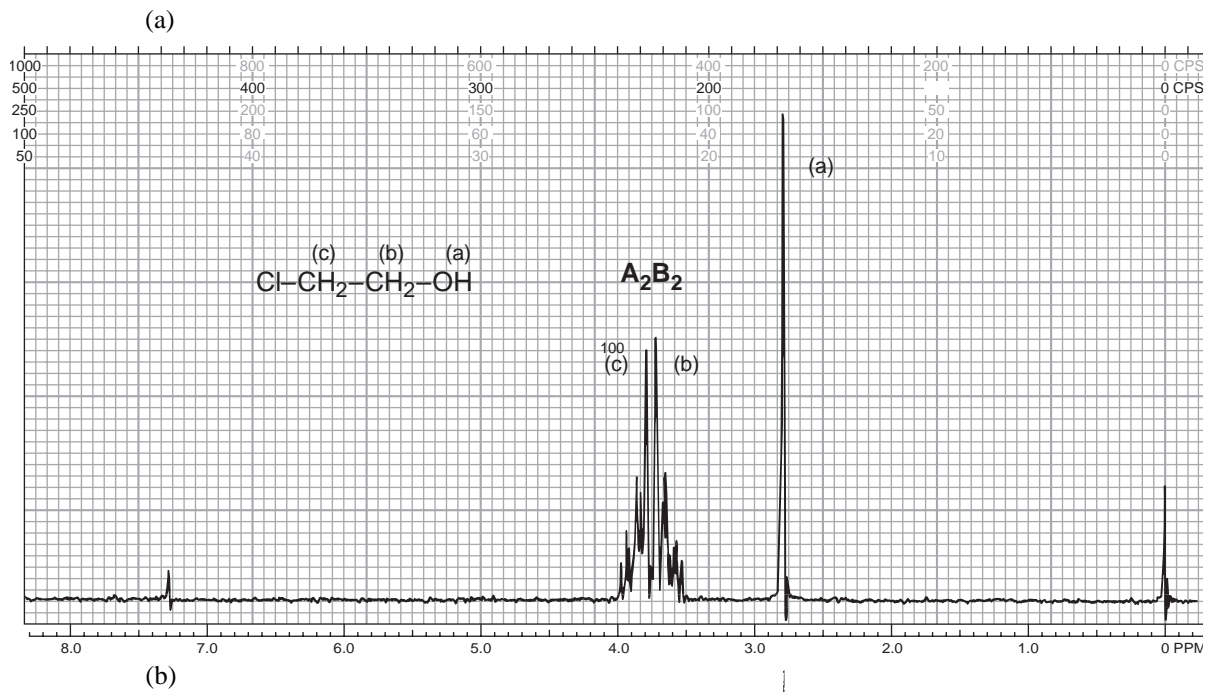
FIGURE 5.43 ^{1}H NMR spectrum of 2-chloroethanol: (a) 60 MHz, (b) 300 MHz (OH not shown), (c) 500 MHz (OH not shown).

approach so closely that the spectrometer cannot resolve them any longer. In these cases, the spectrum would appear to be first order, but in fact it would not quite be so. A common deceptively simple pattern is that encountered with *para*-disubstituted aromatics, an AA'BB' spectrum (see Section 5.10B).

Also notice in Figure 5.36 that the AB spectra with $\Delta v/J$ equal to 3, 6, and 15 all appear roughly first order, but the doublets observed in the range $\Delta v/J = 3$ to 6 have chemical shifts that do not correspond to the center of the doublet (see Fig. 5.37). Unless the worker recognizes the possibility of second-order effects and does a *mathematical* extraction of the chemical shifts, the chemical shift values will be in error. Spectra that appear to be first order, but actually are not, are called **deceptively simple spectra.** The pattern appears to the casual observer to be first order and capable of being explained by the $n + 1$ Rule. However, there may be second-order lines that are either too weak or too closely spaced to observe, and there may be other subtle changes.

Is it important to determine whether a system is deceptively simple? In many cases, the system is so close to first order that it does not matter. However, there is always the possibility that if we assume the spectrum is first order and measure the chemical shifts and coupling constants, we will get incorrect values. Only a complete mathematical analysis tells the truth. For the organic chemist trying to identify an unknown compound, it rarely matters whether the system is deceptively simple. However, if you are trying to use the chemical shift values or coupling constants to prove an important or troublesome structural point, take the time to be more careful. Unless they are obvious cases, we will treat deceptively simple spectra as though they follow the $n + 1$ Rule or as though they can be analyzed by simple tree diagrams. In doing your own work, always realize that there is a considerable margin for error.

5.8 ALKENES

Just as the protons attached to double bonds have characteristic chemical shifts due to a change in hybridization (sp^2 vs. sp^3) and deshielding due to the diamagnetic anisotropy generated by the π electrons of the double bond, alkenyl protons have characteristic splitting patterns and coupling constants. For monosubstituted alkenes, three distinct types of spin interaction are observed:

$$^3J_{AB} = 6\text{–}15 \text{ Hz (typically 9–12 Hz)}$$

$$^3J_{AC} = 14\text{–}19 \text{ Hz (typically 15–18 Hz)}$$

$$^2J_{BC} = 0\text{–}5 \text{ Hz (typically 1–3 Hz)}$$
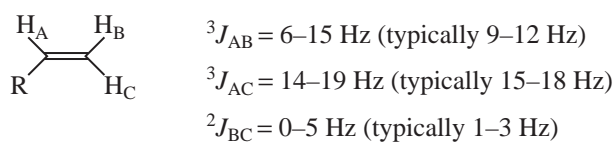
Protons substituted *trans* on a double bond couple most strongly, with a typical value for ^3J of about 16 Hz. The *cis* coupling constant is slightly more than half this value, about 10 Hz. Coupling between terminal methylene protons (geminal coupling) is smaller yet, less than 5 Hz. These coupling constant values decrease with electronegative substituents in an additive fashion, but $^3J_{\text{trans}}$ is always larger than $^3J_{\text{cis}}$ for a given system.

As an example of the ^{1}H NMR spectrum of a simple *trans*-alkene, Figure 5.44 shows the spectrum of *trans*-cinnamic acid. The phenyl protons appear as a large group between 7.4 and 7.6 ppm, and the acid proton is a singlet that appears off scale at 13.2 ppm. The two vinyl protons H_A and H_C split each other into two doublets, one centered at 7.83 ppm downfield of the phenyl resonances and the other at 6.46 ppm upfield of the phenyl resonances. The proton H_C, attached to the carbon bearing the phenyl ring, is assigned the larger chemical shift as it resides on the more electron-poor β-carbon of the α,β-unsaturated carbonyl system in addition to its position in a deshielding area of the anisotropic field generated by the π electrons of the aromatic ring. The coupling constant $^3J_{AC}$ can be determined quite easily from the 300-MHz spectrum shown in Figure 5.44. The *trans* coupling constant in this
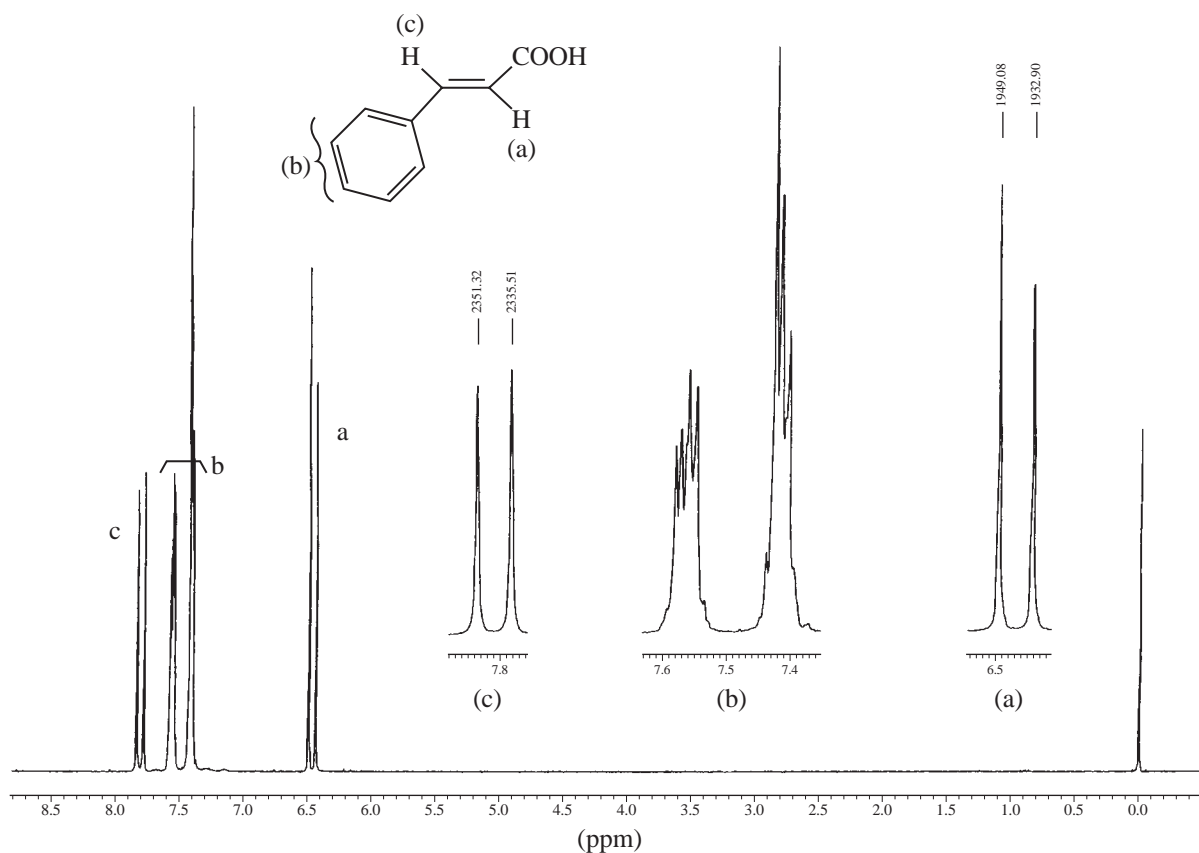
FIGURE 5.44   The ¹H NMR spectrum of *trans*-cinnamic acid.

case is 15.8 Hz—a common value for *trans* proton–proton coupling across a double bond. The *cis* isomer would exhibit a smaller splitting.

A molecule that has a symmetry element (a plane or axis of symmetry) passing through the C=C double bond does not show any *cis* or *trans* splitting since the vinyl protons are chemically and magnetically equivalent. An example of each type can be seen in *cis-* and *trans-*stilbene, respectively. In each compound, the vinyl protons H$_A$ and H$_B$ give rise to only a single *unsplit* resonance peak.

Plane of symmetry
cis-Stilbene

Twofold axis of symmetry
trans-Stilbene

2192.85
2186.60
2178.88
2172.63

1472.57
1471.09
1458.59
1456.75

1374.76
1373.29
1368.51
1367.04

(a) (c)

H   H

H   O—CH₃

(b)

O

7.32 7.28 7.24
(ppm)
(c)

4.92 4.88 4.84
(b)

4.60 4.56
(a)

(c)

(b) (a)

7.5 7.0 6.5 6.0 5.5 5.0 4.5 4.0 3.5 3.0 2.5 2.0 1.5 1.0 0.5 0.0

(ppm)
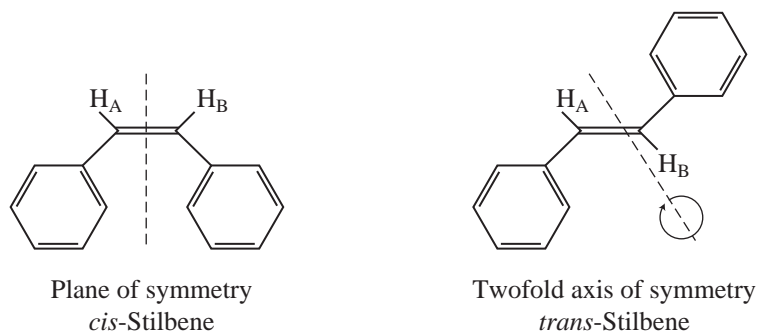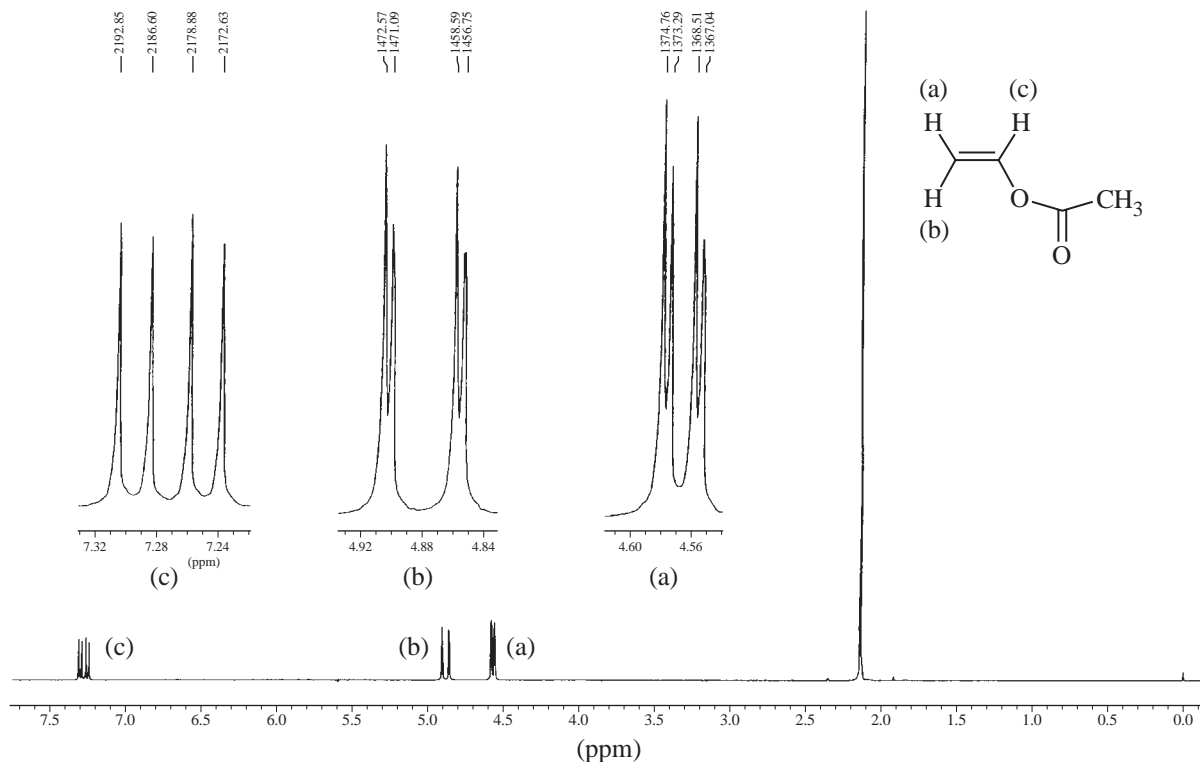
FIGURE 5.45 The ¹H NMR spectrum of vinyl acetate (AMX).

Vinyl acetate gives an NMR spectrum typical of a compound with a terminal alkene. Each alkenyl proton has a chemical shift and a coupling constant different from those of each of the other protons. This spectrum, shown in Figure 5.45 is not unlike that of styrene oxide (Fig. 5.26). Each hydrogen is split into a doublet of doublets (four peaks). Figure 5.46 is a graphical analysis of the vinyl portion. Notice that $^3J_{BC}$ (*trans,* 14 Hz) is larger than $^3J_{AC}$ (*cis,* 6.3 Hz), and that $^2J_{AB}$ (geminal, 1.5 Hz) is very small—the usual situation for vinyl compounds.

H$_C$ H$_B$ H$_A$

J_{BC} J_{BC} J_{AC}

J_{AC} J_{AB} J_{AB}
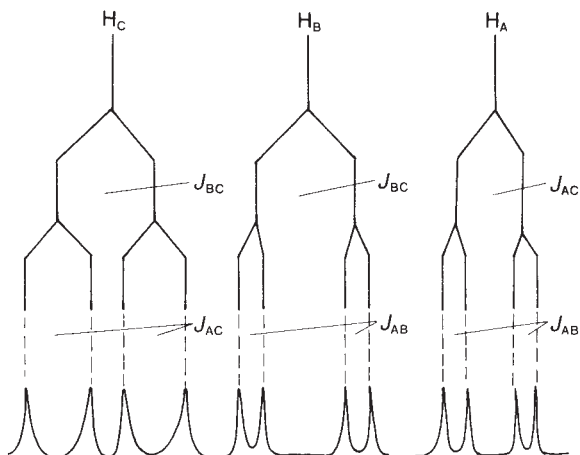
FIGURE 5.46 Graphical analysis of the splittings in vinyl acetate (AMX).
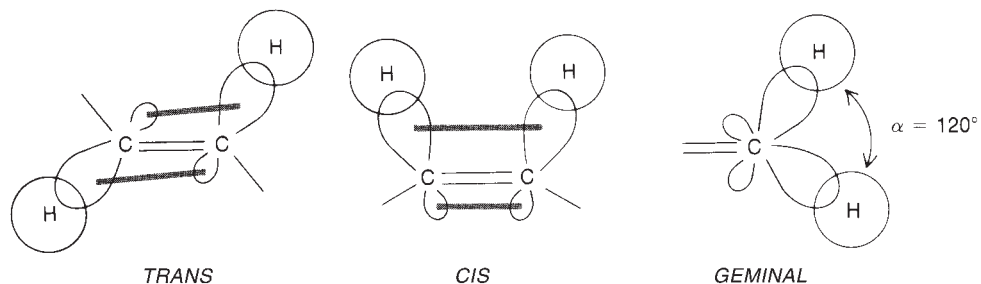
FIGURE 5.47 Coupling mechanisms in alkenes.

The mechanism of *cis* and *trans* coupling in alkenes is no different from that of any other three-bond vicinal coupling, and that of the terminal methylene protons is just a case of two-bond geminal coupling. All three types have been discussed already and are illustrated in Figure 5.47. To obtain an explanation of the relative magnitudes of the ^3J coupling constants, notice that the two C—H bonds are parallel in *trans* coupling, while they are angled away from each other in *cis* coupling. Also note that the H—C—H angle for geminal coupling is nearly 120°, a virtual minimum in the graph of Figure 5.4. In addition to these three types of coupling, alkenes often show small long-range (allylic) couplings (Section 5.2D).

Figure 5.48 is a spectrum of crotonic acid. See if you can assign the peaks and explain the couplings in this compound (draw a tree diagram). The acid peak is not shown on the full-scale
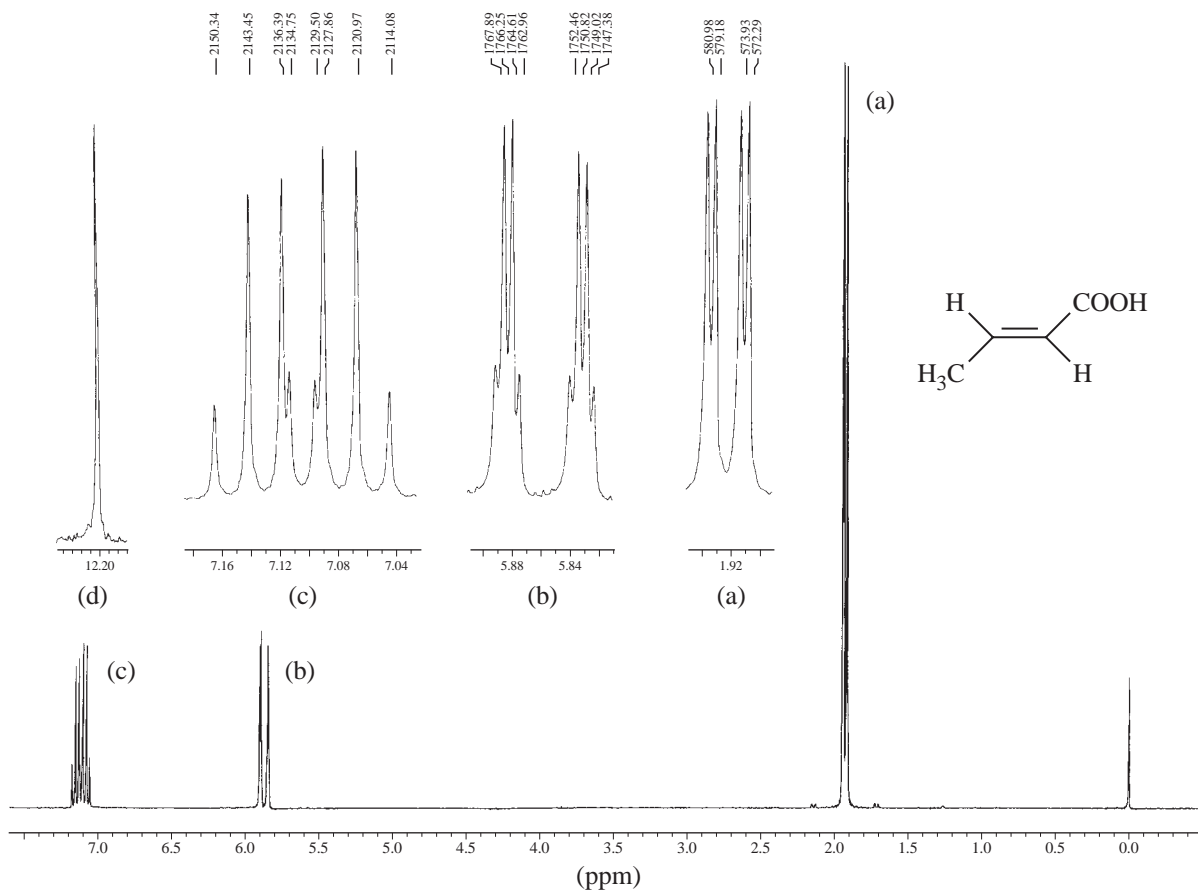
FIGURE 5.48 The 300-MHz ^{1}H NMR spectrum of crotonic acid (AMX$_3$).

spectrum, but is shown in the expansions at 12.2 ppm. Also remember that $^3J_{trans}$ is quite large in an alkene while the allylic couplings will be small. The multiplets may be described as a doublet of doublets (1.92 ppm), a doublet of quartets (5.86 ppm), and a doublet of quartets (7.10 ppm) with the peaks of the two quartets overlapping.

5.9 MEASURING COUPLING CONSTANTS—ANALYSIS OF AN ALLYLIC SYSTEM

In this section, we will work through the analysis of the 300-MHz FT-NMR spectrum of 4-allyloxyanisole. The complete spectrum is shown in Figure 5.49. The hydrogens of the allylic system are labeled a–d. Also shown are the methoxy group hydrogens (three-proton singlet at 3.78 ppm) and the *para*-disubstituted benzene ring resonances (second-order multiplet at 6.84 ppm). The origin of the *para*-disubstitution pattern will be discussed in Section 5.10B. The main concern here will be to explain the allylic splitting patterns and to determine the various coupling constants. The exact assignment of the multiplets in the allylic group depends not only on their chemical shift values, but also on the splitting patterns observed. Some initial analysis must be done before any assignments can be definitely made.
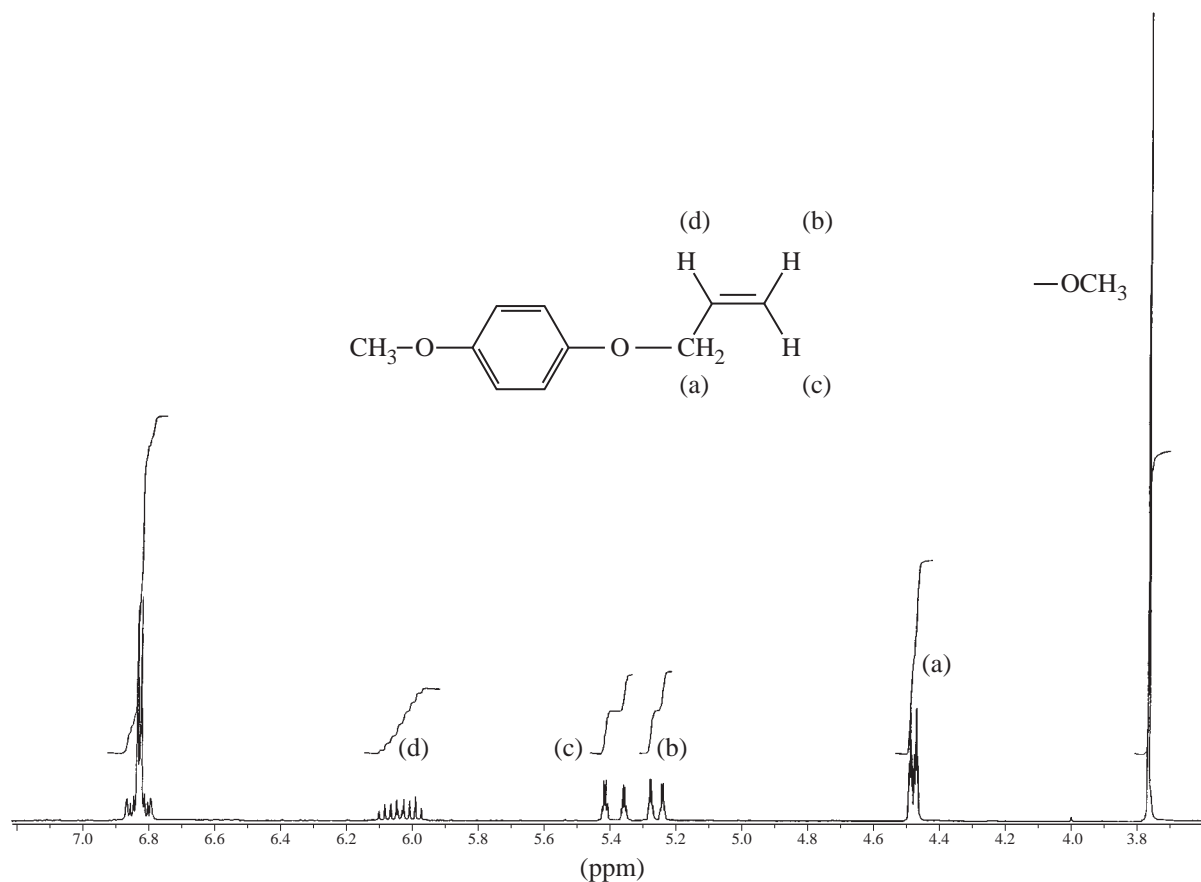
FIGURE 5.49 The 300-MHz ^{1}H NMR spectrum of 4-allyloxyanisole.

Initial Analysis

The allylic OCH_2 group (4.48 ppm) is labeled **a** on the spectrum and is the easiest multiplet to identify since it has an integral of 2H. It is also in the chemical shift range expected for a group of protons on a carbon atom that is attached to an oxygen atom. It has a larger chemical shift than the upfield methoxy group (3.77 ppm) because it is attached to the carbon–carbon double bond as well as the oxygen atom.

The hydrogen attached to the same carbon of the double bond as the OCH_2 group will be expected to have the broadest and most complicated pattern and is labeled **d** on the spectrum. This pattern should be spread out because the first splitting it will experience is a large splitting $^3J_{cd}$ from the *trans*-H_c, followed by another large coupling $^3J_{bd}$ from the *cis*-H_b. The adjacent OCH_2 group will yield additional (and smaller) splitting into triplets $^3J_{ad}$. Finally, this entire pattern integrates for only 1H.

Assigning the two terminal vinyl hydrogens relies on the difference in the magnitude of a *cis* and a *trans* coupling. H_c will have a *wider* pattern than H_b because it will have a *trans* coupling $^3J_{cd}$ to H_d, while H_b will experience a smaller $^3J_{bd}$ *cis* coupling. Therefore, the multiplet with wider spacing is assigned to H_c, and the narrower multiplet is assigned to H_b. Notice also that each of these multiplets integrates for 1H.

The preliminary assignments just given are tentative, and they must pass the test of a full tree analysis with coupling constants. This will require expansion of all the multiplets so that the exact value (in Hertz) of each subpeak can be measured. Within reasonable error limits, all coupling constants must agree in magnitude wherever they appear.

Tree-Based Analysis and Determination of Coupling Constants

The best way to start the analysis of a complicated system is to start with the **simplest** of the splitting patterns. In this case, we will start with the OCH_2 protons in multiplet **a**. The expansion of this multiplet is shown in Figure 5.50a. It appears to be a doublet of triplets (dt). However, examination of the molecular structure (see Fig. 5.49) would lead us to believe that this multiplet should be a doublet of doublets of doublets (ddd), the OCH_2 group being split first by H_d ($^3J_{ad}$), then by H_b ($^4J_{ab}$), and then by H_c ($^4J_{ac}$), each of which is a single proton. A doublet of triplets could result only if (by coincidence) $^4J_{ab} = ^4J_{ac}$. We can find out if this is the case by extracting the coupling constants and constructing a tree diagram. Figure 5.50b gives the positions of the peaks in the multiplet. By taking

(a)	(b)	(c)

(b)

Positions of peaks (Hz)	Differences
1350.13	
1348.66	1.47
1347.18	1.47
	5.15
1344.98	
1343.51	1.47
1342.04	1.47

(c) H_a

$^3J_{ad}$ 5.15 Hz

$^4J_{ab}$ 1.47 Hz

$^4J_{ac}$ 1.47 Hz

lines overlap

4.50   4.48   4.46
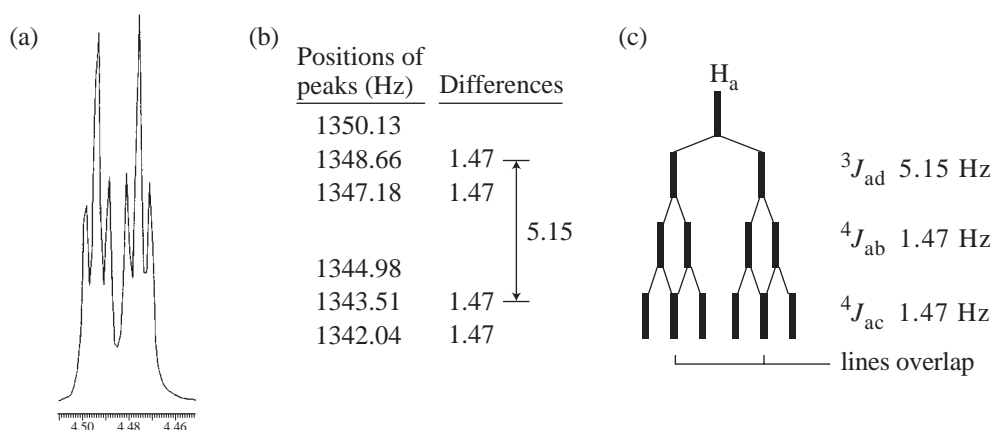
F I G U R E 5 . 5 0 Allyloxyanisole. (a) Expansion of H_a. (b) Peak positions (Hz) and selected frequency differences. (c) Splitting tree diagram showing the origin of the splitting pattern.
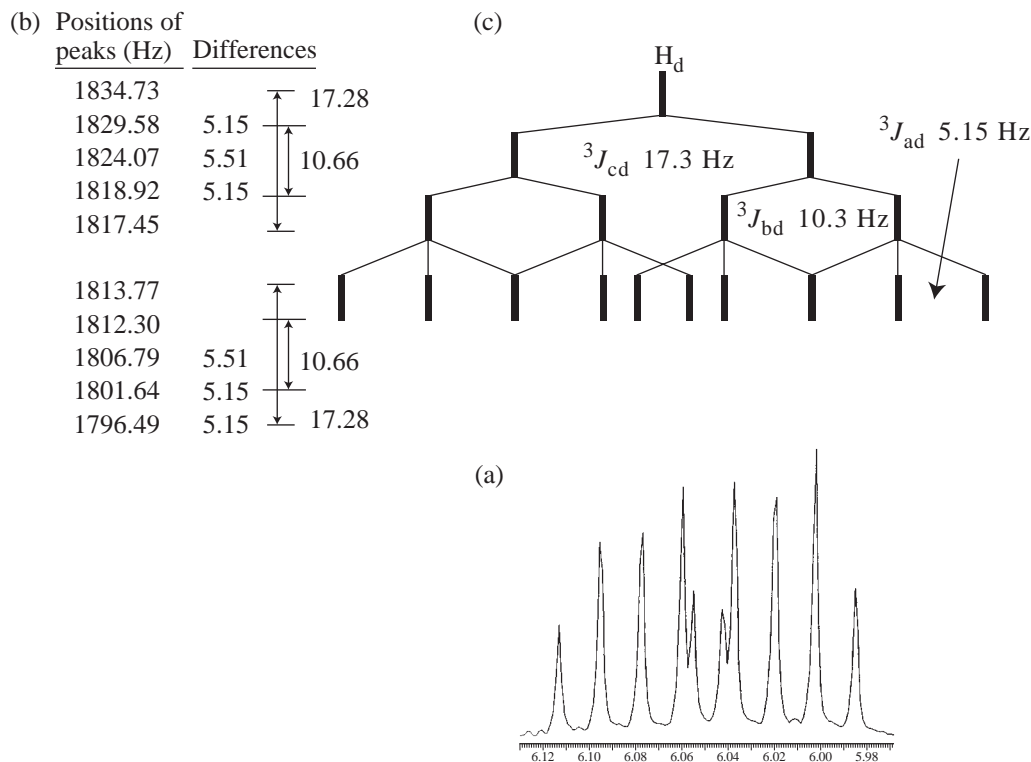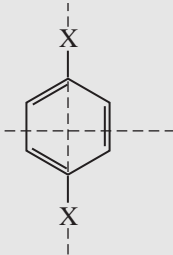
appropriate differences (see Section 5.6), we can extract two coupling constants with magnitudes of 1.5 Hz and 5.2 Hz. The larger value is in the correct range for a vicinal coupling ($^3J_{ad}$), and the smaller value must be identical for both the *cis* and *trans* allylic couplings ($^4J_{ab}$ and $^4J_{ac}$). This would lead to the tree diagram shown in Figure 5.50c. Notice that when the two smaller couplings are equivalent (or nearly equivalent) the central lines in the final doublet coincide, or overlap, and effectively give triplets instead of pairs of doublets. We will begin by assuming that this is correct. If we are in error, there will be a problem in trying to make the rest of the patterns consistent with these values.

Next consider H_b The expansion of this multiplet (Fig. 5.51a) shows it to be an apparent doublet of quartets. The largest coupling should be the *cis* coupling $^3J_{bd}$, which should yield a doublet. The geminal coupling $^2J_{bc}$ should produce another pair of doublets (dd), and the allylic geminal coupling $^4J_{ab}$ should produce triplets (two H_a protons). The expected final pattern would be a doublet of doublet of triplets (ddt) with six peaks in each half of the splitting pattern. Since only four peaks are observed, there must be overlap such as was discussed for H_a. Figure 5.51c shows that could happen if $^2J_{bc}$ and $^4J_{ab}$ are both small and have nearly the same magnitude. In fact, the two *J* values appear to be coincidentally the same (or similar), and this is not unexpected (see the typical geminal and allylic values on pp. 244 and 277). Figure 5.51b also shows that only two different *J* values can be extracted from the positions of the peaks (1.5 and 10.3 Hz). Examine the tree diagram in Figure 5.51c to see the final solution, a doublet of doublet of triplets (ddt) pattern, which appears to be a doublet of quartets due to the coincidental overlap.

H_c is also expected to be a doublet of doublet of triplets (ddt) but shows a doublet of quartets for reasons similar to those explained for H_b. Examination of Figure 5.52 explains how this occurs. Notice that the first coupling ($^3J_{cd}$) is larger than $^3J_{bd}$.

At this point, we have extracted all six of the coupling constants for the system

$$^3J_{cd}\text{-}trans = 17.3 \text{ Hz} \qquad ^2J_{bc}\text{-}gem = 1.5 \text{ Hz}$$

$$^3J_{bd}\text{-}cis = 10.3 \text{ Hz} \qquad ^4J_{ab}\text{-allylic} = 1.5 \text{ Hz}$$

$$^3J_{ad} = 5.2 \text{ Hz} \qquad ^4J_{ac}\text{-allylic} = 1.5 \text{ Hz}$$

(a)

(b) Positions of
peaks (Hz) Differences

1589.12	
1587.65	1.47
1586.18	1.47
1584.71	1.47
	10.30
1578.46	
1577.35	1.11
1575.88	1.47
1574.41	1.47

(c)

H_b

$^3J_{bd}$ 10.3 Hz

$^2J_{bc}$ 1.47 Hz

$^4J_{ab}$ 1.47 Hz

lines overlap

5.30   5.28   5.26   5.24   5.22
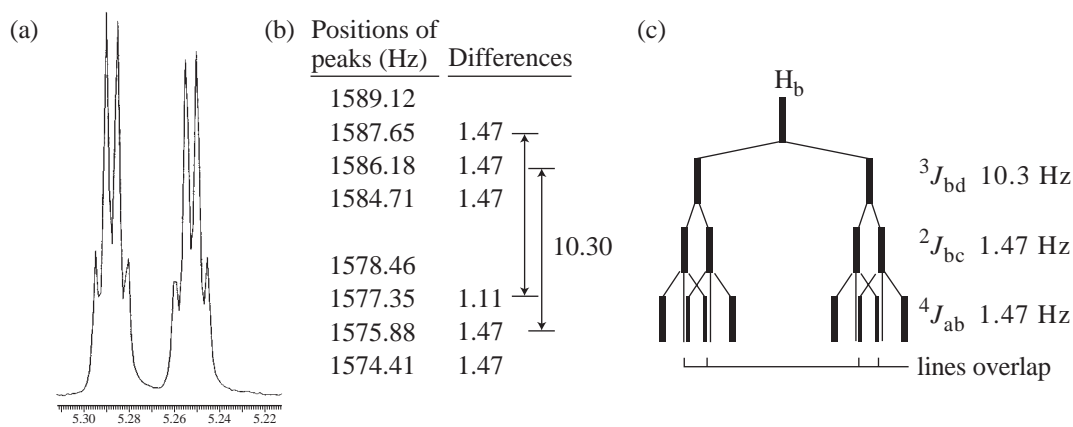
F I G U R E   5 . 5 1   Allyloxyanisole. (a) Expansion of H_b. (b) Peak positions (Hz) and selected frequency differences. (c) Splitting tree diagram showing the origin of the splitting pattern.
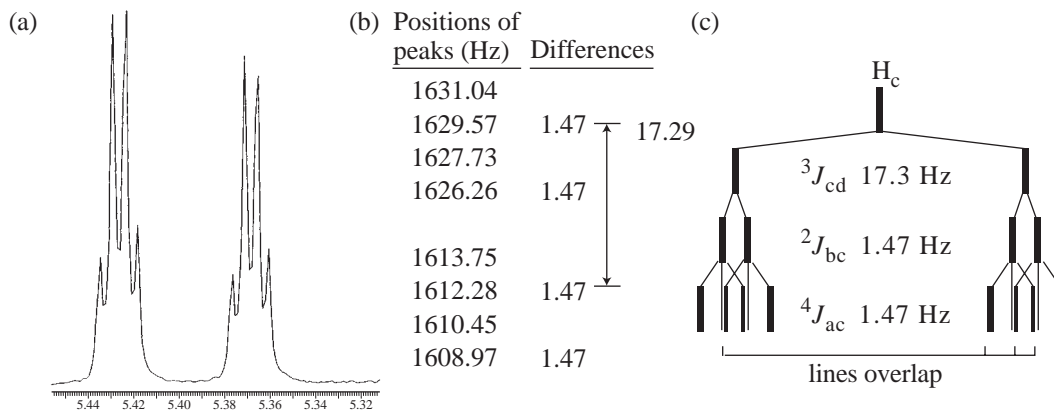
FIGURE 5.52 Allyloxyanisole. (a) Expansion of H_c. (b) Peak positions (Hz) and selected frequency differences. (c) Splitting tree diagram showing the origin of the splitting pattern.

H_d has not been analyzed, but we will do this *by prediction* in the next paragraph. Note that three of the coupling constants (all of which are expected to be small ones) are equivalent or nearly equivalent. This is either pure coincidence or could have to do with an inability of the NMR spectrometer to resolve the very small differences between them more clearly. In any event, note that one small inconsistency is seen in Figure 5.51b; one of the differences is 1.1 Hz instead of the expected 1.5 Hz.

Proton d—A Prediction Based on the *J* Values Already Determined

An expansion of the splitting pattern for H_d is shown in Figure 5.53a, and the peak values in Hz are given in Figure 5.53b. The observed pattern will be predicted using the *J* values just determined as a way of checking our results. If we have extracted the constants correctly, we should be able to correctly predict the splitting pattern. This is done in Figure 5.53c, in which the tree is constructed to scale using the *J* values already determined. The predicted pattern is a doublet of doublet of triplets (ddt), which should have six peaks on each half of the symmetrical multiplet. However, due to overlaps, we see what appear to be two overlapping quintets. This agrees well with the observed spectrum, thereby validating our analysis. Another small inconsistency is seen here. The *cis* coupling ($^3J_{bd}$) measured in Figure 5.51 was 10.3 Hz. The same coupling measured from the H_d multiplet gives $^3J_{bd} = 10.7$ Hz. What is the true value of $^3J_{bd}$? The lines in the H_d resonance are sharper than those in the H_b resonance because H_d does not experience the small long-range allylic couplings that are approximately identical in magnitude. In general, *J* values measured from sharp, uncomplicated resonances are more reliable than those measured from broadened peaks. The true coupling magnitude for $^3J_{bd}$ is likely closer to 10.7 Hz than to 10.3 Hz.

The Method

Notice that we started with the *simplest* pattern, determined its splitting tree, and extracted the relevant coupling constants. Then, we moved to the next most complicated pattern, doing essentially the same procedure, making sure that the values of any coupling constants shared by the two patterns agreed (within experimental error). If they do not agree, something is in error, and you must go back and start again. With the analysis of the third pattern, all of the coupling constants were obtained. Finally, rather than extracting constants from the last pattern, the pattern was predicted using the constants already determined. It is always a good idea to use prediction on the final pattern as a

(b) Positions of
peaks (Hz)   Differences

1834.73	
1829.58	5.15
1824.07	5.51
1818.92	5.15
1817.45	
1813.77	
1812.30	
1806.79	5.51
1801.64	5.15
1796.49	5.15

17.28
10.66

10.66
17.28

(c)

H_d

$^3J_{cd}$ 17.3 Hz

$^3J_{ad}$ 5.15 Hz

$^3J_{bd}$ 10.3 Hz

(a)

6.12   6.10   6.08   6.06   6.04   6.02   6.00   5.98

FIGURE 5.53 Allyloxyanisole. (a) Expansion of H_d. (b) Peak positions (Hz) and selected frequency differences. (c) Splitting tree diagram showing the origin of the splitting pattern.

method of validation. If the predicted pattern matches the experimentally determined pattern, then it is almost certainly correct.

5.10 AROMATIC COMPOUNDS—SUBSTITUTED BENZENE RINGS

Phenyl rings are so common in organic compounds that it is important to know a few facts about NMR absorptions in compounds that contain them. In general, the ring protons of a benzenoid system appear around 7 ppm; however, electron-withdrawing ring substituents (e.g., nitro, cyano, carboxyl, or carbonyl) move the resonance of these protons downfield, and electron-donating ring substituents (e.g., methoxy or amino) move the resonance of these protons upfield. Table 5.8 shows these trends for a series of symmetrically *para*-disubstituted benzene compounds. The *p*-disubstituted compounds were chosen because their two planes of symmetry render all of the hydrogens equivalent. Each compound gives only one aromatic peak (a singlet) in the proton NMR spectrum. Later you will see that some positions are affected more strongly than others in systems with substitution patterns different from this one. Table A6.3 in Appendix 6 enables us to make rough estimates of some of these chemical shifts.

In the sections that follow, we will attempt to cover some of the most important types of benzene ring substitution. In many cases, it will be necessary to examine sample spectra taken at both 60 and 300 MHz. Many benzenoid rings show second-order splittings at 60 MHz but are essentially first order at 300 MHz or higher field.

TABLE 5.8
^{1}H CHEMICAL SHIFTS IN *p*-DISUBSTITUTED BENZENE COMPOUNDS

Substituent X	δ (ppm)	
—OCH$_3$	6.80	Electron donating
—OH	6.60	
—NH$_2$	6.36	
—CH$_3$	7.05	
—H	7.32	
—COOH	8.20	Electron withdrawing
—NO$_2$	8.48	

A. Monosubstituted Rings

Alkylbenzenes

In monosubstituted benzenes in which the substituent is neither a strongly electron-withdrawing nor a strongly electron-donating group, all the ring protons give rise to what appears to be a *single resonance* when the spectrum is determined at 60 MHz. This is a particularly common occurrence in alkyl-substituted benzenes. Although the protons *ortho, meta,* and *para* to the substituent are not chemically equivalent, they generally give rise to a single unresolved absorption peak. All of the protons are nearly equivalent under these conditions. The NMR spectra of the aromatic portions of alkylbenzene compounds are good examples of this type of circumstance. Figure 5.54a is the 60-MHz ^{1}H spectrum of ethylbenzene.

The 300-MHz spectrum of ethylbenzene, shown in Figure 5.54b, presents quite a different picture. With the increased frequency shifts at higher field (see Fig. 3.35), the aromatic protons (that were nearly equivalent at 60 MHz) are neatly separated into two groups. The *ortho* and *para* protons appear upfield from the *meta* protons. The splitting pattern is clearly second order.

Electron-Donating Groups

When electron-donating groups are attached to the aromatic ring, the ring protons are not equivalent, even at 60 MHz. A highly activating substituent such as methoxy clearly increases the electron density at the *ortho* and *para* positions of the ring (by resonance) and helps to give these protons greater shielding than those in the *meta* positions and thus a substantially different chemical shift.
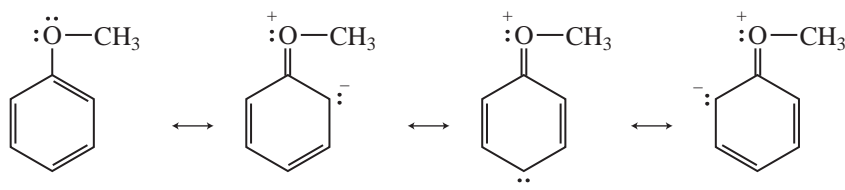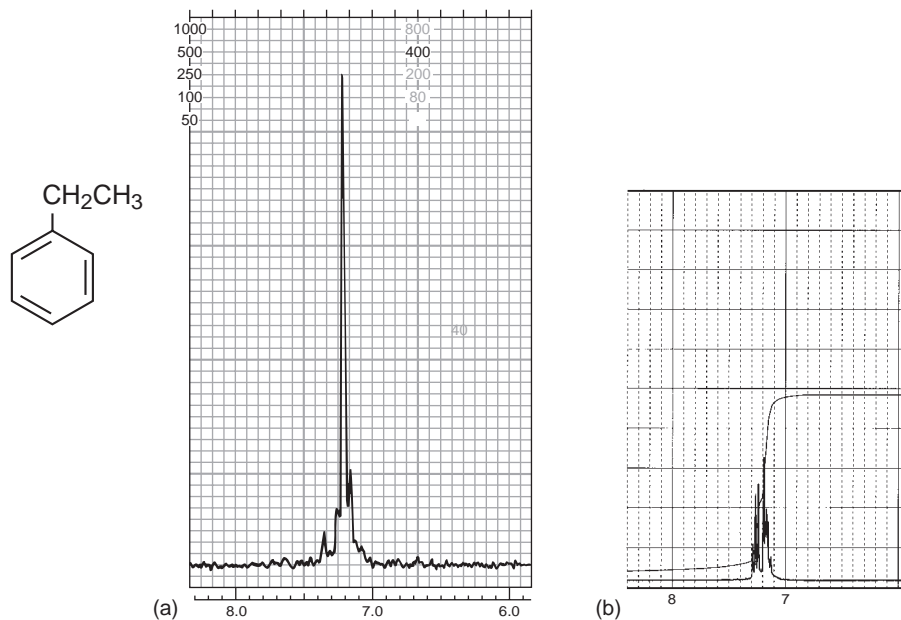
FIGURE 5.54 The aromatic ring portions of the ^{1}H NMR spectrum of ethylbenzene at (a) 60 MHz and (b) 300 MHz.

At 60 MHz, this chemical shift difference results in a complicated second-order splitting pattern for anisole (methoxybenzene), but the protons do fall clearly into two groups, the *ortho/para* protons and the *meta* protons. The 60-MHz NMR spectrum of the aromatic portion of anisole (Fig. 5.55) has a complex multiplet for the *o, p* protons (integrating for three protons) that is upfield from the *meta*
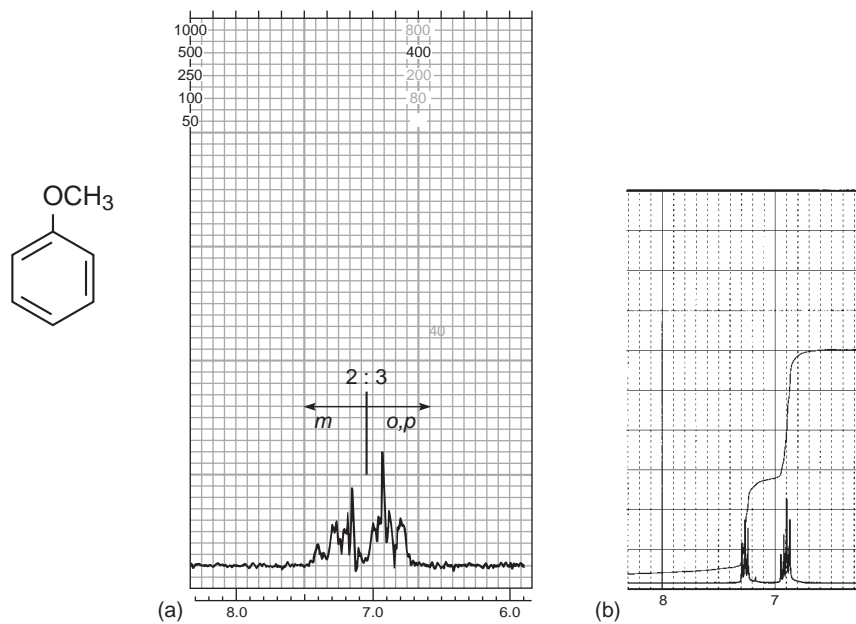
FIGURE 5.55 The aromatic ring portions of the ^{1}H NMR spectrum of anisole at (a) 60 MHz and (b) 300 MHz.
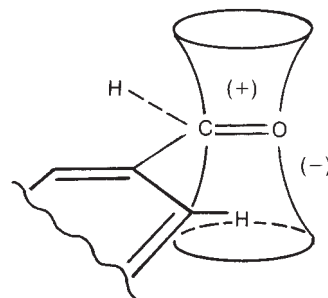
FIGURE 5.56 Anisotropic deshielding of the *ortho* protons of benzaldehyde.

protons (integrating for two protons), with a clear separation between the two types. Aniline (aminobenzene) provides a similar spectrum, also with a 3:2 split, owing to the electron-releasing effect of the amino group.

The 300-MHz spectrum of anisole shows the same separation between the *ortho/para* hydrogens (upfield) and the *meta* hydrogens (downfield). However, because the actual shift Δv (in Hertz) between the two types of hydrogens is greater, there is less second-order interaction, and the lines in the pattern are sharper at 300 MHz. In fact, it might be tempting to try to interpret the observed pattern as if it were first order, but remember that the protons on opposite sides of the ring are not magnetically equivalent even though there is a plane of symmetry (see Section 5.3). Anisole is an AA'BB'C spin system.

Anisotropy—Electron-Withdrawing Groups

A carbonyl or a nitro group would be expected to show (aside from anisotropy effects) a reverse effect since these groups are electron withdrawing. One would expect that the group would act to decrease the electron density around the *ortho* and *para* positions, thus deshielding the *ortho* and *para* hydrogens and providing a pattern exactly the reverse of the one shown for anisole (3:2 ratio, downfield:upfield). Convince yourself of this by drawing resonance structures. Nevertheless, the actual NMR spectra of nitrobenzene and benzaldehyde do not have the appearances that would be predicted on the basis of resonance structures. Instead, the *ortho* protons are much more deshielded than the *meta* and *para* protons due to the magnetic anisotropy of the π bonds in these groups.

Anisotropy is observed when a substituent group bonds a carbonyl group directly to the benzene ring (Fig. 5.56). Once again, the ring protons fall into two groups, with the *ortho* protons downfield from the *meta/para* protons. Benzaldehyde (Fig. 5.57) and acetophenone both show this effect in their NMR spectra. A similar effect is sometimes observed when a carbon–carbon double bond is attached to the ring. The 300-MHz spectrum of benzaldehyde (Fig. 5.57b) is a nearly first-order spectrum (probably a deceptively simple AA'BB'C spectrum) and shows a doublet (H_C, 2 H), a triplet (H_B, 1 H), and a triplet (H_A, 2 H).

B. *para*-Disubstituted Rings

Of the possible substitution patterns of a benzene ring, only a few are easily recognized. One of these is the *para*-disubstituted benzene ring. Examine anethole (Fig. 5.58a) as a first example. Because this compound has a plane of symmetry (passing through the methoxy and propenyl groups), the protons H_a and H_a' (both *ortho* to OCH_3) would be expected to have the same chemical shift. Similarly, the protons H_b and H_b' should have the same chemical shift. This is found to be the case. You might think that both sides of the ring should then have identical splitting patterns. With this assumption, one is tempted to look at each side of the ring separately, expecting a pattern in which proton H_b splits proton H_a into a doublet, and proton H_a splits proton H_b into a second doublet.
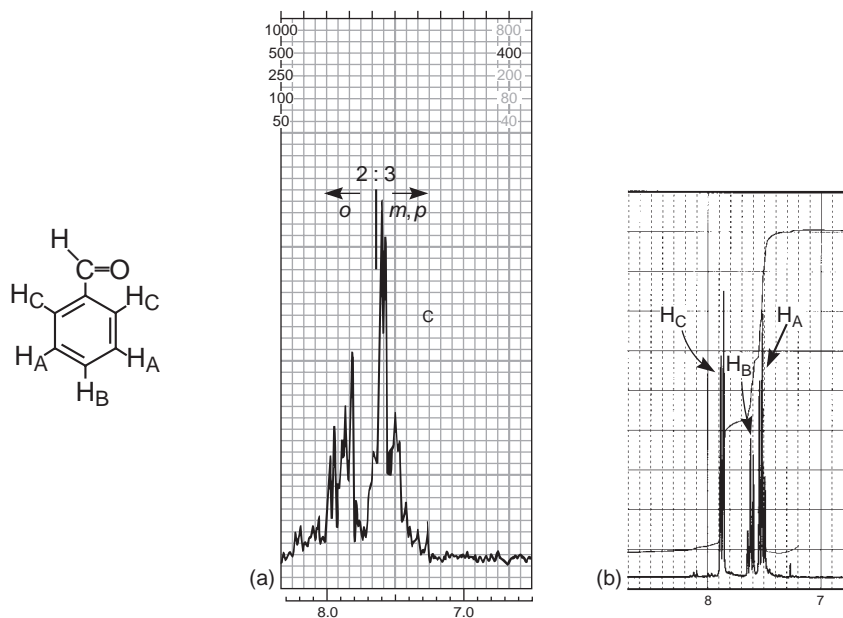
FIGURE 5.57 The aromatic ring portions of the ^1H NMR spectrum of benzaldehyde at (a) 60 MHz and (b) 300 MHz.

Examination of the NMR spectrum of anethole (Fig. 5.59a) shows (crudely) just such a four-line pattern for the ring protons. In fact, a *para*-disubstituted ring is easily recognized by this four-line pattern. However, the four lines do not correspond to a simple first-order splitting pattern. That is because the two protons H_a and H_a' are *not magnetically equivalent* (Section 5.3). Protons H_a and H_a' interact with each other and have finite coupling constant J_{aa}'. Similarly, H_b and H_b' interact with each other and have coupling constant J_{bb}'. More importantly, H_a does not interact equally with H_b (*ortho* to H_a) and with H_b' (*para* to H_a); that is, $J_{ab} \neq J_{ab}'$. If H_b and H_b' are coupled differently to H_a, they cannot be magnetically equivalent. Turning the argument around, H_a and H_a' also cannot be magnetically equivalent because they are coupled differently to H_b and to H_b'. This fact suggests that the situation is more
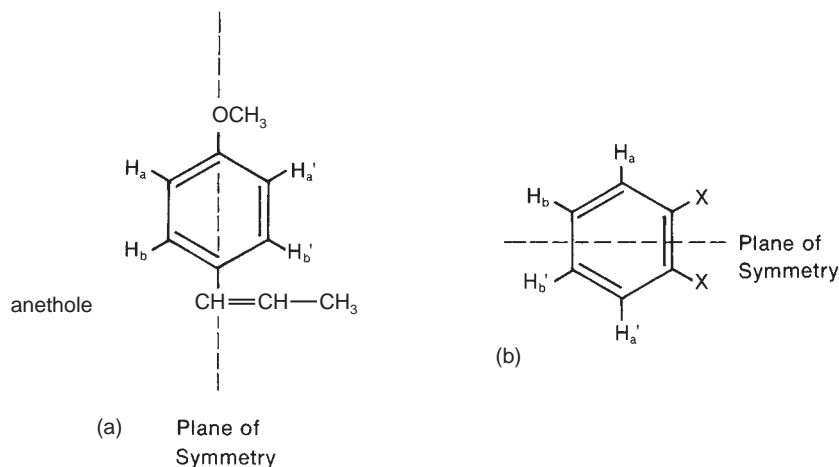
FIGURE 5.58 The planes of symmetry present in (a) a *para*-disubstituted benzene ring (anethole) and (b) a symmetric *ortho*-disubstituted benzene ring.

(a)   (b)
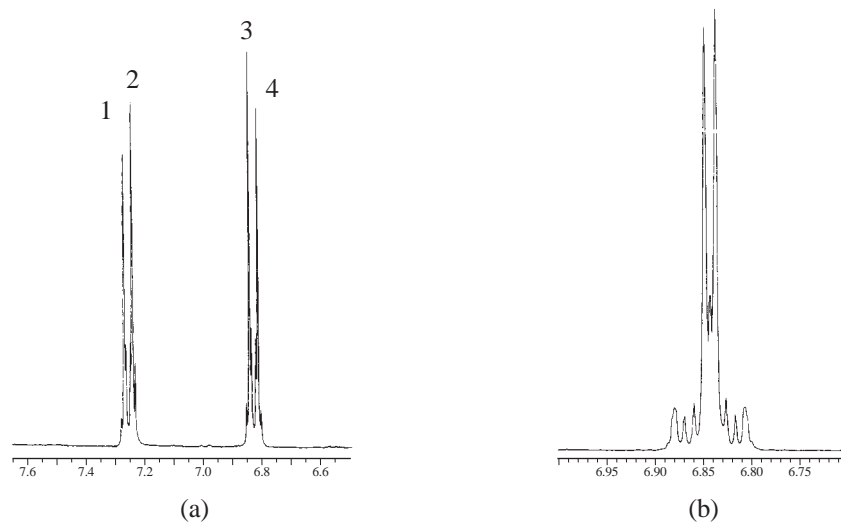
FIGURE 5.59 The aromatic ring portions of the 300-MHz ^{1}H NMR spectra of (a) anethole and (b) 4-allyloxyanisole.

complicated than it might at first appear. A closer look at the pattern in Figure 5.59a shows that this is indeed the case. With an expansion of the parts-per-million scale, this pattern actually resembles four distorted triplets, as shown in Figure 5.60. The pattern is an AA'BB' spectrum.

We will leave the analysis of this second-order pattern to more advanced texts. Note, however, that a crude four-line spectrum is characteristic of a *para*-disubstituted ring. It is also characteristic

(ppm)
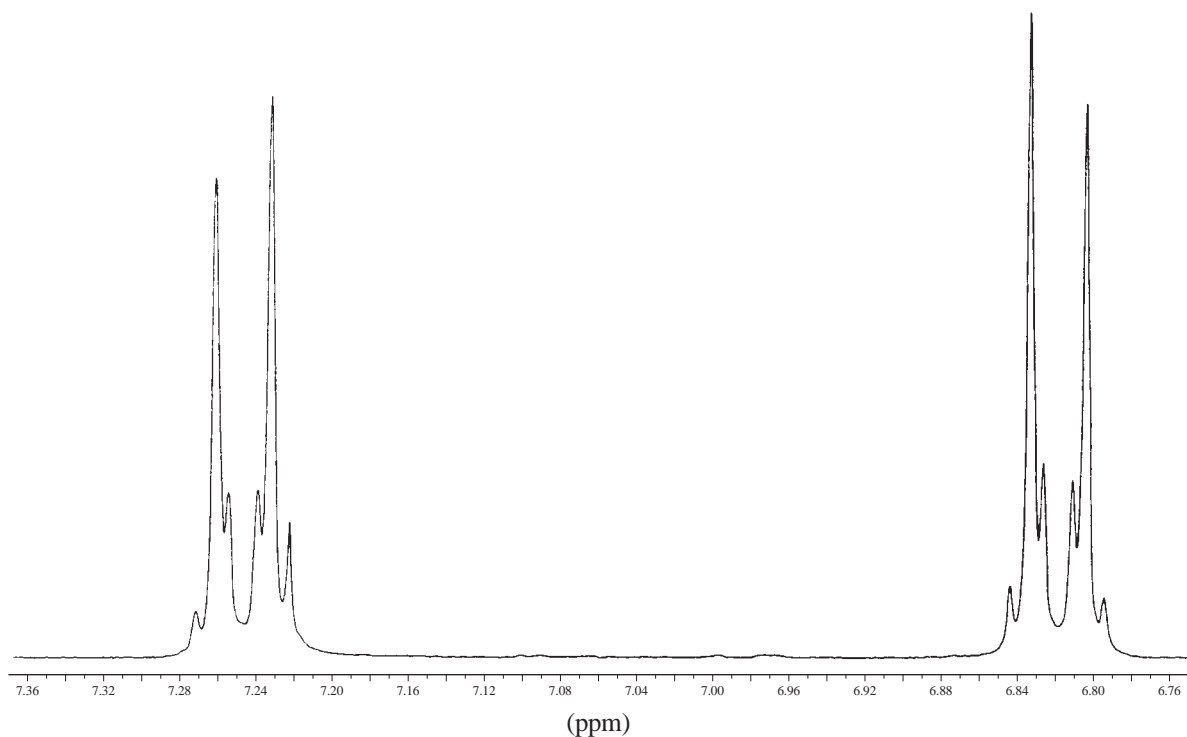
FIGURE 5.60 The expanded *para*-disubstituted benzene AA'BB' pattern.

of an *ortho*-disubstituted ring of the type shown in Figure 5.58b, in which the two *ortho* substituents are identical, leading to a plane of symmetry.

As the chemical shifts of H_a and H_b approach each other, the *para*-disubstituted pattern becomes similar to that of 4-allyloxyanisole (Fig. 5.59b). The inner peaks move closer together, and the outer ones become smaller or even disappear. Ultimately, when H_a and H_b approach each other closely enough in chemical shift, the outer peaks disappear, and the two inner peaks merge into a *singlet*; *p*-xylene, for instance, gives a singlet at 7.05 ppm (Table 5.8). Hence, a single aromatic resonance integrating for four protons could easily represent a *para*-disubstituted ring, but the substituents would obviously be identical.

C. Other Substitution

Other modes of ring substitution can often lead to splitting patterns more complicated than those of the aforementioned cases. In aromatic rings, coupling usually extends beyond the adjacent carbon atoms. In fact, *ortho, meta,* and *para* protons can all interact, although the last interaction (*para*) is not usually observed. Following are typical J values for these interactions:

ortho	*meta*	*para*
$^3J = 7-10$ Hz	$^4J = 1-3$ Hz	$^5J = 0-1$ Hz
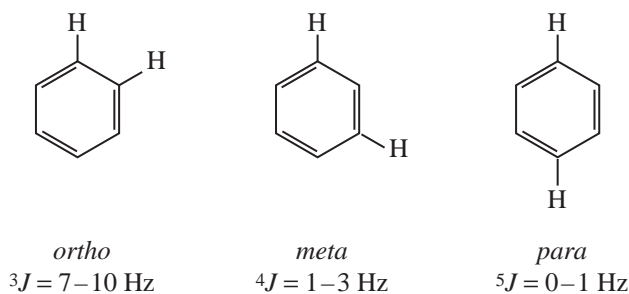
The trisubstituted compound 2,4-dinitroanisole shows all of the types of interactions mentioned. Figure 5.61 shows the aromatic-ring portion of the ^{1}H NMR spectrum of 2,4-dinitroanisole, and Figure 5.62 is its analysis. In this example, as is typical, the coupling between the *para* protons is essentially zero. Also notice the effects of the nitro groups on the chemical shifts of the adjacent pro-
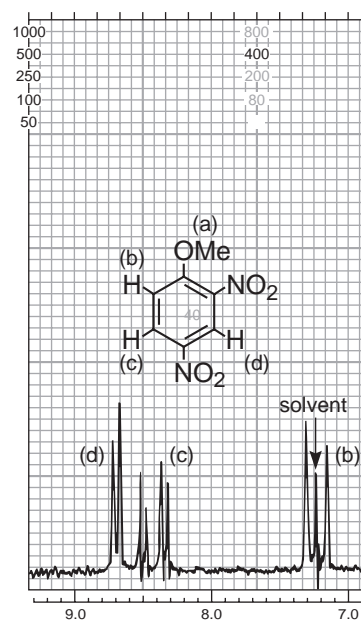
FIGURE 5.61   The aromatic ring portion of the 60-MHz ^{1}H NMR spectrum of 2,4-dinitroanisole.
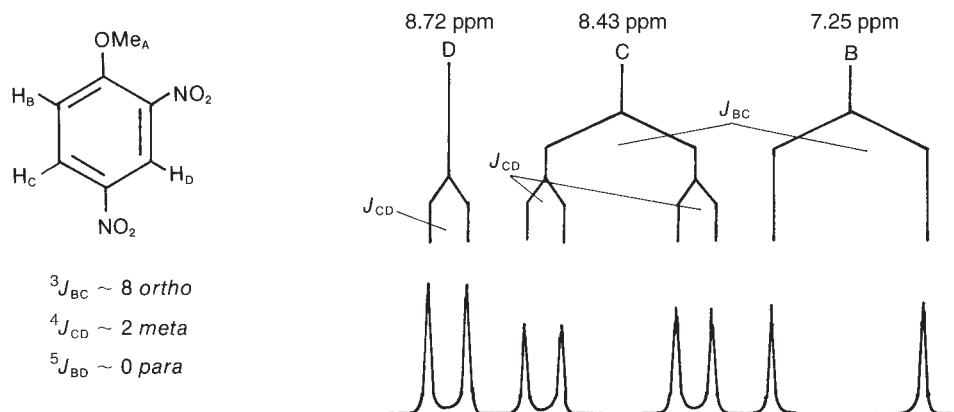
FIGURE 5.62 An analysis of the splitting pattern in the ^{1}H NMR spectrum of 2,4-dinitroanisole.

tons. Proton H_D, which lies between two nitro groups, has the largest chemical shift (8.72 ppm). Proton H_C, which is affected only by the anisotropy of a single nitro group, is not shifted as far downfield.

Figure 5.63 gives the 300-MHz ^{1}H spectra of the aromatic-ring portions of 2-, 3-, and 4-nitroaniline (the *ortho, meta,* and *para* isomers). The characteristic pattern of a *para*-disubstituted ring makes it easy to recognize 4-nitroaniline. Here, the protons on opposite sides of the ring are not magnetically equivalent, and the observed splitting is a second order. In contrast, the splitting patterns for 2- and 3-nitroaniline are simpler, and at 300 MHz a first-order analysis will suffice to explain the spectra. As an exercise, see if you can analyze these patterns, assigning the multiplets to specific protons on the ring. Use the indicated multiplicities (s, d, t, etc.) and expected chemical shifts to help your assign-
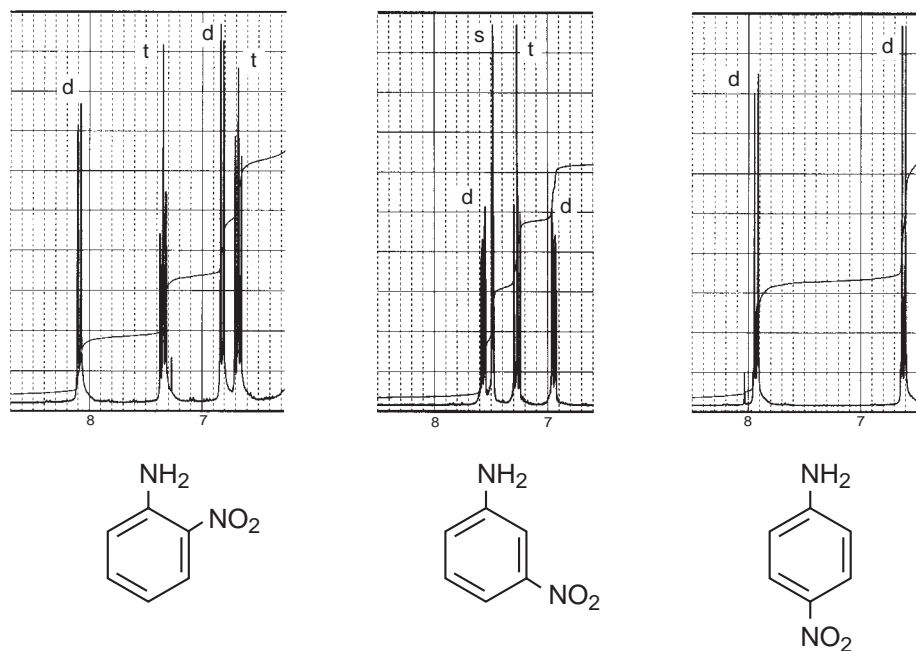
FIGURE 5.63 The 300-MHz ^{1}H NMR spectra of the aromatic ring portions of 2-, 3-, and 4-nitroaniline.
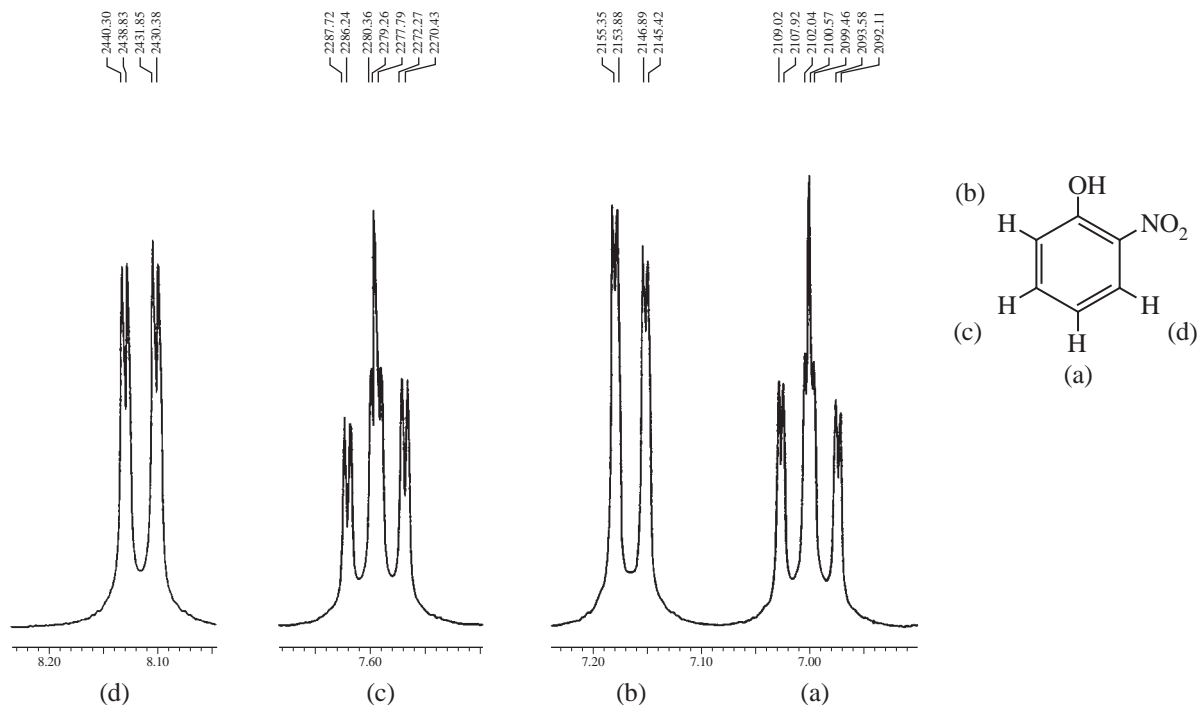
FIGURE 5.64 Expansions of the aromatic ring proton multiplets from the 300-MHz ^{1}H NMR spectrum of 2-nitrophenol. The hydroxyl resonance is not shown.

ments. You may ignore any *meta* or *para* interactions, remembering that ^4J and ^5J couplings will be too small in magnitude to be observed on the scale that these figures are presented.

In Figures 5.64 and 5.65 the expanded ring-proton spectra of 2-nitrophenol and 3-nitrobenzoic acid are presented. The phenol and acid resonances, respectively, are not shown. In these spectra, the position of each subpeak is given in Hertz. For these spectra, it should be possible not only to assign peaks to specific hydrogens but also to derive tree diagrams with discrete coupling constants for each interaction (see Problem 1 at the end of this chapter).

5.11 COUPLING IN HETEROAROMATIC SYSTEMS

Heteroaromatic systems (furans, pyrroles, thiophenes, pyridines, etc.) show couplings analogous to those in benzenoid systems. In furan, for instance, couplings occur between all of the ring protons. Typical values of coupling constants for furanoid rings follow. The analogous couplings in pyrrole systems are similar in magnitude.
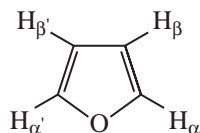
$$^3J_{\alpha\beta} = 1.6 - 2.0 \text{ Hz}$$

$$^4J_{\alpha\beta'} = 0.3 - 0.8 \text{ Hz}$$

$$^4J_{\alpha\alpha'} = 1.3 - 1.8 \text{ Hz}$$

$$^3J_{\beta\beta'} = 3.2 - 3.8 \text{ Hz}$$
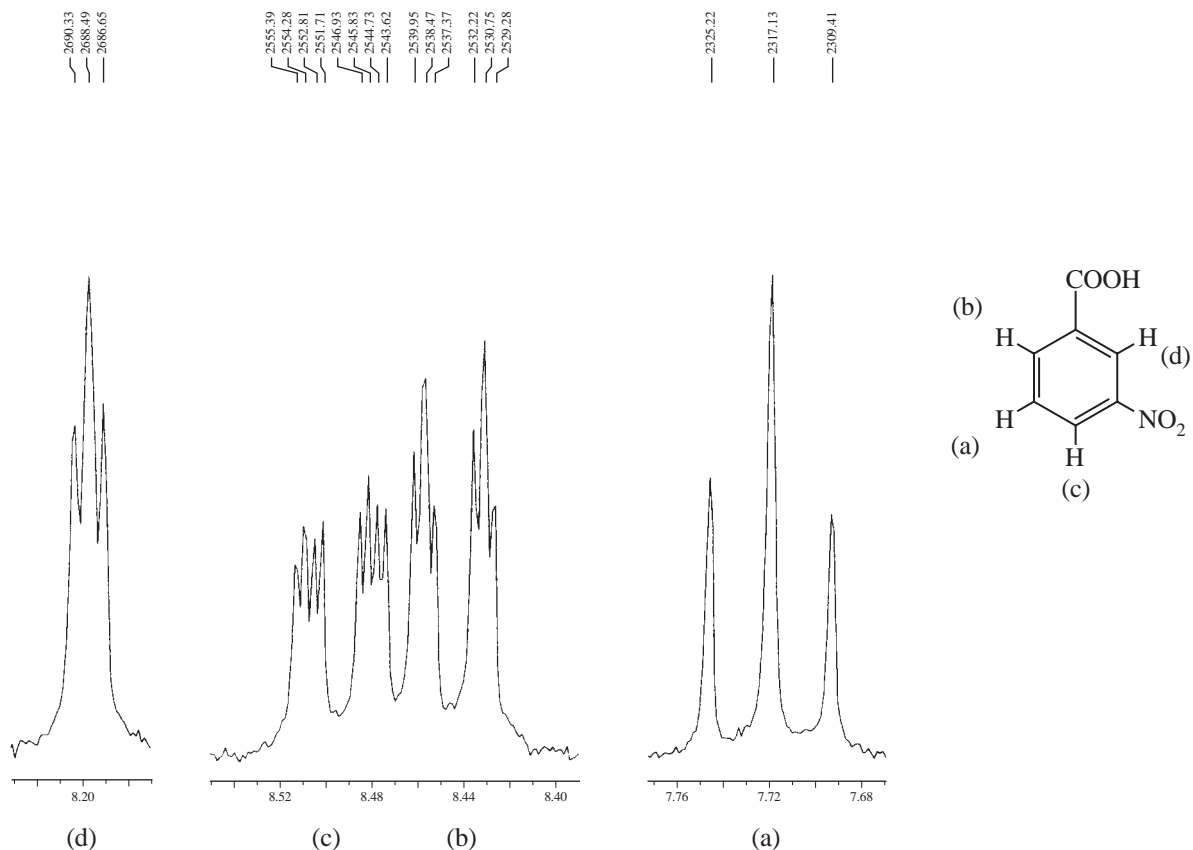
F I G U R E 5 . 6 5   Expansions of the aromatic ring proton multiplets from the 300-MHz ^{1}H NMR spectrum of 3-nitrobenzoic acid. The acid resonance is not shown.

The structure and spectrum for furfuryl alcohol are shown in Figure 5.66. Only the ring hydrogens are shown—the resonances of the hydroxymethyl side chain (—CH$_2$OH) are not included. Determine a tree diagram for the splittings shown in this molecule and determine the magnitude of the coupling constants (see Problem 1 at the end of this chapter). Notice that proton H$_a$ not only shows coupling to the other two ring hydrogens (H$_b$ and H$_c$) but also appears to have small unresolved *cis*-allylic interaction with the methylene (CH$_2$) group.

Figure 5.67 shows the ring-proton resonances of 2-picoline (2-methylpyridine)—the methyl resonance is not included. Determine a tree diagram that explains the observed splittings and extract the values of the coupling constants (see Problem 1 at the end of this chapter). Typical values of coupling constants for a pyridine ring are different from the analogous couplings in benzene:

$^3J_{ab} = 4-6$ Hz $^3J_{bc} = 7-9$ Hz

$^4J_{ac} = 0-2.5$ Hz $^4J_{bd} = 0.5-2$ Hz

$^5J_{ad} = 0-2.5$ Hz

$^4J_{ae} = <1$ Hz
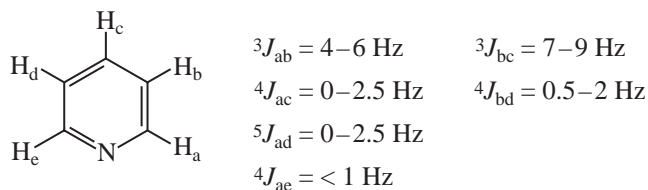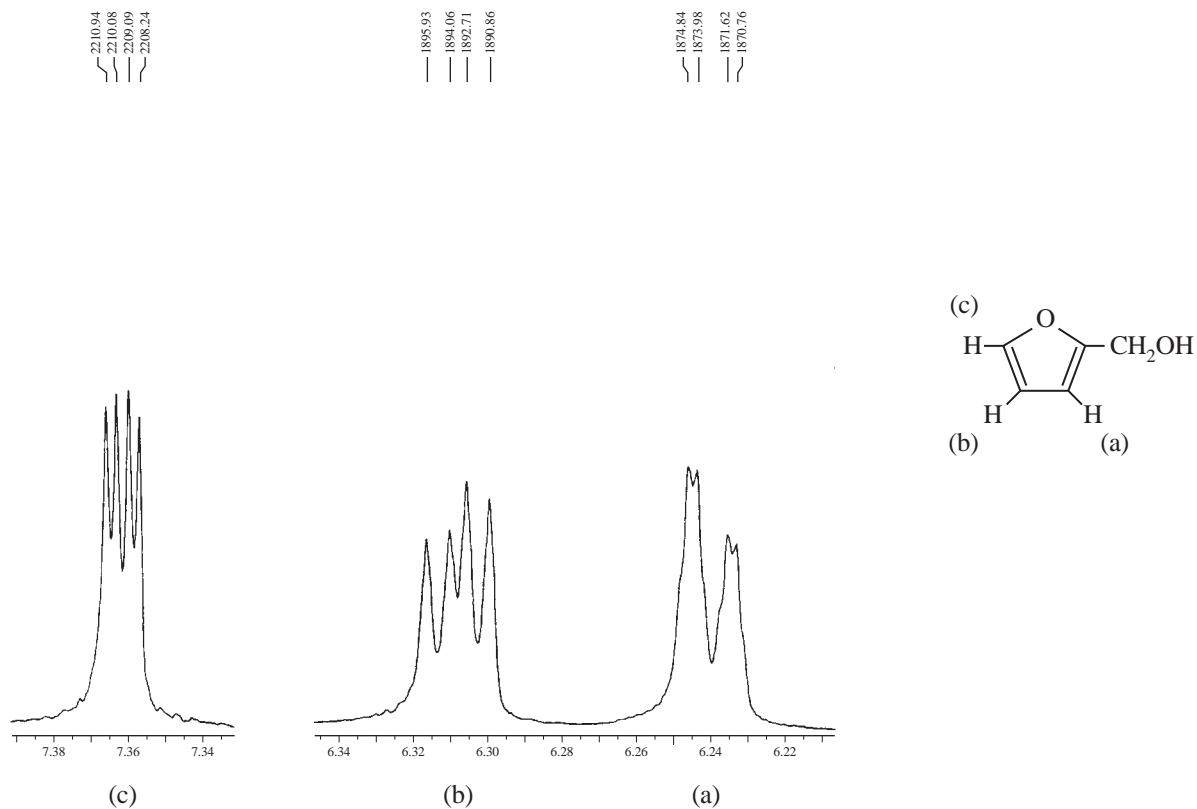
FIGURE 5.66 Expansions of the ring proton resonances from the 300-MHz ^{1}H NMR spectrum of furfuryl alcohol. The resonances from the hydroxymethyl side chain are not shown.

Notice that the peaks originating from proton H_d are quite broad, suggesting that some long-range splitting interactions may not be completely resolved. There may also be some coupling of this hydrogen to the adjacent nitrogen ($I = 1$) or a quadrupole-broadening effect operating (Section 6.5). Coupling constant values for other heterocycles may be found in Appendix 5, p. A15.
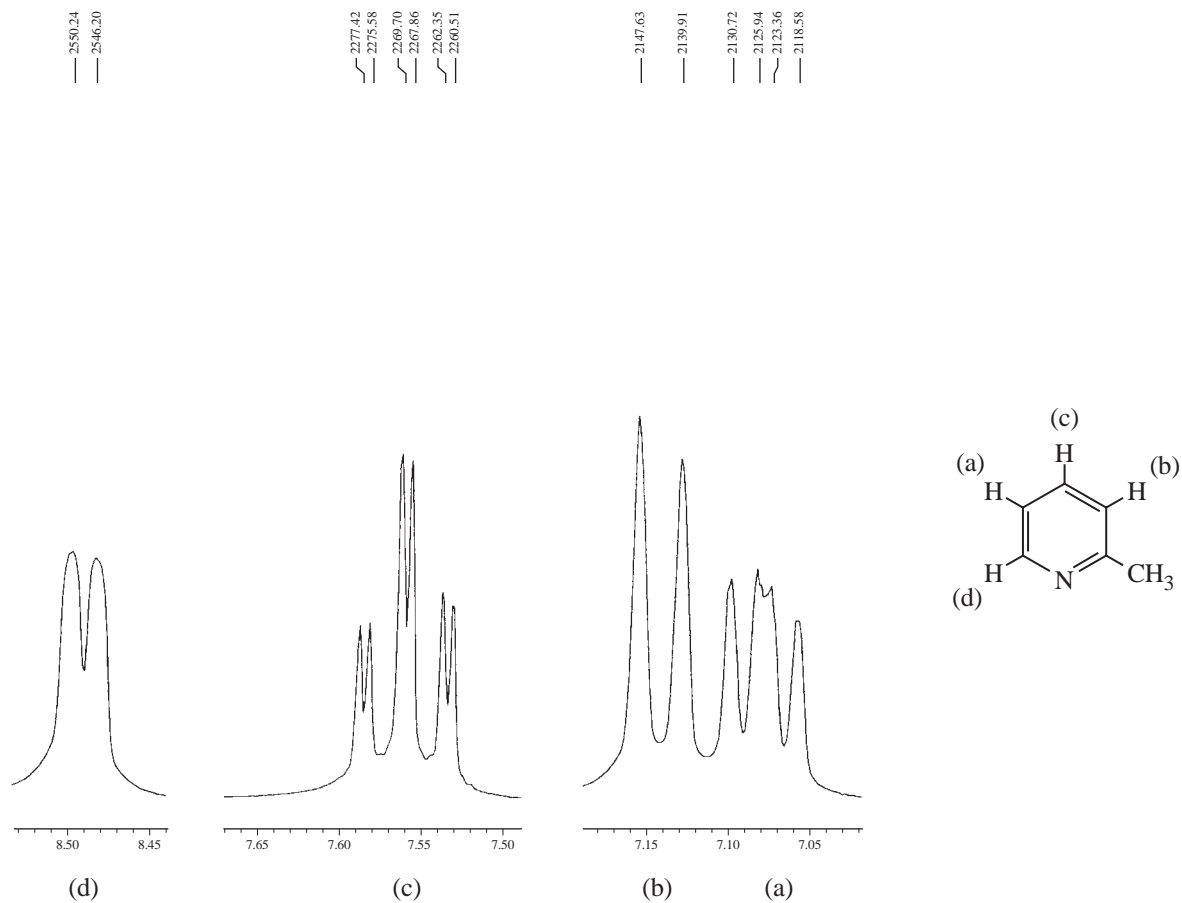
FIGURE 5.67   Expansions of the ring proton resonances from the 300-MHz ^{1}H NMR spectrum of 2-picoline (2-methylpyridine). The methyl resonance is not shown.

PROBLEMS

*1. Determine the coupling constants for the following compounds from their NMR spectra shown in this chapter. Draw tree diagrams for each of the protons.

(a) Vinyl acetate (Fig. 5.45).

(b) Crotonic acid (Fig. 5.48).

(c) 2-Nitrophenol (Fig. 5.64).

(d) 3-Nitrobenzoic acid (Fig. 5.65).

(e) Furfuryl alcohol (Fig. 5.66).

(f) 2-Picoline (2-methylpyridine) (Fig. 5.67).

*2. Estimate the expected splitting (*J* in Hertz) for the lettered protons in the following compounds; i.e., give J_{ab}, J_{ac}, J_{bc}, and so on. You may want to refer to the tables in Appendix 5.

(a)

H_a, Cl / H_b, Cl

(b)

H_a, H_b / Cl, CH_3

(c)

H_a, H_b / Cl, Cl

(d)

H_a H_b ... Cl Cl (cyclopentane ring)

(e)

H_a / H_b (cyclopentene ring)

(f)

OCH_3 H_a / H_b (cyclohexene ring)

(g)

H_a, CH_3 / CH_3, H_b

(h)

H_a, Cl / Cl, H_b

(i)

H_a, H_b / Cl, H_c
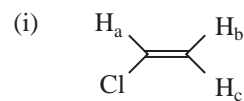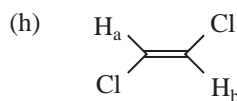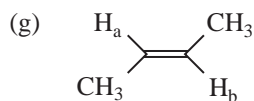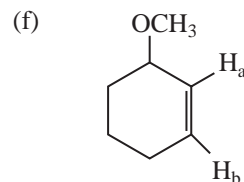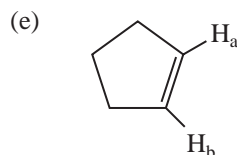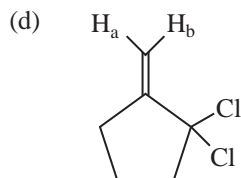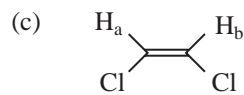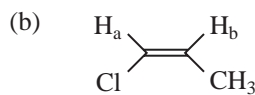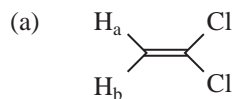
*3. Determine the coupling constants for methyl vinyl sulfone. Draw tree diagrams for each of the three protons shown in the expansions, using Figures 5.50–5.53 as examples. Assign the protons to the structure shown using the letters a, b, c, and d. Hertz values are shown above each of the peaks in the expansions.

1997.78 1987.87 1981.23 1971.31   1878.84 1862.24   1799.71 1789.79

d   c   b

(ppm)
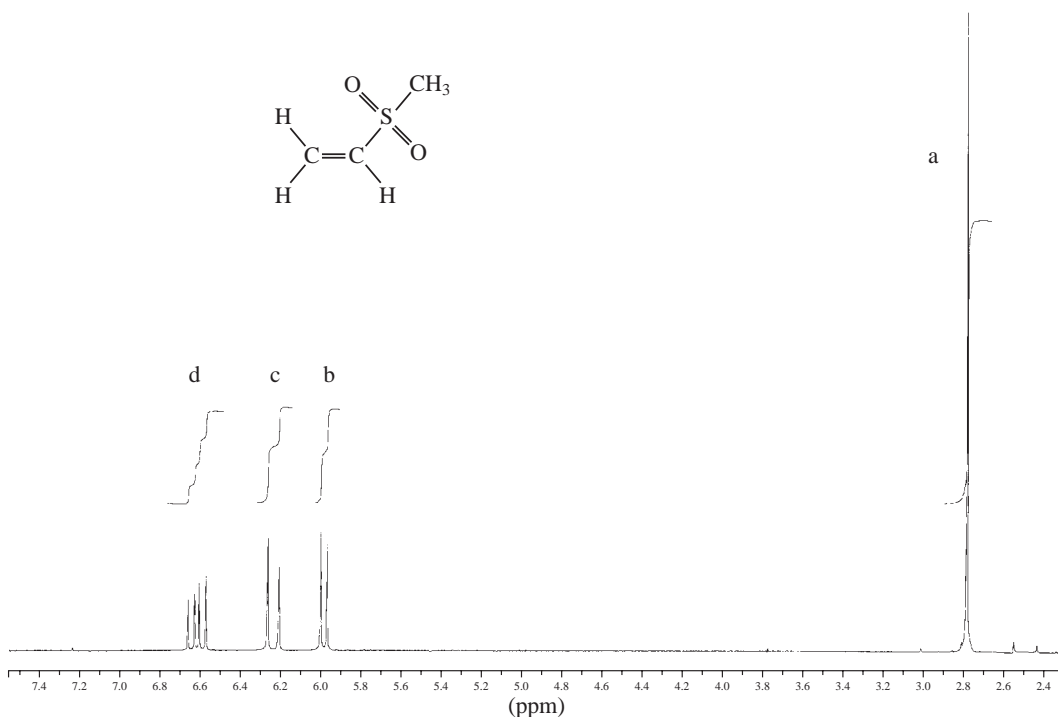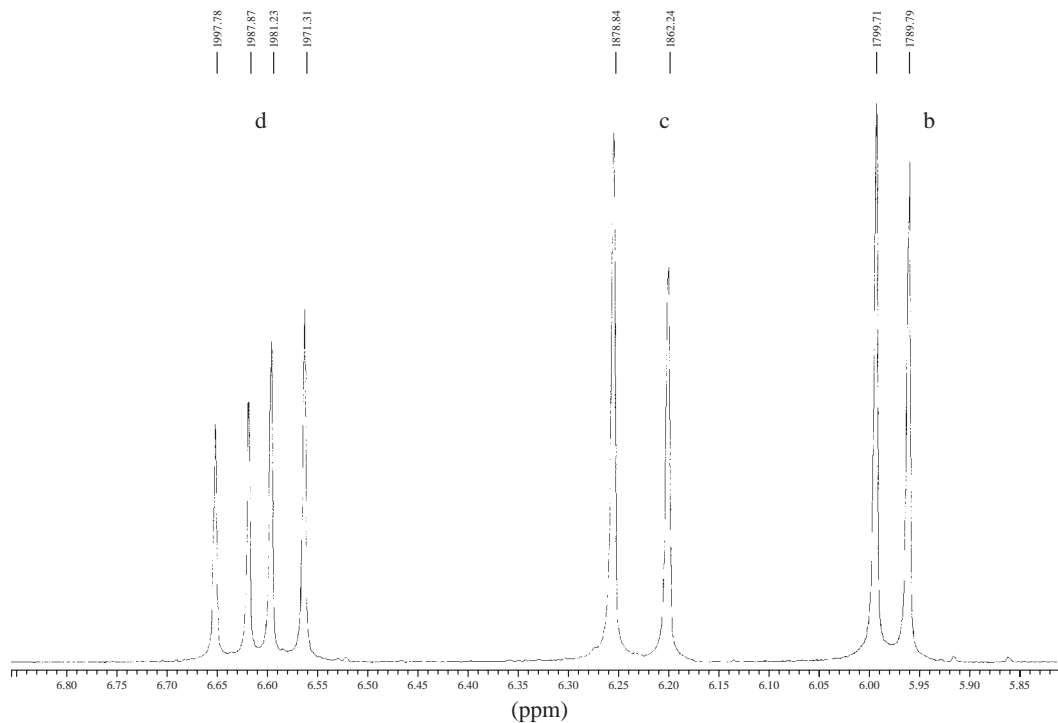
*4. The proton NMR spectrum shown in this problem is of *trans*-4-hexen-3-one. Expansions are shown for each of the five unique types of protons in this compound. Determine the coupling constants. Draw tree diagrams for each of the protons shown in the expansions and label them with the appropriate coupling constants. Also determine which of the coupling constants are ^3J and which are ^4J. Assign the protons to the structure using the letters a, b, c, d, and e. Hertz values are shown above each of the peaks in the expansions.

b

a

c

e   d

(ppm)

e

2016.57
2009.75
2002.94
2000.86
1996.12
1994.05
1987.24
1980.42

6.72   6.68   6.64   6.60
(ppm)

d

1787.54
1785.91
1784.28
1782.50
1771.83
1770.06
1768.43
1766.80

5.96   5.92   5.88
(ppm)

c

719.42
712.02
704.76
697.35

2.40   2.36   2.32
(ppm)

b

513.06
511.43
506.24
504.61

1.72   1.68
(ppm)

a

271.14
263.88
256.47

0.92   0.88   0.84
(ppm)
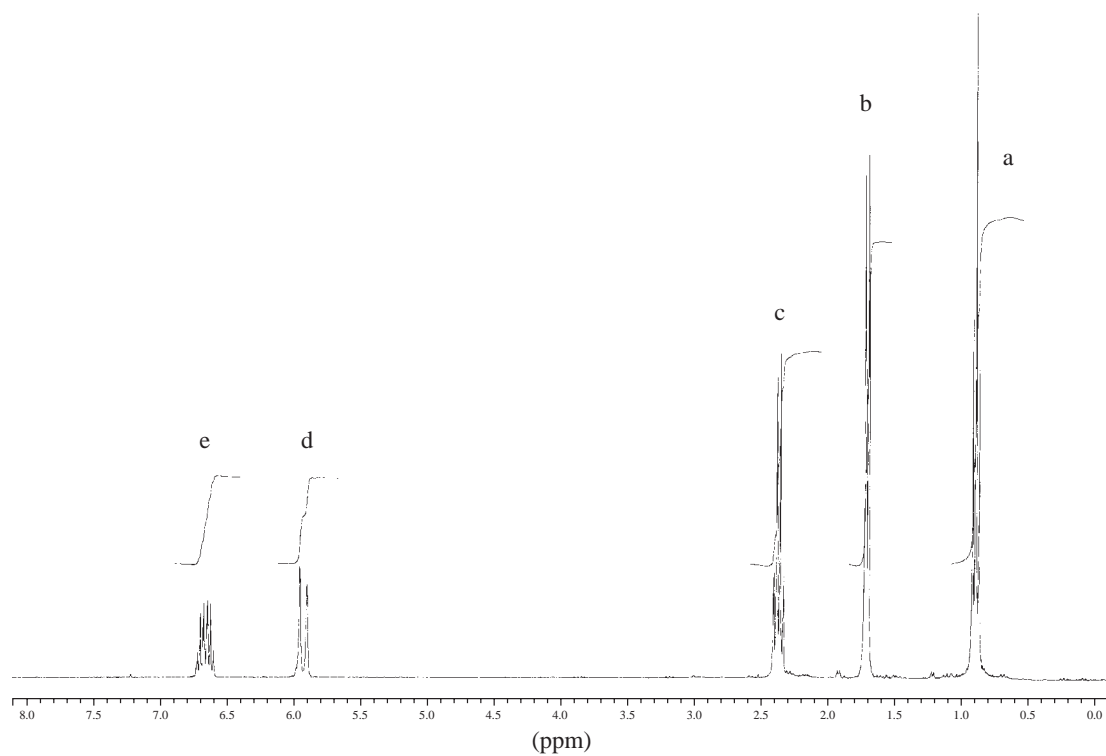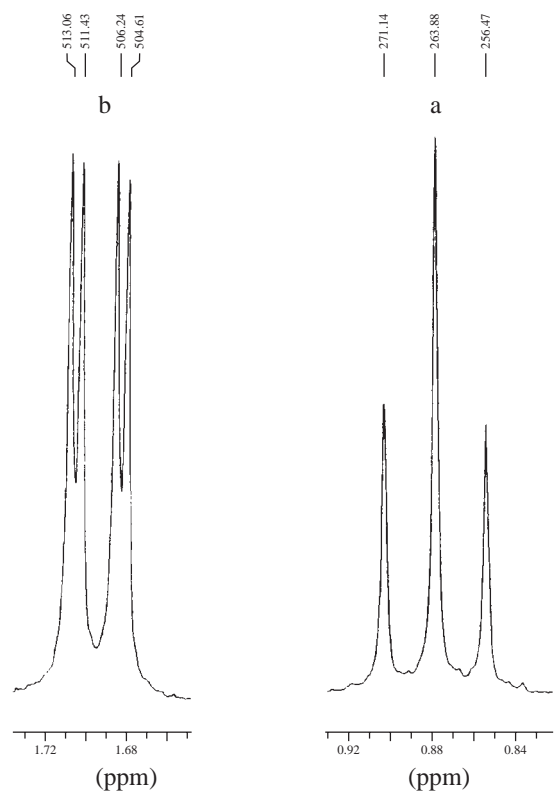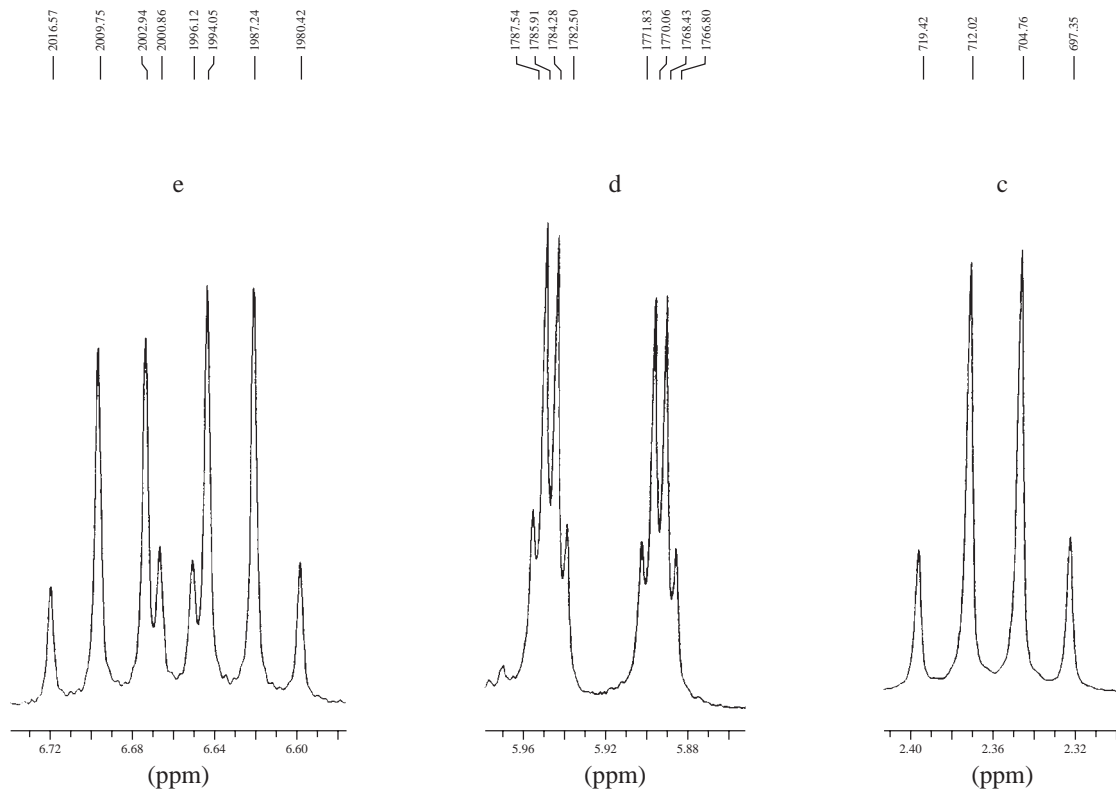
*5. The proton NMR spectrum shown in this problem is of *trans*-2-pentenal. Expansions are shown for each of the five unique types of protons in this compound. Determine the coupling constants. Draw tree diagrams for each of the protons shown in the expansions and label them with the appropriate coupling constants. Also determine which of the coupling constants are ^3J and which are ^4J. Assign the protons to the structure using the letters a, b, c, d, and e. Hertz values are shown above each of the peaks in the expansions.

e

2808.72
2801.00

d

2048.35
2042.10
2035.85
2032.54
2026.66
2020.41

c

1797.96
1796.49
1795.02
1790.24
1788.77
1786.93
1782.52
1781.05
1779.21
1774.43
1772.96
1771.49

9.36 9.34 9.32
(ppm)

6.84 6.82 6.80 6.78 6.76 6.74 6.72
(ppm)

6.00 5.98 5.96 5.94 5.92 5.90 5.88
(ppm)

b

678.37
676.90
671.02
669.55
663.30
657.41
655.94
650.06
648.22

a

295.25
287.89
280.54

2.26 2.24 2.22 2.20 2.18 2.16 2.14
(ppm)

1.00 0.98 0.96 0.94 0.92
(ppm)
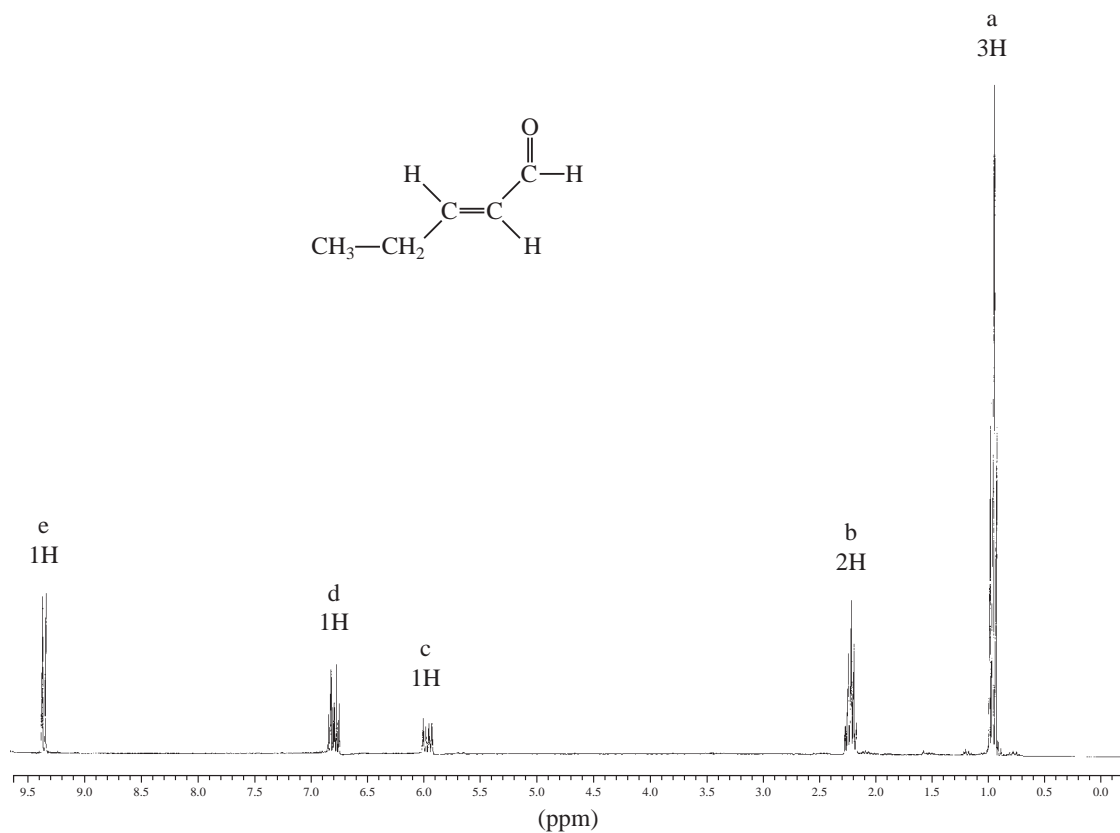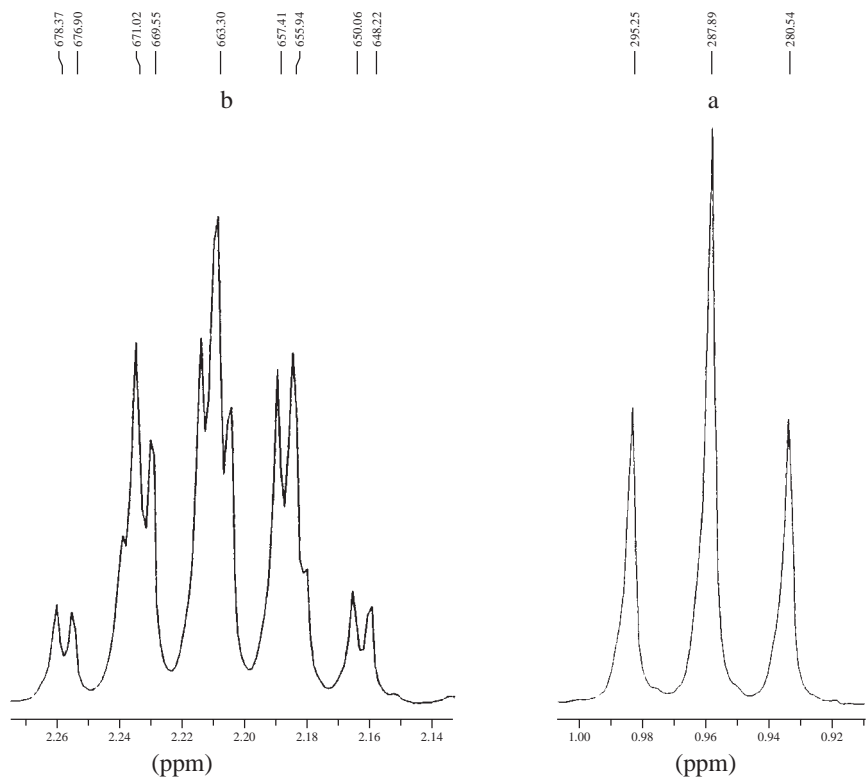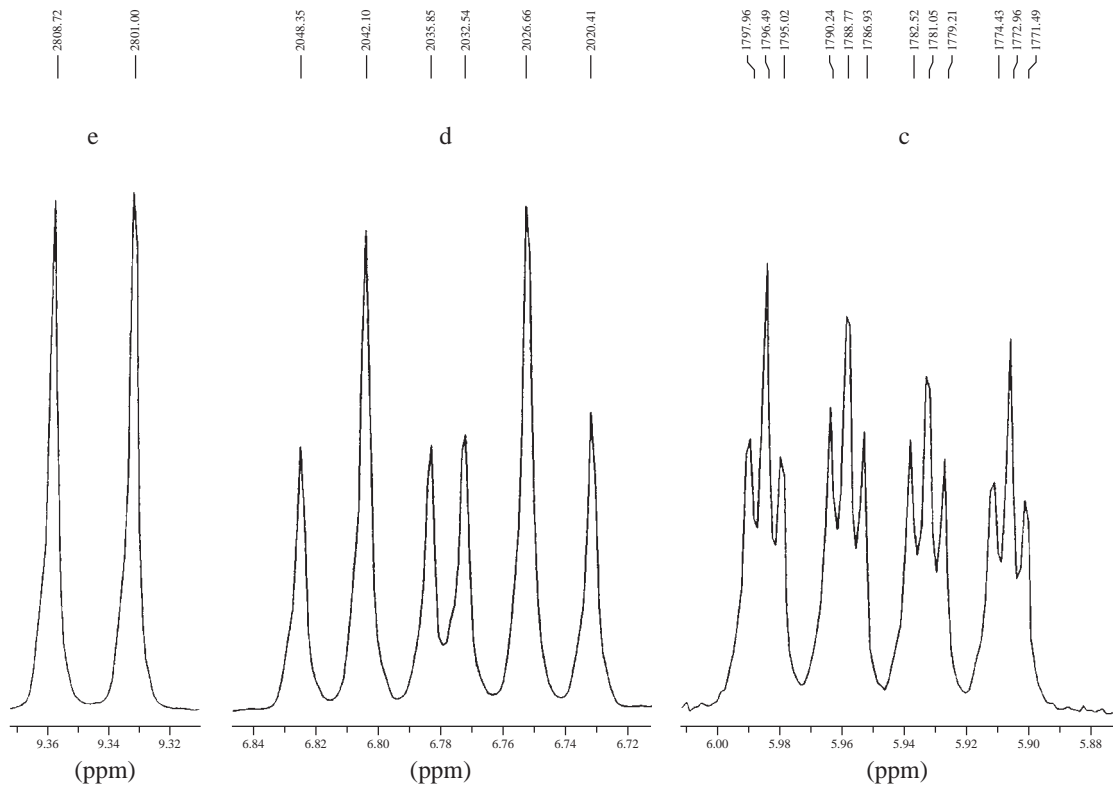
*6. In which of the following two compounds are you likely to see allylic (^4J) coupling?

A   B
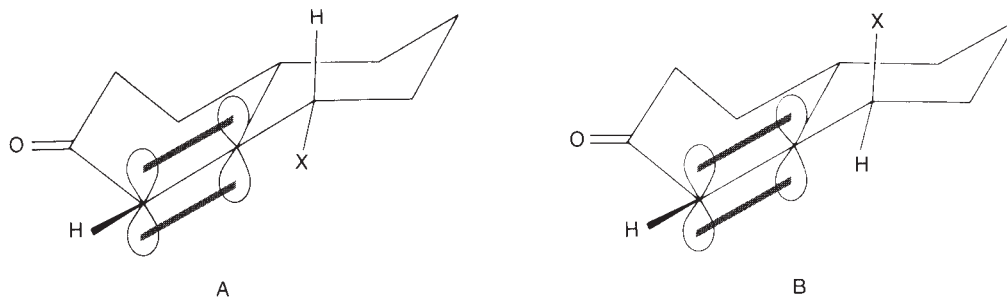
7. The reaction of dimethyl malonate with acetaldehyde (ethanal) under basic conditions yields a compound with formula $C_7H_{10}O_4$. The proton NMR is shown here. The normal carbon-13 and the DEPT experimental results are tabulated:

Normal Carbon	DEPT-135	DEPT-90
16 ppm	Positive	No peak
52.2	Positive	No peak
52.3	Positive	No peak
129	No peak	No peak
146	Positive	Positive
164	No peak	No peak
166	No peak	No peak

Determine the structure and assign the peaks in the proton NMR spectrum to the structure.
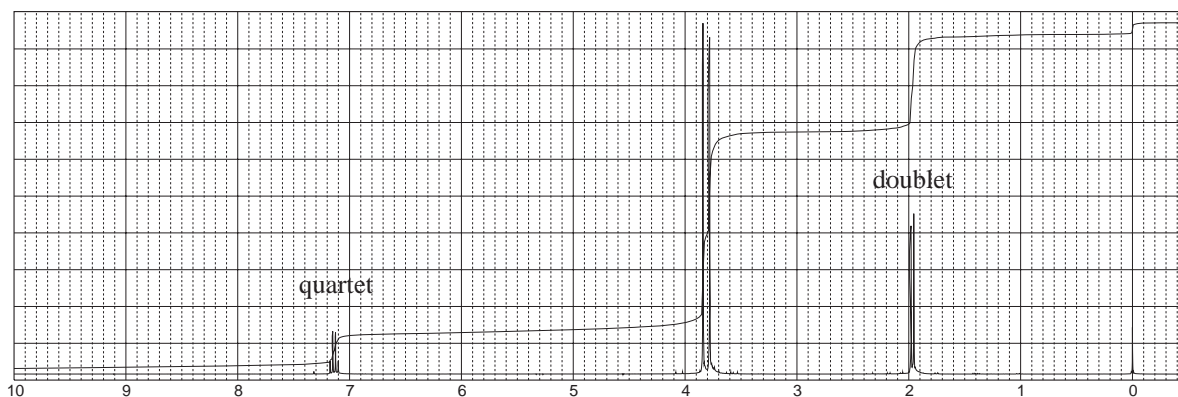
8. Diethyl malonate can be monoalkylated and dialkylated with bromoethane. The proton NMR spectra are provided for each of these alkylated products. Interpret each spectrum and assign an appropriate structure to each spectrum.
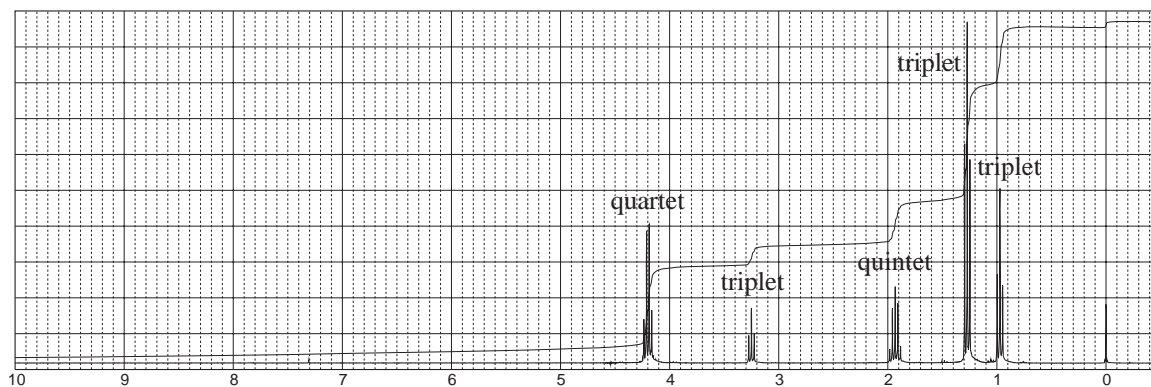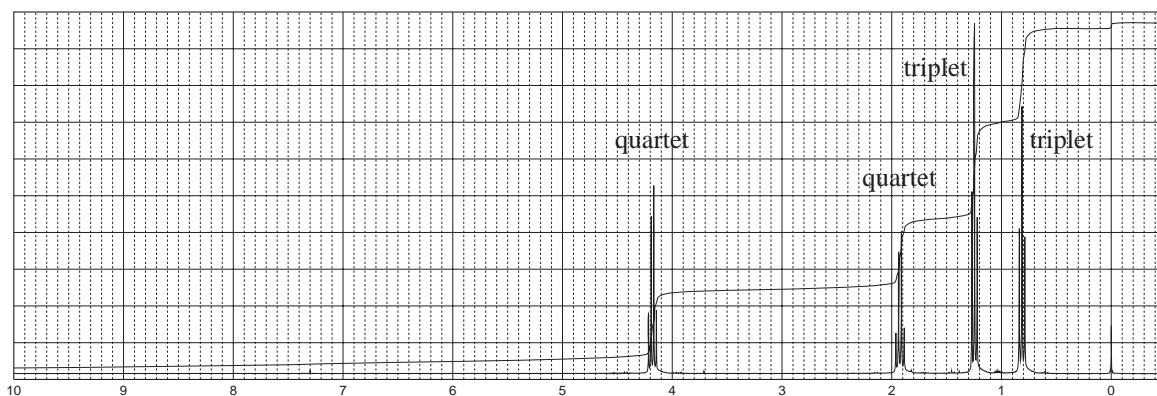
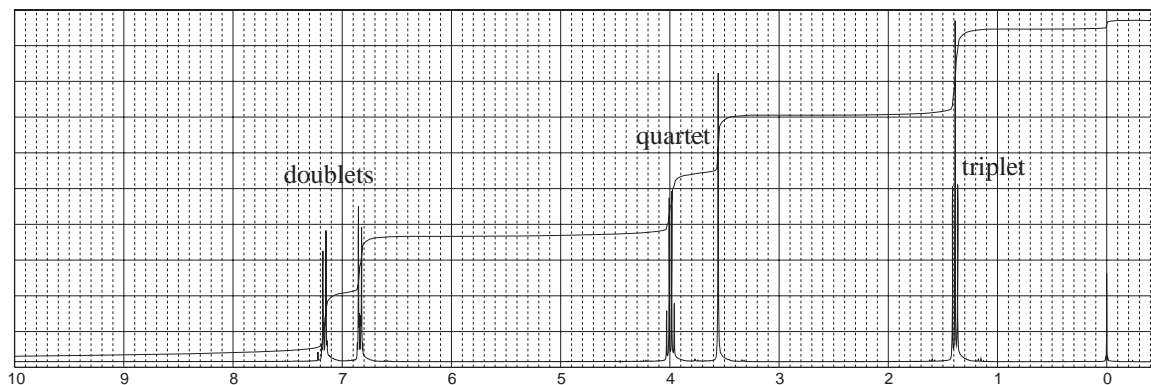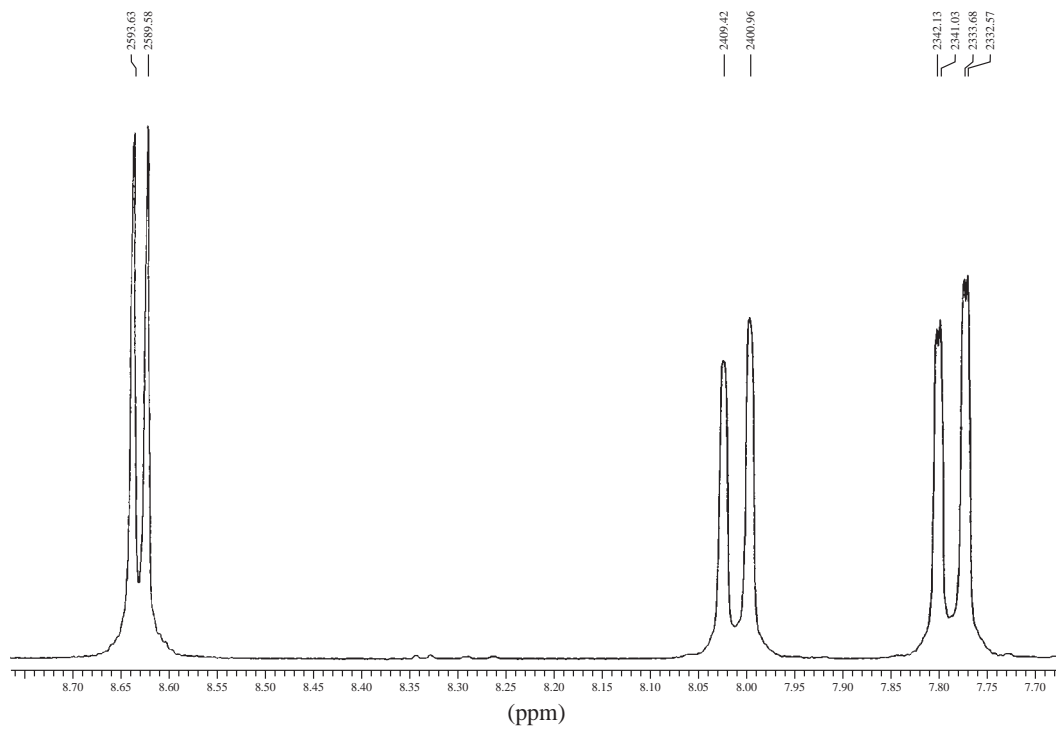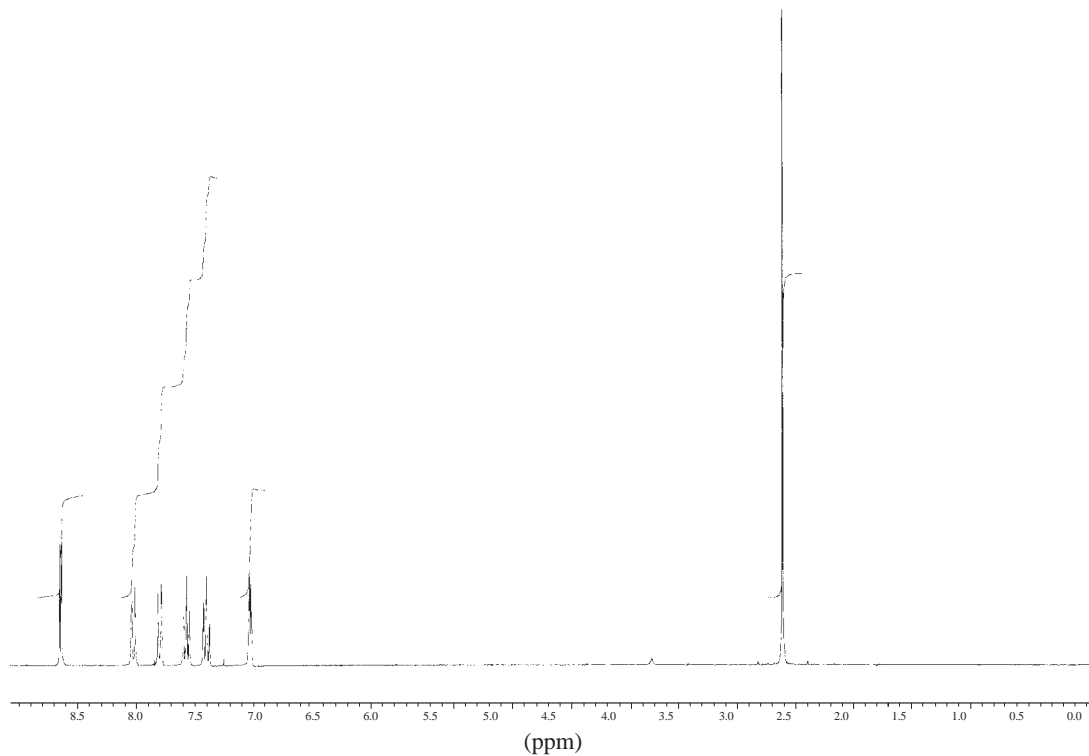9. The proton NMR spectral information shown in this problem is for a compound with formula $C_{10}H_{10}O_3$. A disubstituted aromatic ring is present in this compound. Expansions are shown for each of the unique protons. Determine the J values and draw the structure of this compound. The doublets at 6.45 and 7.78 ppm provide an important piece of information. Likewise, the broad peak at about 12.3 ppm provides information on one of the functional groups present in this compound. Assign each of the peaks in the spectrum.
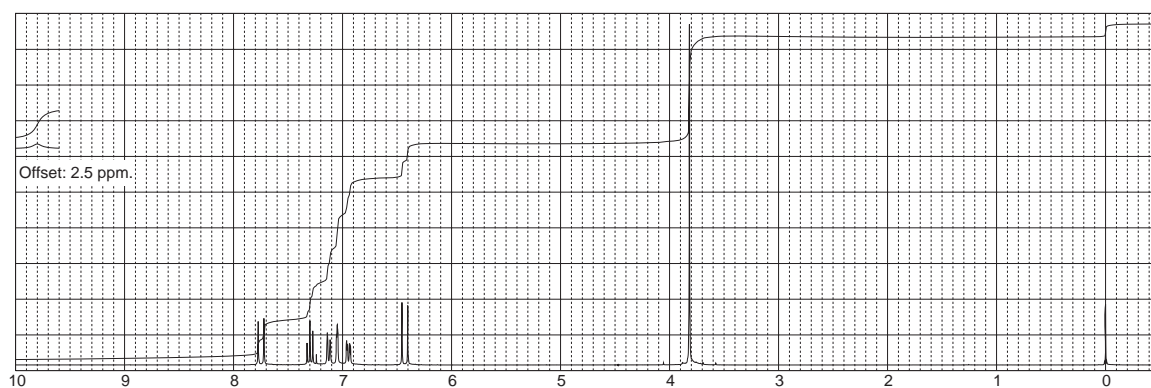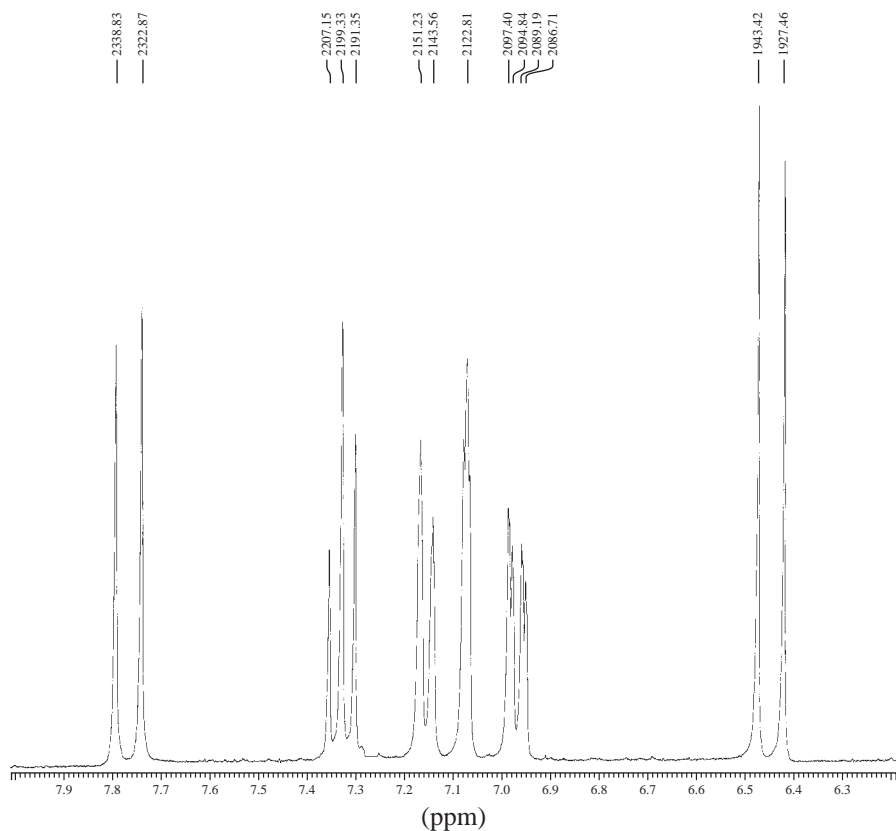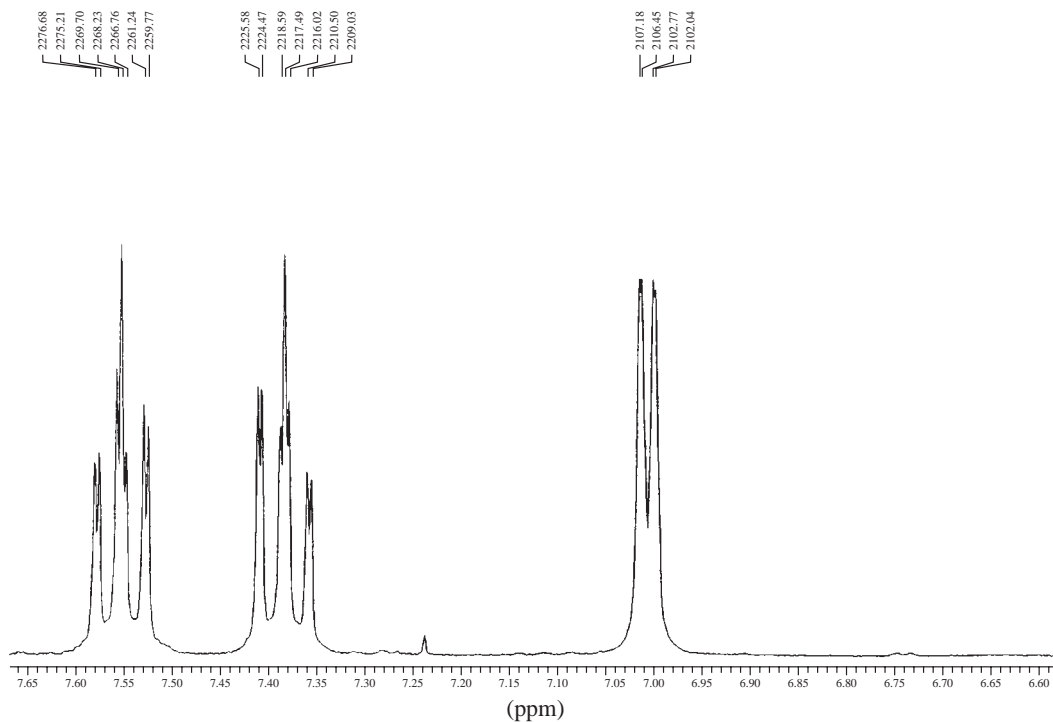
10. The proton NMR spectral information shown in this problem is for a compound with formula $C_8H_8O_3$. An expansion is shown for the region between 8.2 and 7.0 ppm. Analyze this region to determine the structure of this compound. A broad peak (1H) appearing near 12.0 ppm is not shown in the spectrum. Draw the structure of this compound and assign each of the peaks in the spectrum.

2456.11
2448.02

2283.87
2275.58
2267.88

2149.83
2142.11
2134.78
2127.04
2118.58

8.30 8.20 8.10 8.00 7.90 7.80 7.70 7.60 7.50 7.40 7.30 7.20 7.10 7.00

(ppm)
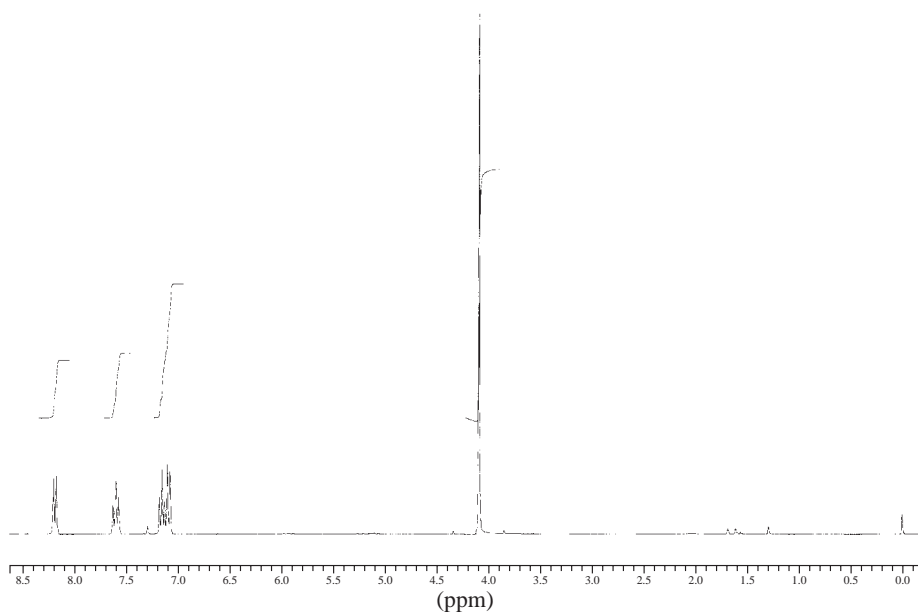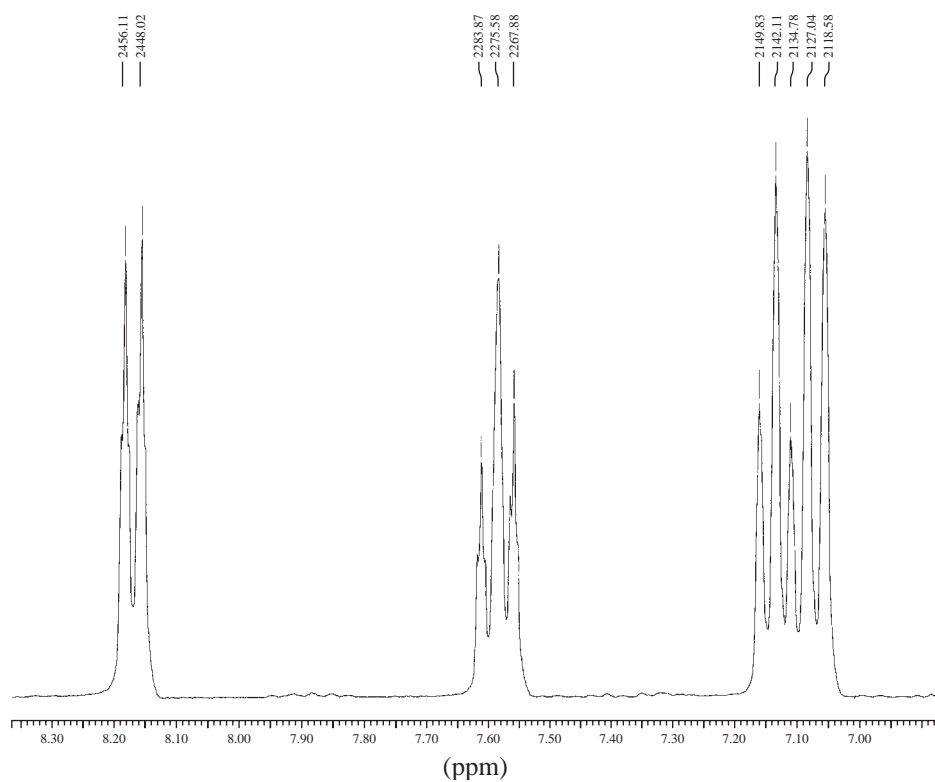
11. The proton NMR spectral information shown in this problem is for a compound with formula $C_{12}H_8N_2O_4$. An expansion is shown for the region between 8.3 and 7.2 ppm. No other peaks appear in the spectrum. Analyze this region to determine the structure of this compound. Strong bands appear at 1352 and 1522 cm^{-1} in the infrared spectrum. Draw the structure of this compound.

2473.89
2472.75
2465.85
2464.47

2317.73
2316.35
2310.26
2308.88
2302.80
2301.33

2290.05
2288.43
2281.85
2280.31
2274.39
2272.85

2196.55
2195.09
2189.00
2187.54

8.32 8.28 8.24 8.20 8.16 8.12 8.08 8.04 8.00 7.96 7.92 7.88 7.84 7.80 7.76 7.72 7.68 7.64 7.60 7.56 7.52 7.48 7.44 7.40 7.36 7.32 7.28 7.24 7.20

(ppm)
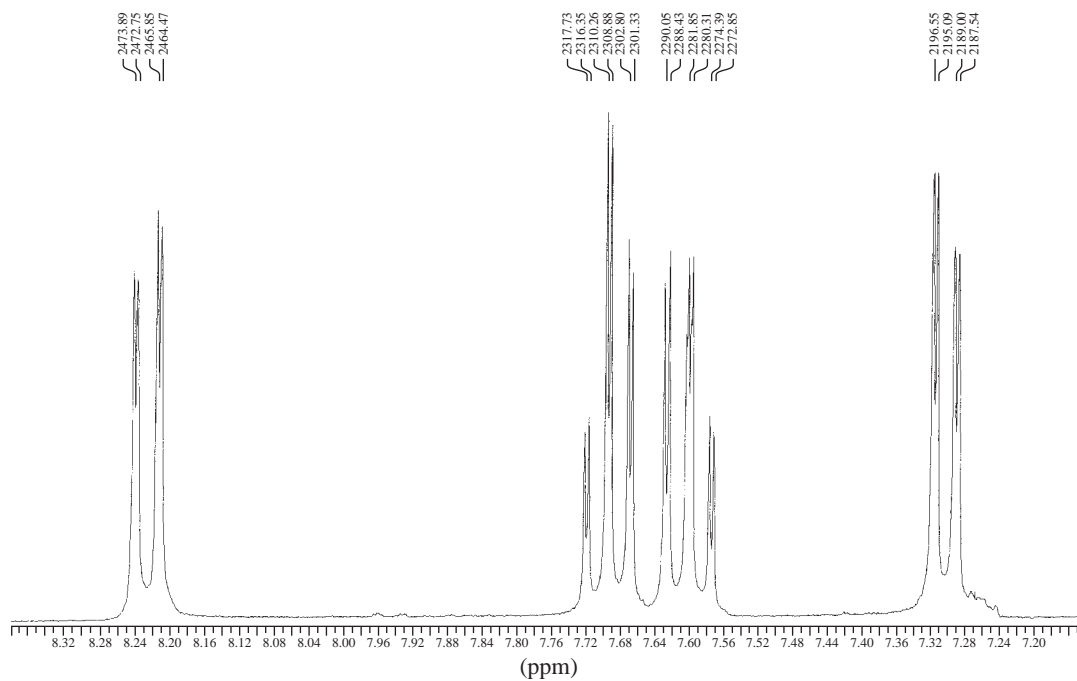
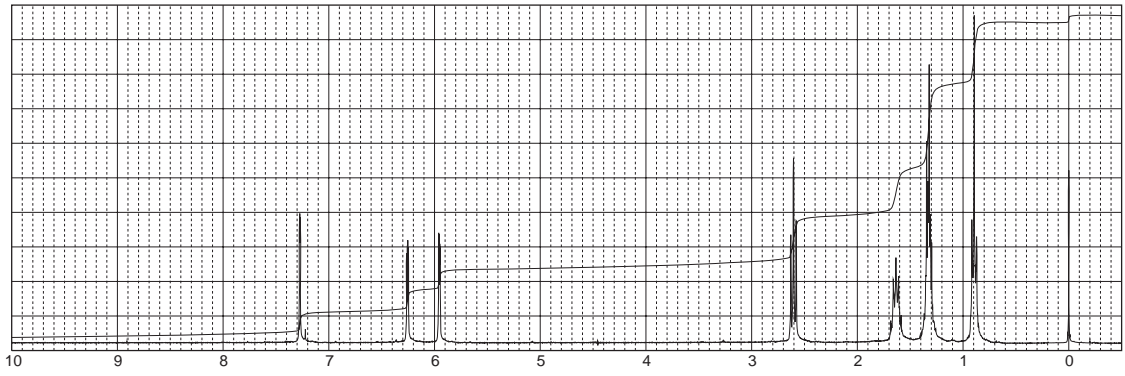**12.** The proton NMR spectral information shown in this problem is for a compound with formula $C_9H_{11}NO$. Expansions of the protons appearing in the range 9.8 and 3.0 ppm are shown. No other peaks appear in the full spectrum. The usual aromatic and aliphatic C–H stretching bands appear in the infrared spectrum. In addition to the usual C–H bands, two weak bands also appear at 2720 and 2842 cm^{-1}. A strong band appears at 1661 cm^{-1} in the infrared spectrum. Draw the structure of this compound.
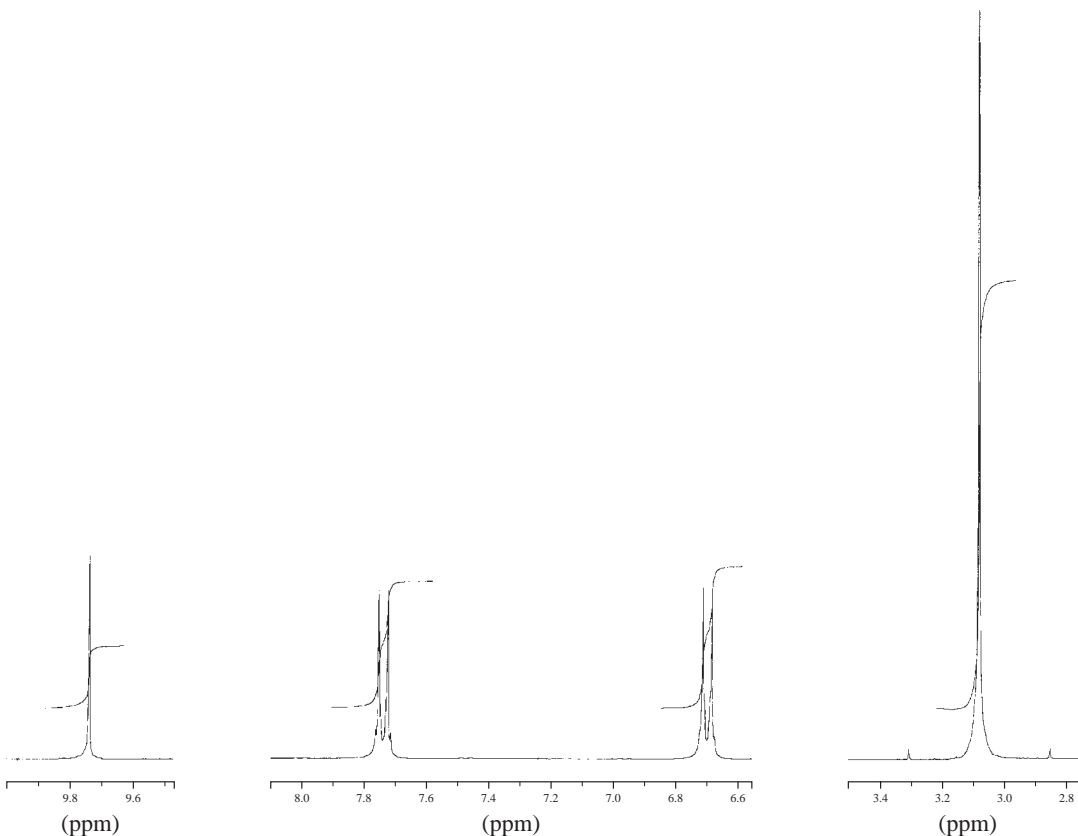
13. The fragrant natural product anethole ($C_{10}H_{12}O$) is obtained from anise by steam distillation. The proton NMR spectrum of the purified material follows. Expansions of each of the peaks are also shown, except for the singlet at 3.75 ppm. Deduce the structure of anethole, including stereochemistry, and interpret the spectrum.

7.30 7.25 7.20 7.15 7.10 7.05 7.00 6.95 6.90 6.85 6.80
(ppm)
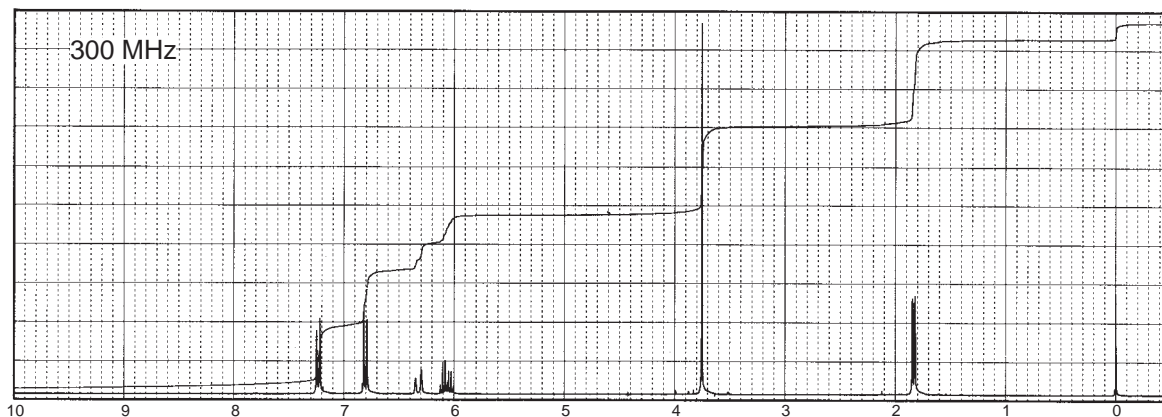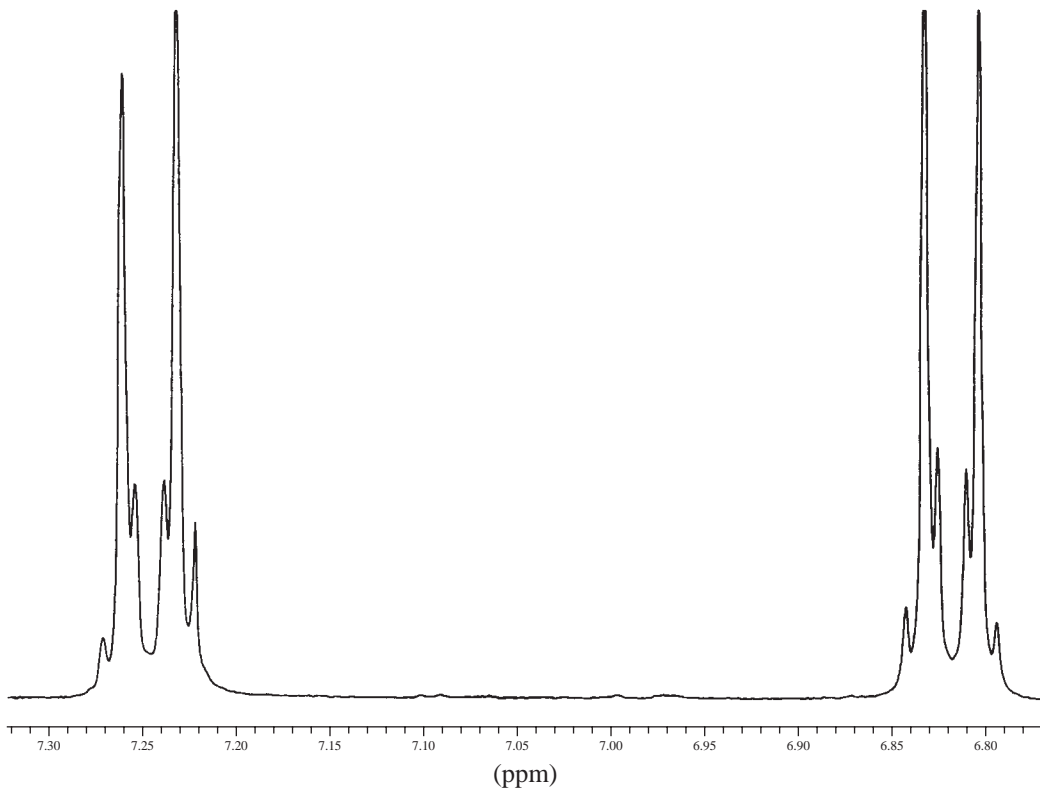
1909.76
1908.19
1893.95
1892.39
1842.15
1835.58
1829.00
1826.34
1822.43
1819.77
1813.20
1806.62
558.06
556.34
551.49
549.93

6.40 6.35 6.30 6.25 6.20 6.15 6.10 6.05 6.00
(ppm)

1.90 1.85 1.80
(ppm)
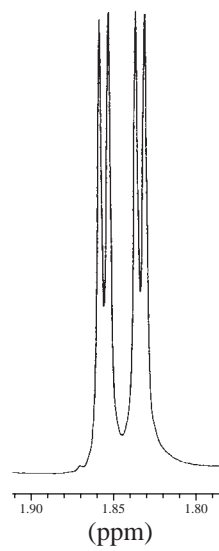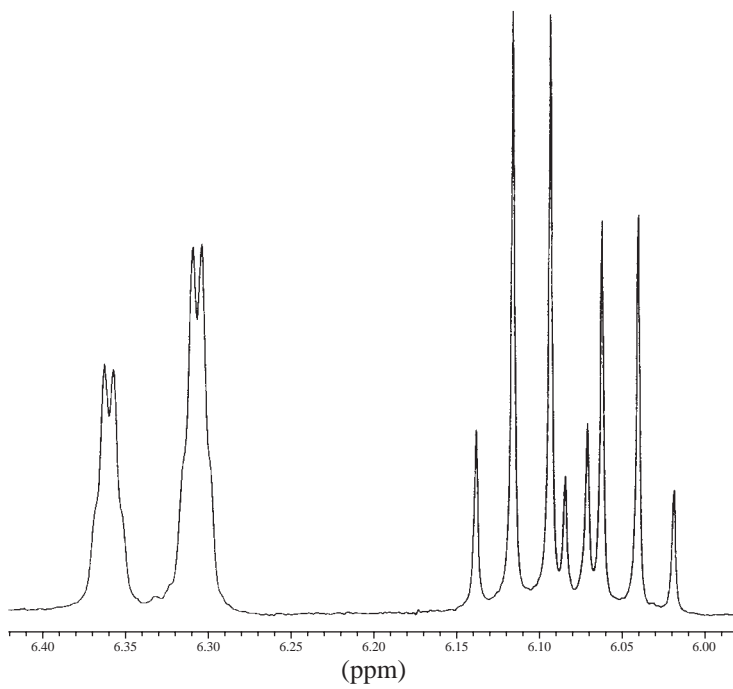
*14. Determine the structure of the following aromatic compound with formula C_8H_7BrO:
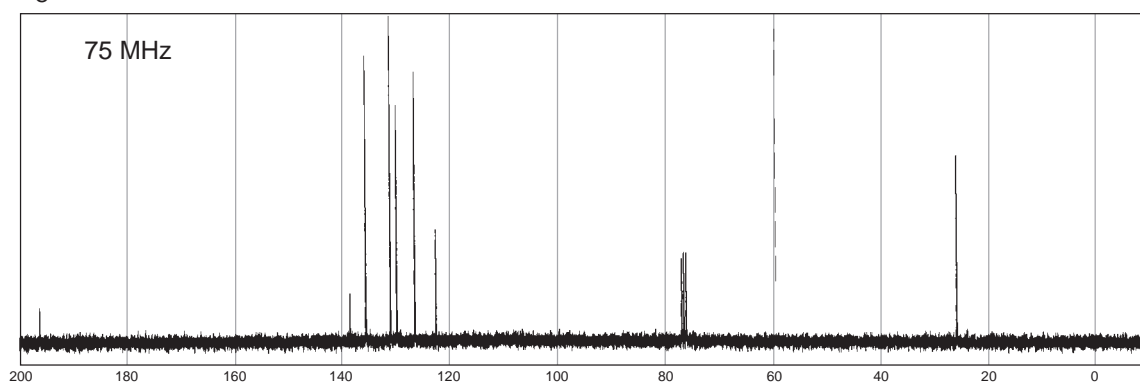
*15. The following spectrum of a compound with formula $C_5H_{10}O$ shows interesting patterns at about 2.4 and 9.8 ppm. Expansions of these two sets of peaks are shown. Expansions of the other patterns (not shown) in the spectrum show the following patterns: 0.92 ppm (triplet), 1.45 ppm (sextet), and 1.61 ppm (quintet). Draw a structure of the compound. Draw tree diagrams of the peaks at 2.4 and 9.8 ppm, including coupling constants.

7.4 Hz

1.9-Hz
spacings

9.8 ppm

2.4 ppm
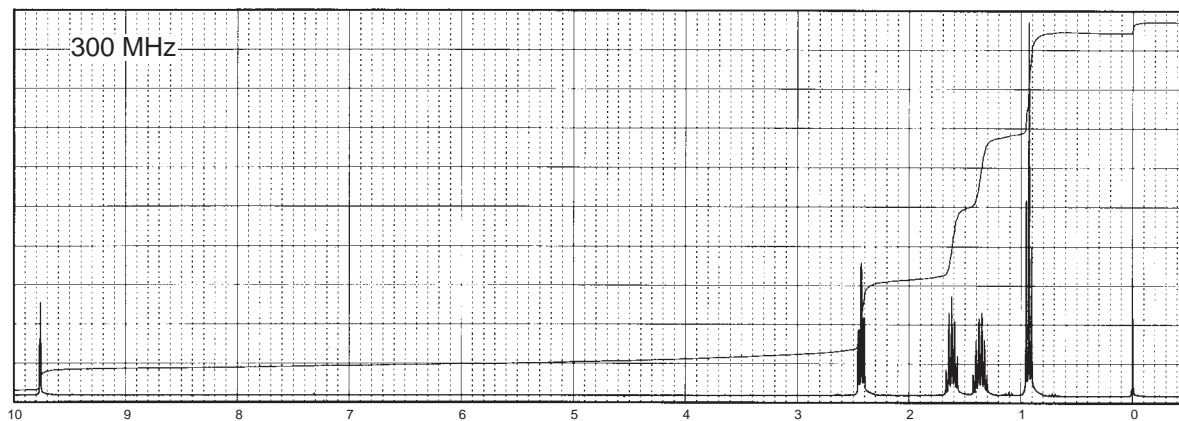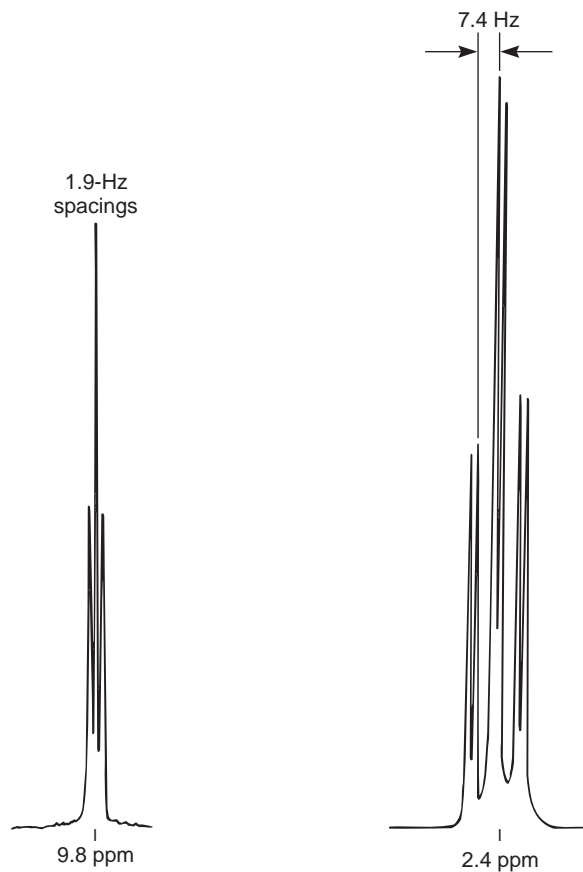
*16. The proton NMR spectral information shown in this problem is for a compound with formula $C_{10}H_{12}O_3$. A broad peak appearing at 12.5 ppm is not shown in the proton NMR reproduced here. The normal carbon-13 spectral results, including DEPT-135 and DEPT-90 results, are tabulated:

Normal Carbon	DEPT-135	DEPT-90
15 ppm	Positive	No peak
40	Negative	No peak
63	Negative	No peak
115	Positive	Positive
125	No peak	No peak
130	Positive	Positive
158	No peak	No peak
179	No peak	No peak

Draw the structure of this compound.

17. The proton NMR spectral information shown in this problem is for a compound with formula $C_{10}H_9N$. Expansions are shown for the region from 8.7 to 7.0 ppm. The normal carbon-13 spectral results, including DEPT-135 and DEPT-90 results, are tabulated:

Normal Carbon	DEPT-135	DEPT-90
19 ppm	Positive	No peak
122	Positive	Positive
124	Positive	Positive
126	Positive	Positive
128	No peak	No peak
129	Positive	Positive
130	Positive	Positive
144	No peak	No peak
148	No peak	No peak
150	Positive	Positive

Draw the structure of this compound and assign each of the protons in your structure. The coupling constants should help you to do this (see Appendix 5).

2276.68 2275.21 2269.70 2268.23 2266.76 2261.24 2259.77

2225.58 2224.47 2218.59 2217.49 2216.02 2210.50 2209.03

2107.18 2106.45 2102.77 2102.04

(ppm)

18. The proton NMR spectral information shown in this problem is for a compound with formula $C_9H_{14}O$. Expansions are shown for all the protons. The normal carbon-13 spectral results, including DEPT-135 and DEPT-90 results, are tabulated:

Normal Carbon	DEPT-135	DEPT-90
14 ppm	Positive	No peak
22	Negative	No peak
27.8	Negative	No peak
28.0	Negative	No peak
32	Negative	No peak
104	Positive	Positive
110	Positive	Positive
141	Positive	Positive
157	No peak	No peak

Draw the structure of this compound and assign each of the protons in your structure. The coupling constants should help you to do this (see Appendix 5).

2189.54	1884.74	1792.82	
2188.81	1882.90	1792.08	
2187.71	1881.80	1789.87	
2186.97	1879.96	1789.14	
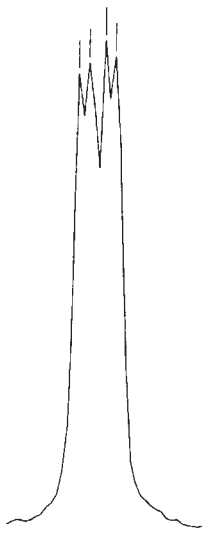
7.30   7.28

(ppm)
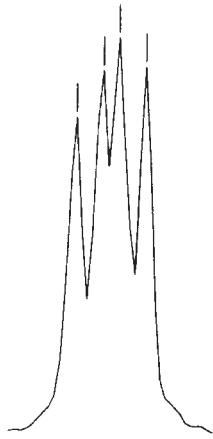
6.28   6.26

(ppm)

5.98   5.96   5.94

(ppm)

2.70   2.60   2.50   1.70   1.60   1.40   1.30   1.20   1.00   0.90   0.80
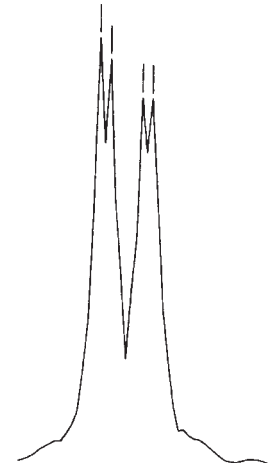
(ppm)
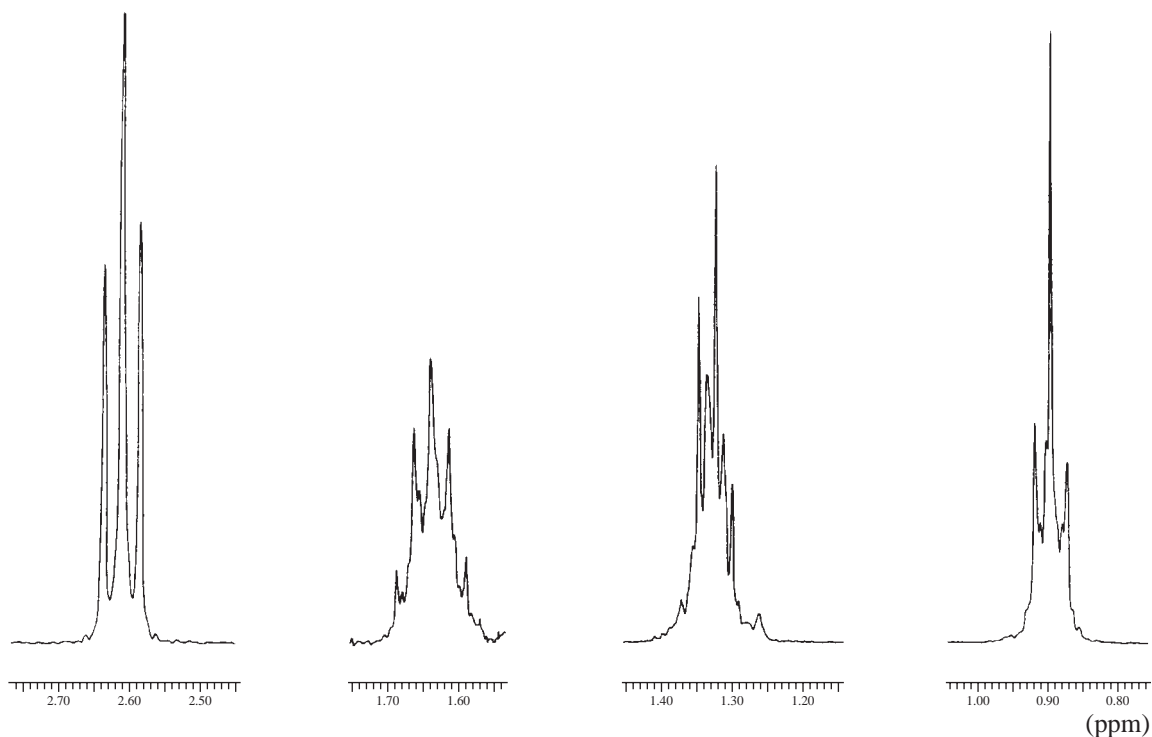
19. The proton NMR spectral information shown in this problem is for a compound with formula $C_{10}H_{12}O_2$. One proton, not shown, is a broad peak that appears at about 12.8 ppm. Expansions are shown for the protons absorbing in the region from 3.5 to 1.0 ppm. The monosubstituted benzene ring is shown at about 7.2 ppm but is not expanded because it is uninteresting. The normal carbon-13 spectral results, including DEPT-135 and DEPT-90 results, are tabulated:

Normal Carbon	DEPT-135	DEPT-90
22 ppm	Positive	No peak
36	Positive	Positive
43	Negative	No peak
126.4	Positive	Positive
126.6	Positive	Positive
128	Positive	Positive
145	No peak	No peak
179	No peak	No peak

Draw the structure of this compound and assign each of the protons in your structure. Explain why the interesting pattern is obtained between 2.50 and 2.75 ppm. Draw tree diagrams as part of your answer.
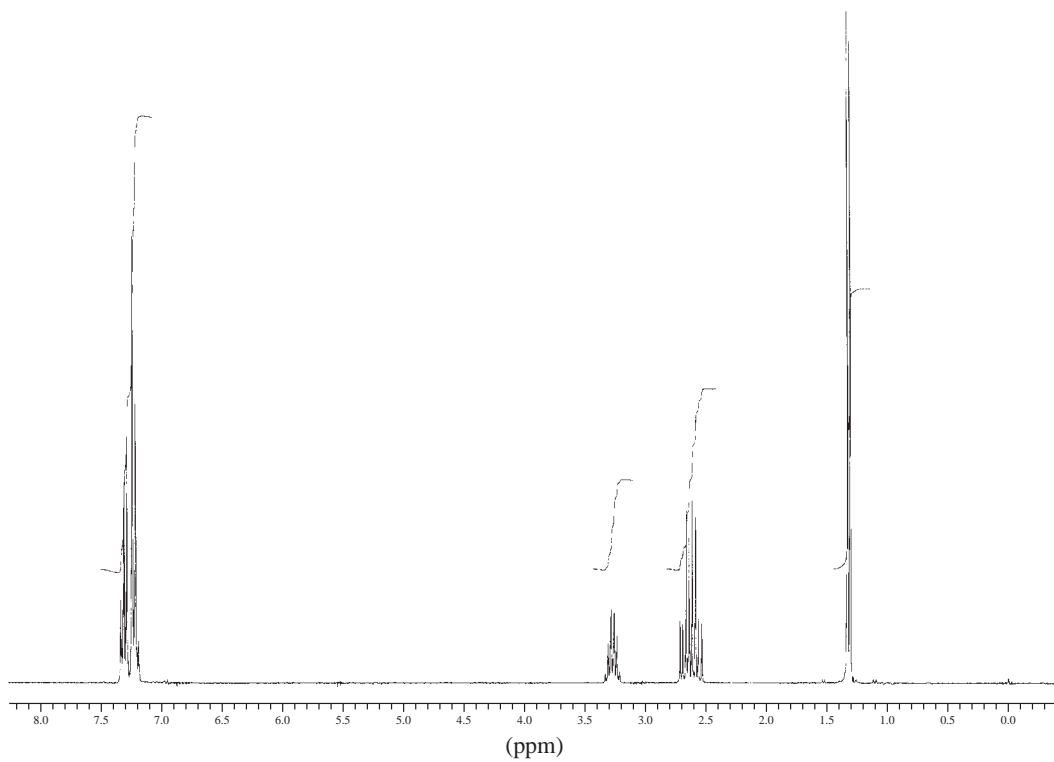
998.91
991.78
984.75
976.89
969.86
962.91

813.16
806.30
797.62
790.77
783.00
774.78
767.47
759.25

398.34
391.39
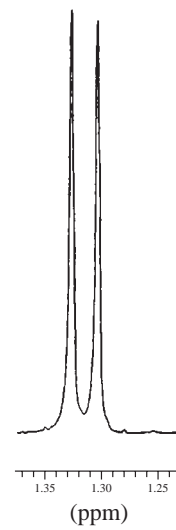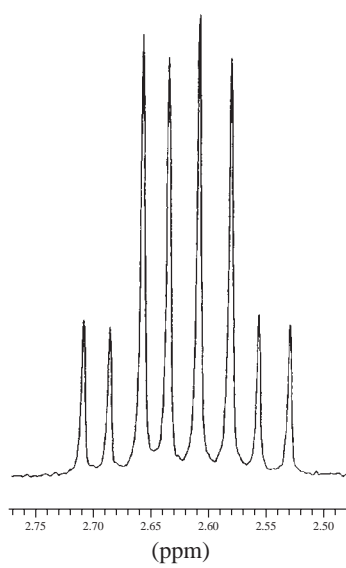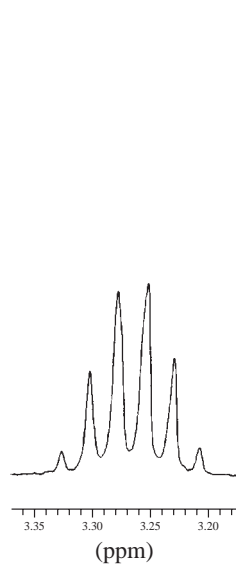
20. The spectrum shown in this problem is of 1-methoxy-1-buten-3-yne. Expansions are shown for each proton. Determine the coupling constants for each of the protons and draw tree diagrams for each. The interesting part of this problem is the presence of significant long-range coupling constants. There are ^3J, ^4J, and ^5J couplings in this compound. Be sure to include all of them in your tree diagram (graphical analysis).
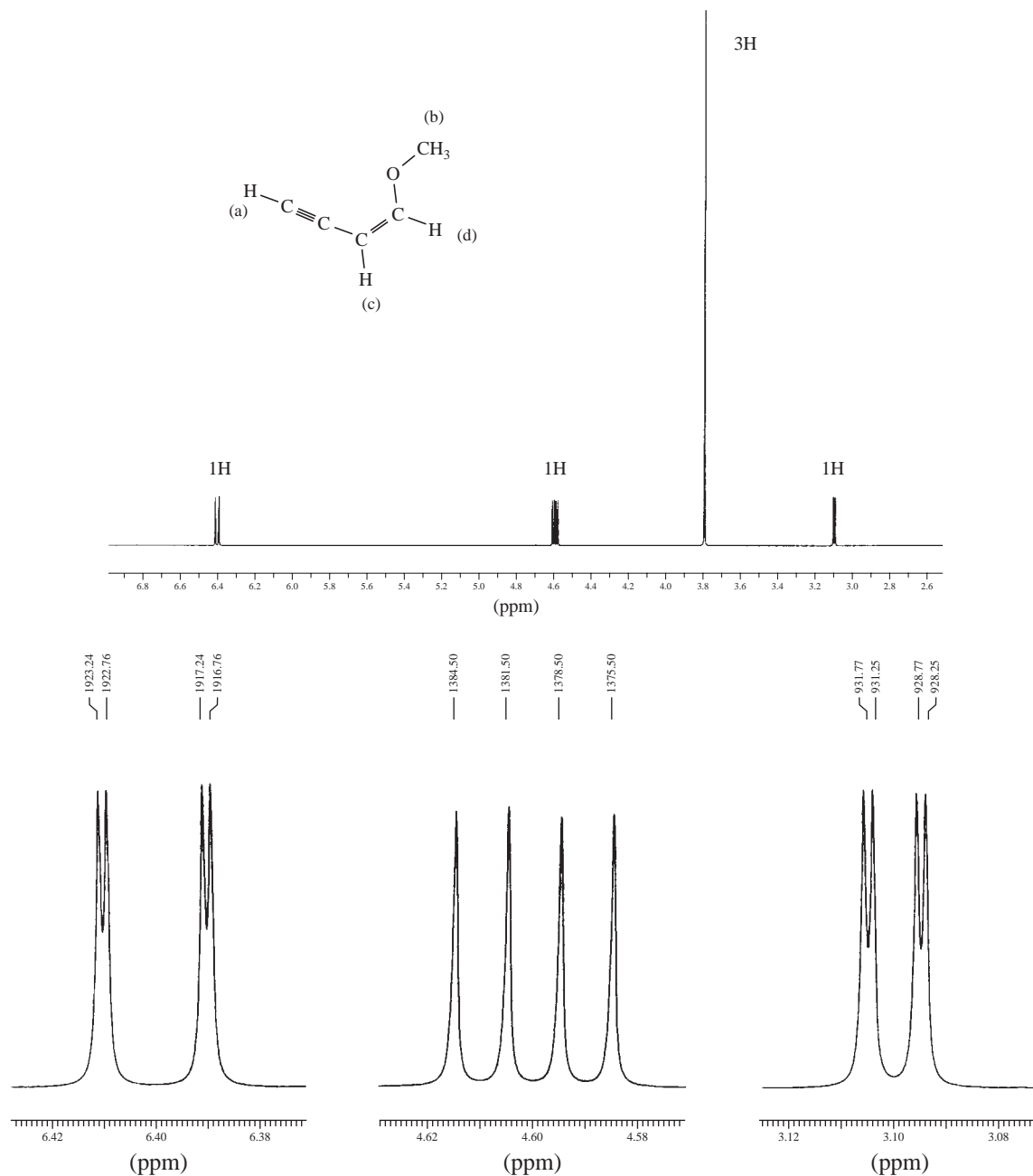
21. The partial proton NMR spectra (**A** and **B**) are given for the *cis* and *trans* isomers of the compound shown below (the bands for the three phenyl groups are not shown in either NMR). Draw the structures for each of the isomers and use the magnitude of the coupling constants to assign a structure to each spectrum. It may be helpful to use a molecular modeling program to determine the dihedral angles for each compound. The finely spaced doublet at 3.68 ppm in spectrum **A** is the band for the O—H peak. Assign each of the peaks in spectrum **A** to the structure. The O—H peak is not shown in spectrum **B**, but assign the pair of doublets to the structure using chemical shift information.
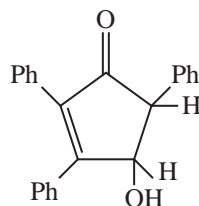
Spectrum A   Spectrum B

(ppm)
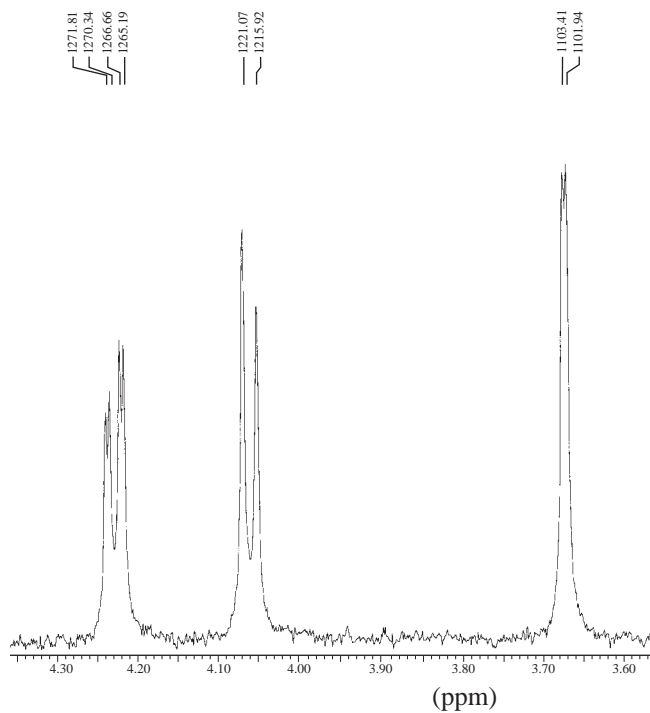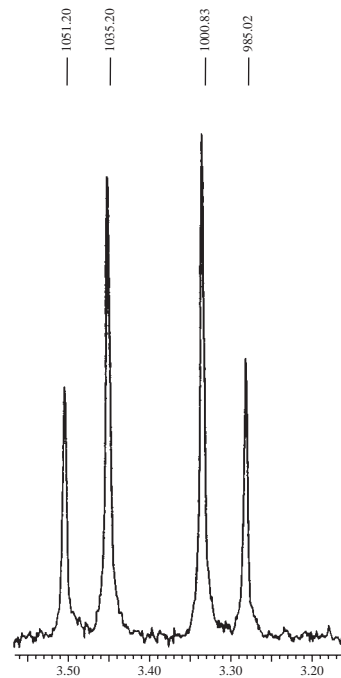
22. The proton NMR spectrum is shown for a compound with formula $C_6H_8Cl_2O_2$. The two chlorine atoms are attached to the same carbon atom. The infrared spectrum displays a strong band 1739 cm^{-1}. The normal carbon-13 and the DEPT experimental results are tabulated. Draw the structure of this compound.

Normal Carbon	DEPT-135	DEPT-90
18 ppm	Positive	No peak
31	Negative	No peak
35	No peak	No peak
53	Positive	No peak
63	No peak	No peak
170	No peak	No peak
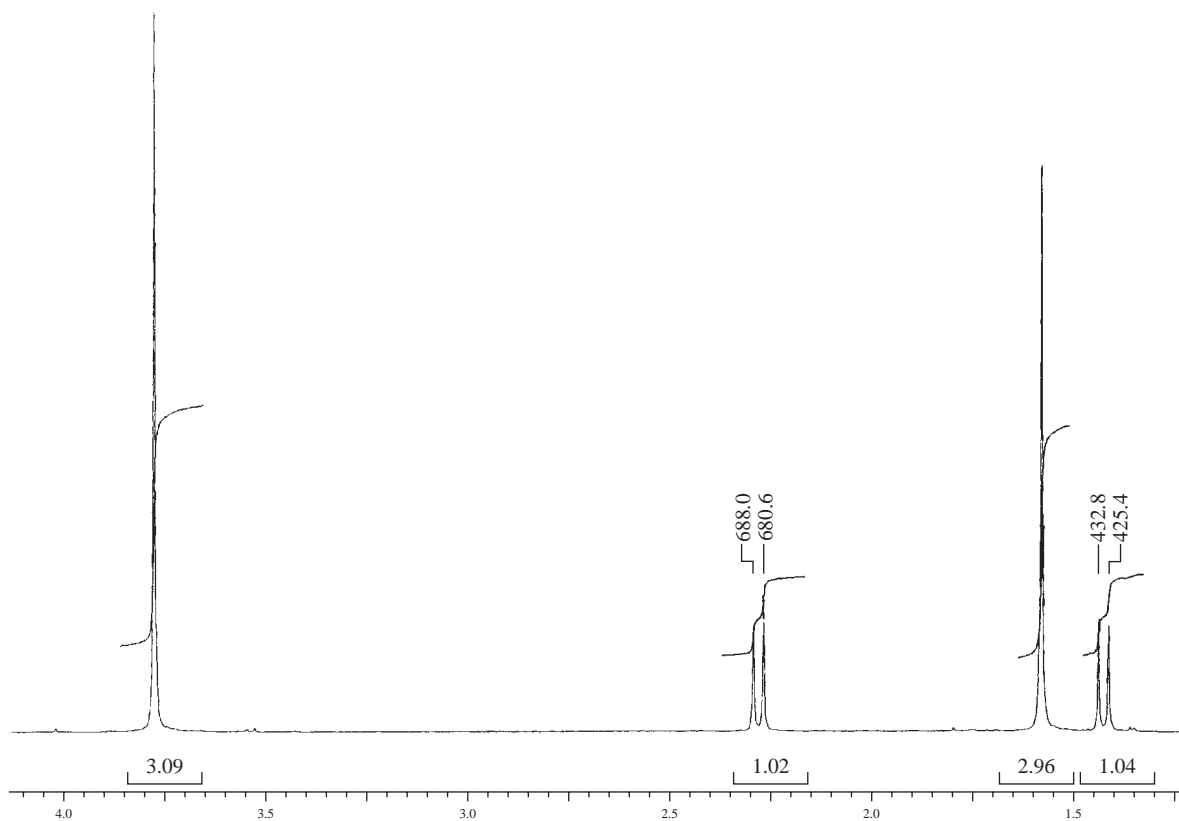
23. The proton NMR spectrum of a compound with formula $C_8H_{14}O_2$ is shown. The DEPT experimental results are tabulated. The infrared spectrum shows medium-sized bands at 3055, 2960, 2875, and 1660 cm^{-1} and strong bands at 1725 and 1185 cm^{-1}. Draw the structure of this compound.

Normal Carbon	DEPT-135	DEPT-90
10.53 ppm	Positive	No peak
12.03	Positive	No peak
14.30	Positive	No peak
22.14	Negative	No peak
65.98	Negative	No peak
128.83	No peak	No peak
136.73	Positive	Positive
168.16	No peak	No peak (C=O)
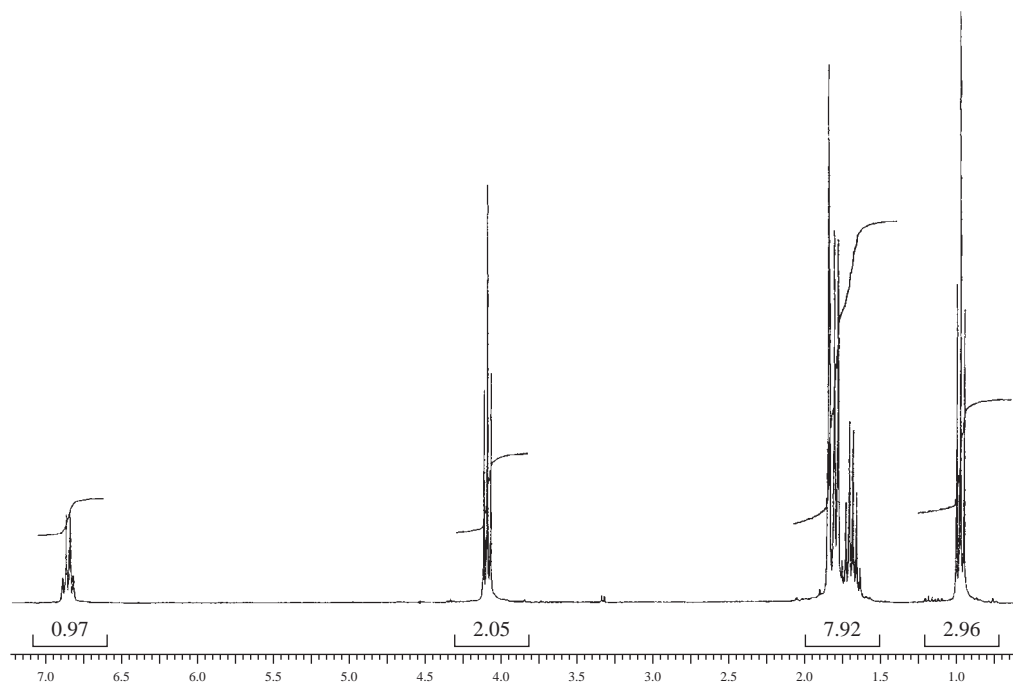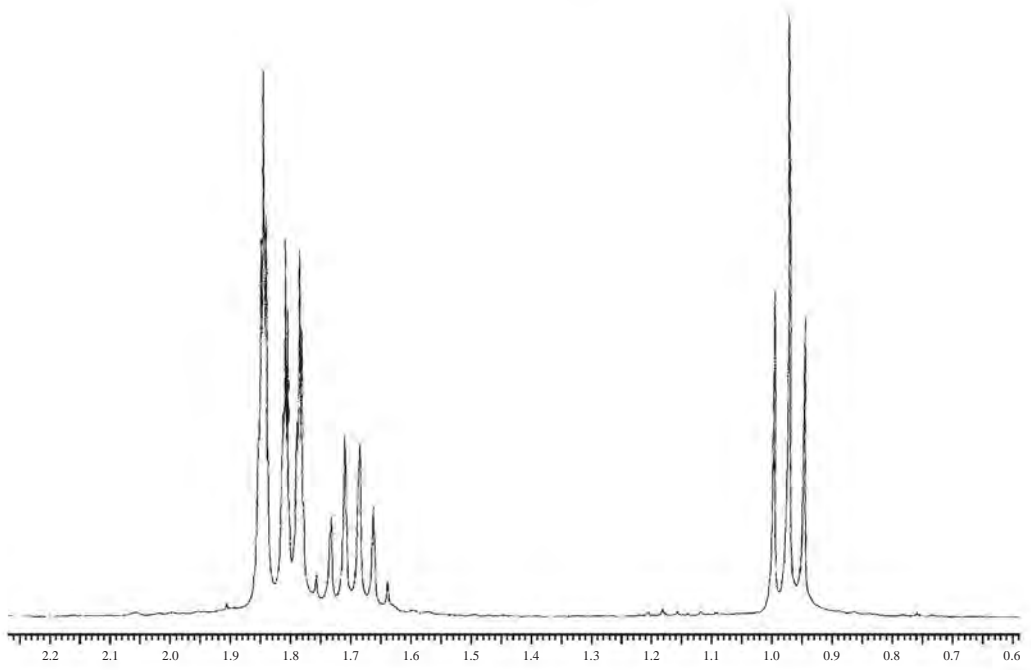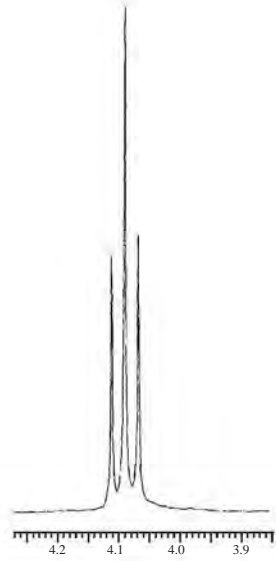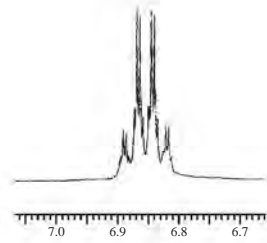
24. The proton NMR spectrum of a compound with formula $C_5H_{10}O$ is shown. The DEPT experimental results are tabulated. The infrared spectrum shows medium-sized bands at 2968, 2937, 2880, 2811, and 2711 cm^{-1} and strong bands at 1728 cm^{-1}. Draw the structure of this compound.

Normal Carbon	DEPT-135	DEPT-90
11.35 ppm	Positive	No peak
12.88	Positive	No peak
23.55	Negative	No peak
47.78	Positive	Positive
205.28	Positive	Positive (C=O)
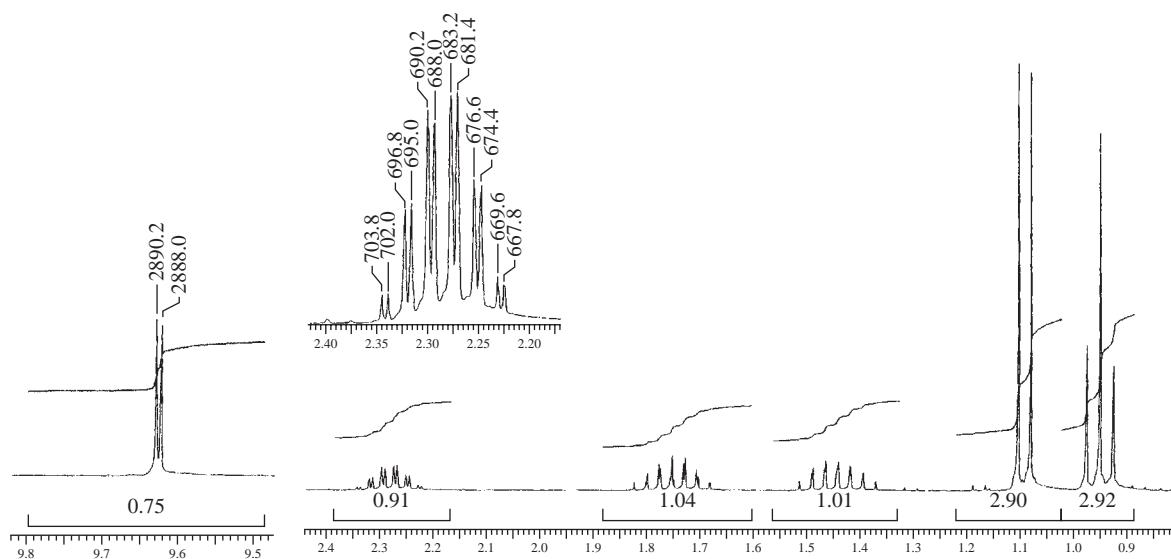
*25. Coupling constants between hydrogen and fluorine nuclei are often quite large: $^3J_{HF} \cong 3–25$ Hz and $^2J_{HF} \cong 44–81$ Hz. Since fluorine-19 has the same nuclear spin quantum number as a proton, we can use the $n + 1$ Rule with fluorine-containing organic compounds. One often sees larger H–F coupling constants, as well as smaller H–H couplings, in proton NMR spectra.

(a) Predict the appearance of the proton NMR spectrum of $F–CH_2–O–CH_3$.

(b) Scientists using modern instruments directly observe many different NMR-active nuclei by changing the frequency of the spectrometer. How would the fluorine NMR spectrum for $F–CH_2–O–CH_3$ appear?

*26. The proton NMR spectral information shown in this problem is for a compound with formula $C_9H_8F_4O$. Expansions are shown for all of the protons. The aromatic ring is disubstituted. In the region from 7.10 to 6.95 ppm, there are two doublets (1H each). One of the doublets is partially overlapped with a singlet (1H). The interesting part of the spectrum is the one proton pattern found in the region from 6.05 to 5.68 ppm. Draw the structure of the compound and draw a tree diagram for this pattern (see Appendix 5 and Problem 25 for proton-to-fluorine coupling constants).

Peak listings (left group): 2177.65, 2176.48, 2170.09, 2169.00, 2162.75, 2161.52

2121.99, 2114.07, 2106.00, 2098.66

1814.34, 1811.44, 1808.53

1761.23, 1758.32, 1755.41

1708.04, 1705.13, 1702.30

(ppm)
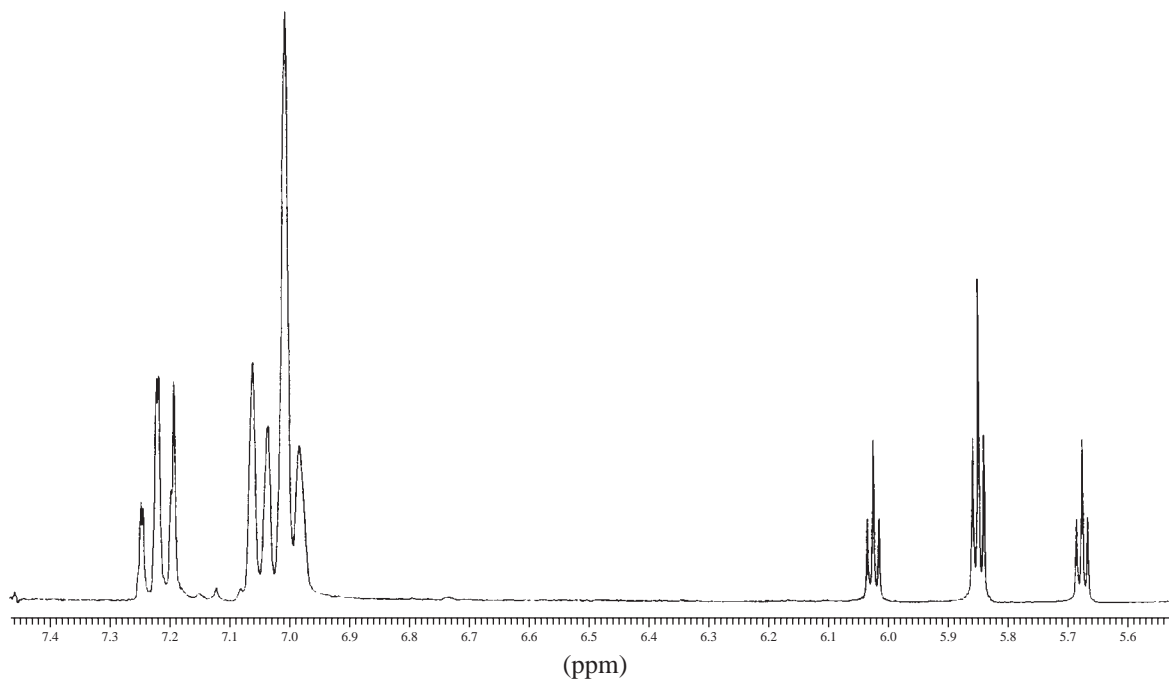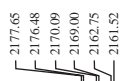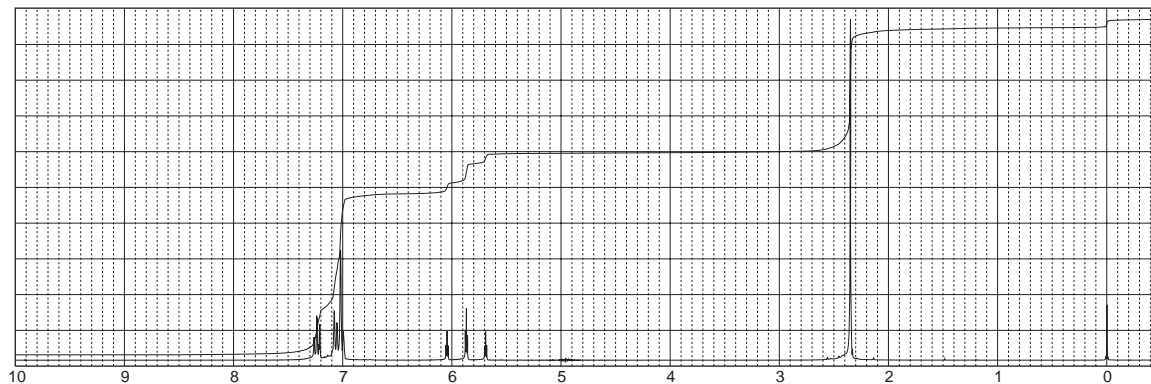
27. A compound with the formula C_2H_4BrF has the following NMR spectrum. Draw the structure for this compound. Using the Hertz values on the expansions, calculate the coupling constants. Completely explain the spectrum.

300 MHz

1433.66 1427.91 1422.16

1387.00 1381.25 1375.50

1084.59 1078.73 1072.98 1063.58 1057.83 1052.08

4.80 4.76 4.72 4.68 4.64 4.60 4.56

3.64 3.60 3.56 3.52 3.48

(ppm)   (ppm)
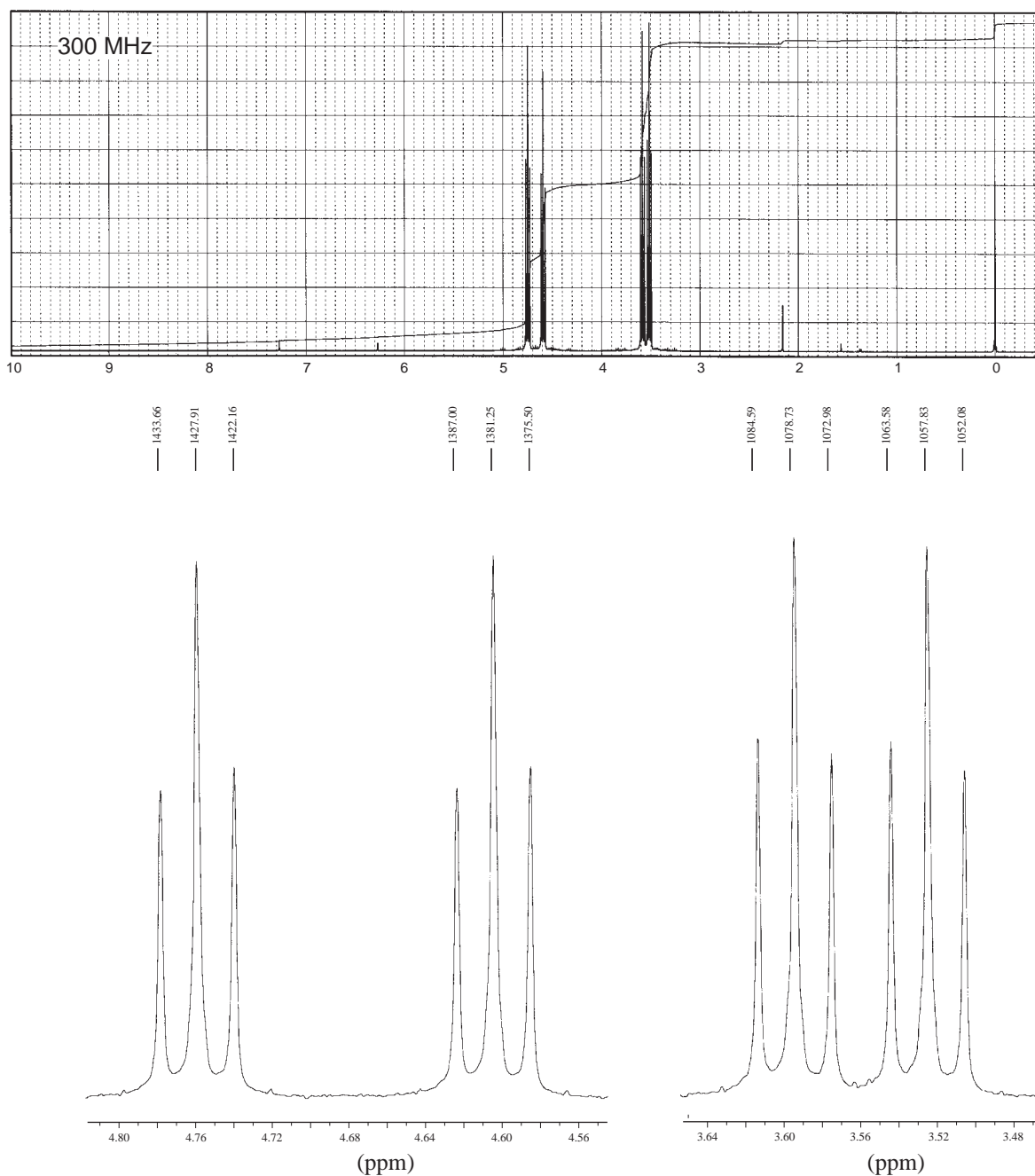
*28. Predict the proton and deuterium NMR spectra of $D-CH_2-O-CH_3$, remembering that the spin quantum number for deuterium = 1. Compare the proton spectrum to that of $F-CH_2-O-CH_3$ (Problem 25a).

*29. Although the nuclei of chlorine ($I = \frac{3}{2}$), bromine ($I = \frac{3}{2}$), and iodine ($I = \frac{5}{2}$) exhibit nuclear spin, the geminal and vicinal coupling constants, J_{HX} (vic) and J_{HX} (gem), are normally zero. These atoms are simply too large and diffuse to transmit spin information via their plethora of electrons. Owing to strong electrical quadrupole moments, these halogens are completely decoupled from directly attached protons or from protons on adjacent carbon atoms. Predict the proton NMR spectrum of $Br-CH_2-O-CH_3$ and compare it to that of $F-CH_2-O-CH_3$ (Problem 25a).

*30. In addition to $H-^{19}F$ coupling, it is possible to observe the influence of phosphorus-31 on a proton spectrum ($H-^{31}P$). Although proton–phosphorus coupling constants vary considerably according to the hybridization of phosphorus, phosphonate esters have ^2J and ^3J H–P coupling constants of about 13 Hz and 8 Hz, respectively. Since phosphorus-31 has the same nuclear-spin quantum number as a proton, we can use the $n + 1$ Rule with phosphorus-containing organic compounds. Explain the following spectrum for dimethyl methylphosphonate (see Appendix 5).
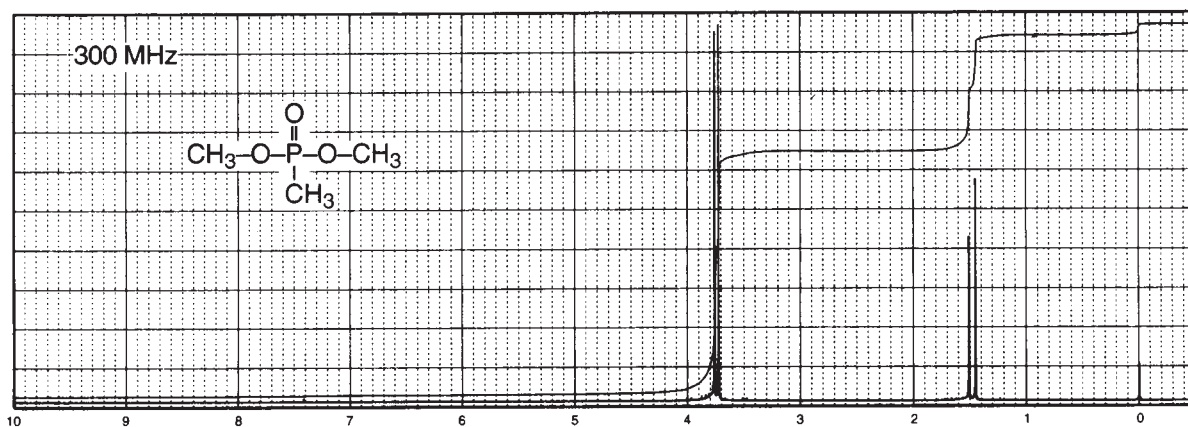
31. The proton NMR spectra for methyltriphenylphosphonium halide and its carbon-13 analogue are shown in this problem. Concentrating your attention on the doublet at 3.25 ppm and the pair of doublets between 2.9 and 3.5 ppm, interpret the two spectra. You may need to refer to Appendix 5 and Appendix 9. Estimate the coupling constants in the two spectra. Ignore the phenyl groups in your interpretation.

$$(C_6H_5)_3 - \overset{+}{P} - {}^{13}CH_3$$

$$X^-$$
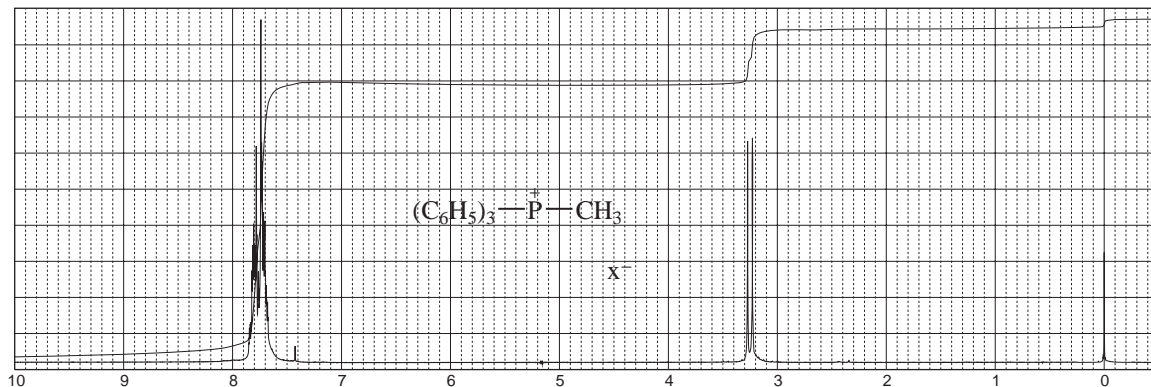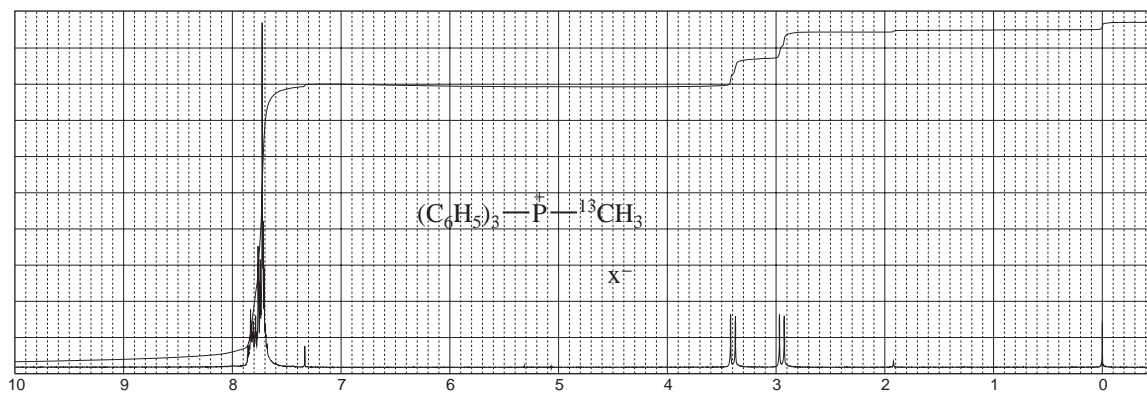
32. All three of the compounds, a, b, and c, have the same mass (300.4 amu). Identify each compound and assign as many peaks as you can, paying special attention to methyl and vinyl hydrogens. There is a small $CHCl_3$ peak near 7.3 ppm in each spectrum that should be ignored when analyzing the spectra.
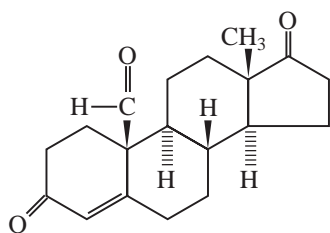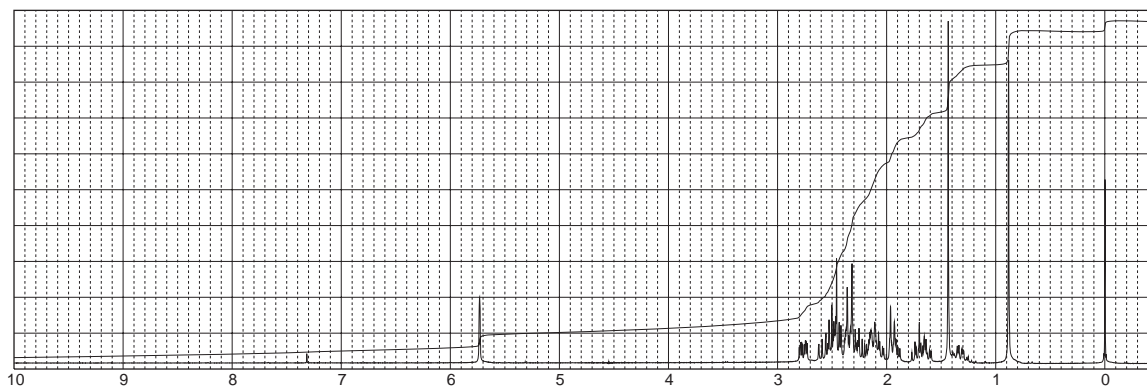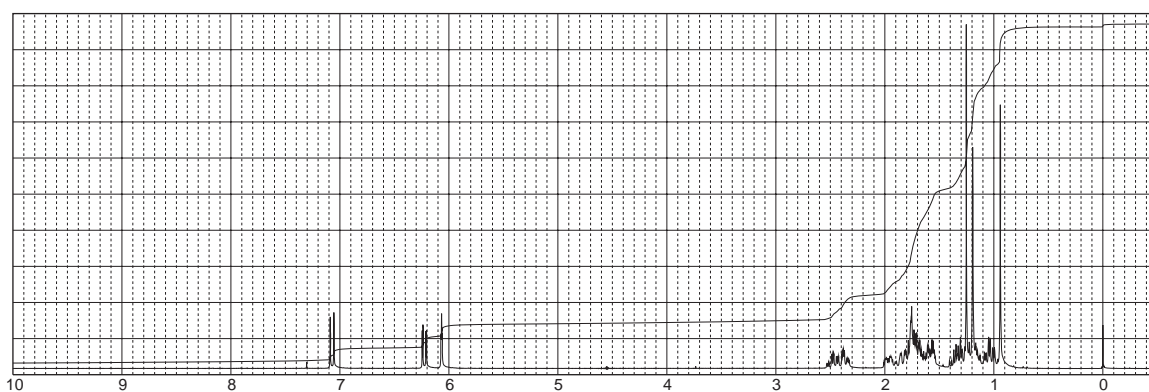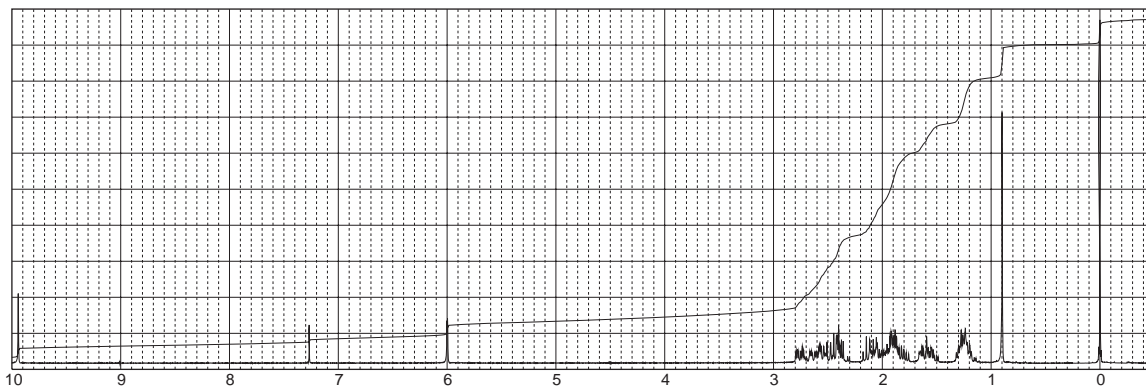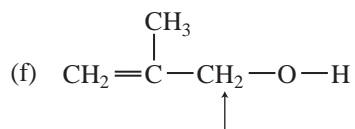

(a)
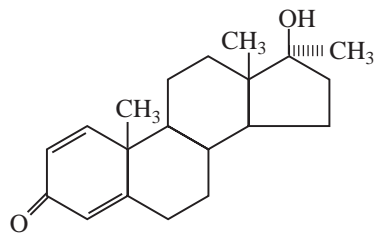
(b)
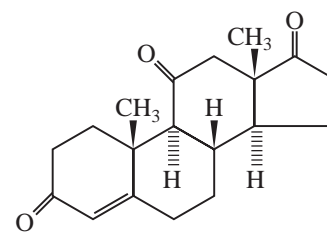
(c)

*33. Calculate the chemical shifts for the indicated protons using Table A6.1 in Appendix 6.

(a) $CH_3-\underset{\underset{\displaystyle \uparrow}{\overset{\overset{\displaystyle O}{\|}}{C}}}{}-CH_3$

(b) $CH_3-\underset{\underset{\displaystyle \uparrow}{}}{CH_2}-\overset{\overset{\displaystyle O}{\|}}{C}-\underset{\underset{\displaystyle \uparrow}{}}{CH_2}-\overset{\overset{\displaystyle O}{\|}}{C}-O-CH_3$

(c) $Cl-\underset{\underset{\displaystyle \uparrow}{}}{CH_2}-\overset{\overset{\displaystyle O}{\|}}{C}-O-CH_3$

(d) $CH_3-CH_2-\underset{\underset{\displaystyle \uparrow}{}}{CH_2}-C\equiv C-H$

(e) $CH_3-CH_2-\underset{\underset{\displaystyle Cl}{\overset{\displaystyle Cl}{|}}}{C}-\underset{\uparrow}{H}$

(f) $CH_2=\underset{\overset{\displaystyle CH_3}{|}}{C}-\underset{\underset{\displaystyle \uparrow}{}}{CH_2}-O-H$
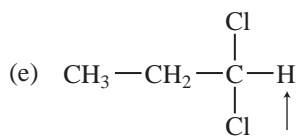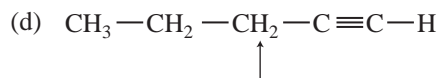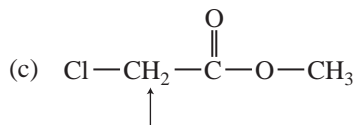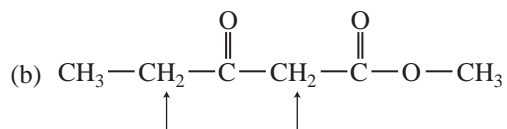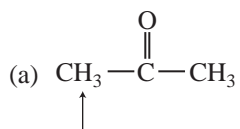
*34. Calculate the chemical shifts for the vinyl protons using Table A6.2 in Appendix 6.

(a)

(b)

(c)

(d)

(e)

(f)
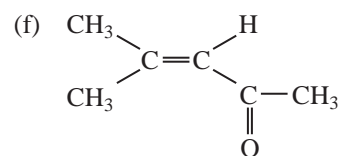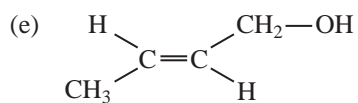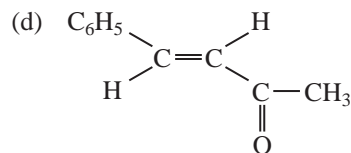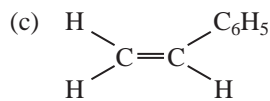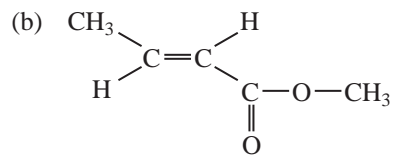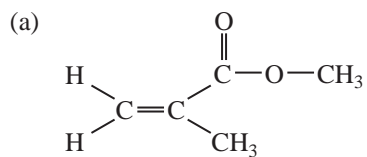
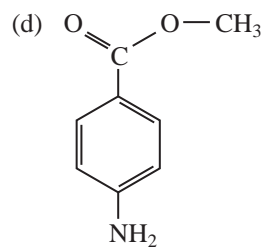***35.** Calculate the chemical shifts for the aromatic protons using Table A6.3 in Appendix 6.

(a)

(b)

(c)

(d)

(e)

(f)

(g)

(h)

(i)
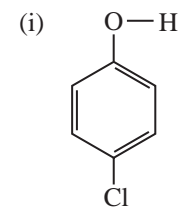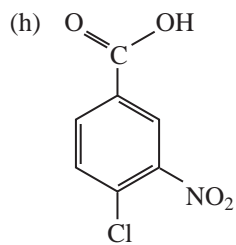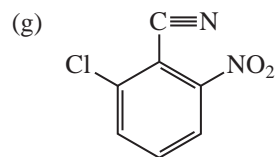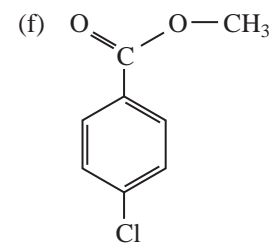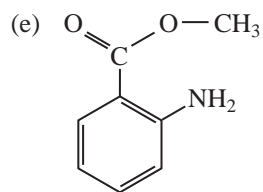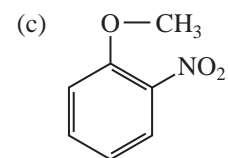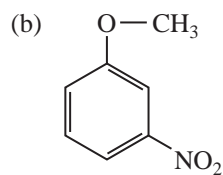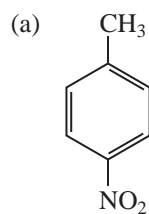
REFERENCES

Books and Monographs

Becker, E. D., *High Resolution NMR: Theory and Chemical Applications,* 3rd ed., Academic Press, New York, 1999.

Bovey, F. A., *NMR Spectroscopy,* Academic Press, New York, 1969.

Breitmaier, E., *Structure Elucidation by NMR in Organic Chemistry: A Practical Guide,* 3rd ed., John Wiley and Sons, New York, 2002.

Claridge, T. D. W., *High Resolution NMR Techniques in Organic Chemistry,* Pergamon, Oxford, England, 1999.

Crews, P., J. Rodriguez, and M. Jaspars, *Organic Structure Analysis,* Oxford University Press, New York, 1998.

Derome, A. E., *Modern NMR Techniques for Chemistry Research,* Pergamon Press, Oxford, England, 1987.

Friebolin, H., *Basic One- and Two-Dimensional NMR Spectroscopy,* 4th ed., Wiley-VCH, Weinheim, 2004.

Günther, H., *NMR Spectroscopy,* 2nd ed., John Wiley and Sons, New York, 1995.

Jackman, L. M., and S. Sternhell, *Applications of Nuclear Magnetic Resonance Spectroscopy in Organic Chemistry,* 2nd ed., Pergamon Press, London, 1969.

Lambert, J. B., H. F. Shurvell, D. A. Lightner, and T. G. Cooks, *Organic Structural Spectroscopy,* Prentice Hall, Upper Saddle River, NJ, 1998.

Macomber, R. S., *NMR Spectroscopy—Essential Theory and Practice,* College Outline Series, Harcourt, Brace Jovanovich, New York, 1988.

Macomber, R. S., *A Complete Introduction to Modern NMR Spectroscopy,* John Wiley and Sons, New York, 1998.

Nelson, J. H., *Nuclear Magnetic Resonance Spectroscopy,* Prentice Hall, Upper Saddle River, NJ, 2003.

Pople, J. A., W. C. Schneider, and H. J. Bernstein, *High Resolution Nuclear Magnetic Resonance,* McGraw–Hill, New York, 1959.

Pretsch, E., P. Buhlmann, and C. Affolter, *Structure Determination of Organic Compounds. Tables of Spectral Data,* 3rd ed., Springer-Verlag, Berlin, 2000.

Roberts, J. D., *Nuclear Magnetic Resonance: Applications to Organic Chemistry,* McGraw–Hill, New York, 1959.

Roberts, J. D., *An Introduction to the Analysis of Spin–Spin Splitting in High Resolution Nuclear Magnetic Resonance Spectra,* W. A. Benjamin, New York, 1962.

Roberts, J. D., *ABCs of FT-NMR,* University Science Books, Sausolito, CA, 2000.

Sanders, J. K. M., and B. K. Hunter, *Modern NMR Spectroscopy—A Guide for Chemists,* 2nd ed., Oxford University Press, Oxford, England, 1993.

Silverstein, R. M., F. X. Webster, and D. Kiemle, *Spectrometric Identification of Organic Compounds,* 7th ed., John Wiley and Sons, New York, 2005.

Vyvyan, J. R., Ph.D. thesis, University of Minnesota, 1995.

Wiberg, K. B., and B. J. Nist, *The Interpretation of NMR Spectra,* W. A. Benjamin, New York, 1962.

Compilations of Spectra

Ault, A., and M. R. Ault, *A Handy and Systematic Catalog of NMR Spectra,* 60 MHz with some 270 MHz, University Science Books, Mill Valley, CA, 1980.

Pouchert, C. J., and J. Behnke, *The Aldrich Library of ^{13}C and ^{1}H FT-NMR Spectra,* 300 MHz, Aldrich Chemical Company, Milwaukee, WI, 1993.

Computer Programs

Bell, H., Virginia Tech, Blacksburg, VA. (Dr. Bell has a number of NMR programs available from http://www.chemistry.vt.edu/chem-dept/hbell/bellh.htm or e-mail: hmbell@vt.edu.)

Reich, H. J., University of Wisconsin, WINDNMR-Pro, a Windows program for simulating high-resolution NMR spectra. http://www.chem.wisc.edu/areas/reich/plt/windnmr.htm.

Papers

Mann, B. "The Analysis of First-Order Coupling Patterns in NMR Spectra," *Journal of Chemical Education, 72* (1995): 614.

Hoye, T. R., P. R. Hanson, and J. R. Vyvyan, "A Practical Guide to First-Order Multiplet Analysis in ^{1}H NMR Spectroscopy," *Journal of Organic Chemistry 59* (1994): 4096.

Hoye, T. R., and H. Zhao, "A Method for Easily Determining Coupling Constant Values: An Addendum to 'A Practical Guide to First-Order Multiplet Analysis in ^{1}H NMR Spectroscopy'", *Journal of Organic Chemistry 67* (2002): 4014.

Websites

http://www.nmrfam.wisc.edu/
NMRFAM, Madison.

http://www.magnet.fsu.edu/scientificdivisions/nmr/overview.html
National High Magnetic Field Laboratory.

http://www.aist.go.jp/RIODB/SDBS/menu-e.html
Integrated Spectral DataBase System for Organic Compounds, National Institute of Materials and Chemical Research, Tsukuba, Ibaraki 305-8565, Japan. This database includes infrared, mass spectra, and NMR data (proton and carbon-13) for a number of compounds.

http://www.chem.ucla.edu/~webspectra/
UCLA Department of Chemistry and Biochemistry, in connection with Cambridge University Isotope Laboratories, maintains a website, WebSpectra, that provides NMR and IR spectroscopy problems for students to interpret. They provide links to other sites with problems for students to solve.

http://www.nd.edu/~smithgrp/structure/workbook.html
Combined structure problems provided by the Smith group at the University of Notre Dame.